

University of Alberta

Development of Novel Non-Scarring Tissue Engineered Skin to Treat Burn Patients and Others with Extensive Skin Loss.

by

Mathew Varkey

A thesis submitted to the Faculty of Graduate Studies and Research
in partial fulfillment of the requirements for the degree of

Doctor of Philosophy

in

Experimental Surgery

Department of Surgery

©Mathew Varkey

Spring 2013

Edmonton, Alberta

Permission is hereby granted to the University of Alberta Libraries to reproduce single copies of this thesis and to lend or sell such copies for private, scholarly or scientific research purposes only. Where the thesis is converted to, or otherwise made available in digital form, the University of Alberta will advise potential users of the thesis of these terms.

The author reserves all other publication and other rights in association with the copyright in the thesis and, except as herein before provided, neither the thesis nor any substantial portion thereof may be printed or otherwise reproduced in any material form whatsoever without the author's prior written permission.



Library and Archives
Canada

Published Heritage
Branch

395 Wellington Street
Ottawa ON K1A 0N4
Canada

Bibliothèque et
Archives Canada

Direction du
Patrimoine de l'édition

395, rue Wellington
Ottawa ON K1A 0N4
Canada

Your file Votre référence

ISBN: 978-0-494-96414-9

Our file Notre référence

ISBN: 978-0-494-96414-9

NOTICE:

The author has granted a non-exclusive license allowing Library and Archives Canada to reproduce, publish, archive, preserve, conserve, communicate to the public by telecommunication or on the Internet, loan, distribute and sell theses worldwide, for commercial or non-commercial purposes, in microform, paper, electronic and/or any other formats.

The author retains copyright ownership and moral rights in this thesis. Neither the thesis nor substantial extracts from it may be printed or otherwise reproduced without the author's permission.

AVIS:

L'auteur a accordé une licence non exclusive permettant à la Bibliothèque et Archives Canada de reproduire, publier, archiver, sauvegarder, conserver, transmettre au public par télécommunication ou par l'Internet, prêter, distribuer et vendre des thèses partout dans le monde, à des fins commerciales ou autres, sur support microforme, papier, électronique et/ou autres formats.

L'auteur conserve la propriété du droit d'auteur et des droits moraux qui protègent cette thèse. Ni la thèse ni des extraits substantiels de celle-ci ne doivent être imprimés ou autrement reproduits sans son autorisation.

In compliance with the Canadian Privacy Act some supporting forms may have been removed from this thesis.

While these forms may be included in the document page count, their removal does not represent any loss of content from the thesis.

Conformément à la loi canadienne sur la protection de la vie privée, quelques formulaires secondaires ont été enlevés de cette thèse.

Bien que ces formulaires aient inclus dans la pagination, il n'y aura aucun contenu manquant.

Canada

Abstract

Tissue engineered skin containing autologous fibroblasts and keratinocytes on collagen-glycosaminoglycan (C-GAG) matrices are the preferred skin substitutes for wound repair when loss of skin is extensive as in burns. A significant negative outcome of wound healing is hypertrophic scarring (HTS), a dermal-fibroproliferative disorder, that leads to considerable morbidity. Dermal fibroblasts, the cells that mediate wound healing and HTS are heterogeneous; they consist of superficial (SF), deep (DF) and hair follicle fibroblasts. Previous studies have shown that DF may be responsible for HTS. The goal of this project was therefore to further characterize SF and DF, explore new targets for treatment of HTS and develop tissue engineered skin with anti-scarring properties, for use in patients with extensive skin loss.

Biochemical and biomechanical assessment of C-GAG matrices independently seeded with SF or DF revealed differential matrix remodelling. Matrices with DF were more contracted and stiffer and had significantly higher osteopontin, angiotensin-II, peroxisome-proliferator-activated receptor (PPAR)- α , and significantly less tumor necrosis factor- α , PPAR- β/δ , PPAR- γ , and the proteoglycan, fibromodulin compared to matrices with SF. These targets could potentially be used for treatment of HTS. Further, when SF or DF were independently co-cultured with keratinocytes on matrices, the resulting engineered skin with SF formed a continuous epidermis with increased epidermal barrier function and higher levels of keratin-5 and E-cadherin, compared to that

with DF, which had an intermittent epidermis. Also, engineered skin with SF formed better basement membrane with more laminin-5, nidogen, collagen typeVII, and the proteoglycan, perlecan, compared to that with DF. Furthermore, assessment of epidermal effect on matrix remodelling by SF and DF revealed a significant keratinocytes-mediated inhibition of matrix contraction, TGF- β 1 and collagen production, and myofibroblast-differentiation for DF and not for SF. Also, co-culture of keratinocytes resulted in reduced gene expression of pro-fibrotic, CTGF and fibronectin and increased expression of anti-fibrotic, MMP-1, decorin and fibromodulin for DF and not SF. Taken together, the specific use of SF in tissue engineered skin may be more beneficial than heterogeneous dermal fibroblasts to promote adhesion of newly-formed skin and anti-fibrotic wound healing, and promising for use in treatment of extensive skin loss and other basement membrane disorders.

Acknowledgement

I would like to express my sincere gratitude to my supervisor Dr. Edward Tredget for all his support and guidance throughout my Ph.D. program. I would also like to thank Dr. Ding for her support. I would like to thank all past and present members of the Tredget lab for their friendship. I would also like to thank members of my supervisory committee Dr. Hasan Uludağ and Dr. Robert Burrell for their helpful suggestions. I am grateful to my family for their unwavering support without which this endeavor would not have been possible.

I would like to acknowledge the Department of Surgery for providing me with Graduate Research Assistantships throughout my PhD program, and CIHR and the Firefighter's Burn Trust Fund for funding this project.

Table of Contents

| | | |
|-------|---|----|
| 1 | Introduction | 2 |
| 1.1 | Skin | 2 |
| 1.1.1 | Skin Injury from Burns..... | 3 |
| 1.1.2 | Tissue Engineering of Skin | 5 |
| 1.1.3 | Wound Healing and Fibrosis..... | 6 |
| 1.2 | Skin Substitutes | 9 |
| 1.2.1 | Features of Skin Substitutes..... | 10 |
| 1.2.2 | Types of Skin Substitutes..... | 10 |
| 1.2.3 | Commercially Available Skin Substitutes..... | 11 |
| 1.2.4 | Limitations of Commercially Available Skin Substitutes..... | 16 |
| 1.3 | Cultured Skin Substitutes..... | 17 |
| 1.3.1 | Scaffold | 18 |
| 1.3.2 | Design Specifications for Collagen-GAG Scaffolds | 21 |
| 1.3.3 | Advantages of Using Collagen-GAG Scaffolds | 22 |
| 1.3.4 | Cells | 23 |
| 1.4 | Preparation of CSS..... | 27 |
| 1.4.1 | Preparation of Collagen-GAG Suspension | 28 |
| 1.4.2 | Fabrication of Collagen-GAG Scaffolds | 28 |
| 1.4.3 | Cross-Linking of Collagen-GAG Scaffolds..... | 30 |
| 1.4.4 | Culture Conditions..... | 32 |
| 1.4.5 | Advantages of Co-culture of Fibroblasts and Keratinocytes..... | 33 |
| 1.5 | Advantages of CSS..... | 35 |
| 1.6 | Limitations of CSS..... | 36 |
| 1.7 | Thesis Research Project | 37 |
| 1.8 | Table and Figures | 40 |
| 1.9 | References | 45 |
| 2 | Differential Collagen-Glycosaminoglycan Matrix Remodeling by Superficial and Deep Dermal Fibroblasts: Potential Therapeutic Targets for Hypertrophic Scar.. | 62 |

| | | |
|--------|---|-----|
| 2.1 | Introduction | 62 |
| 2.2 | Materials and Methods | 65 |
| 2.2.1 | Preparation of C-GAG Matrices | 65 |
| 2.2.2 | Determination of Pore Structure and Sizes of C-GAG Matrices | 66 |
| 2.2.3 | Isolation of Fibroblasts and Cell Culture | 67 |
| 2.2.4 | Assessment of Cell Viability on C-GAG Matrices | 68 |
| 2.2.5 | Analysis of Contraction of C-GAG Matrices with Fibroblasts | 68 |
| 2.2.6 | Biomechanical Testing of C-GAG Matrices with Fibroblasts | 69 |
| 2.2.7 | Assessment of Collagen Content in Fibroblast-Populated C-GAG Matrices and Conditioned Medium | 69 |
| 2.2.8 | Histological Analysis | 70 |
| 2.2.9 | Immunohistochemical Analysis | 71 |
| 2.2.10 | Gene Expression Studies | 72 |
| 2.2.11 | Protein Expression Analysis | 73 |
| 2.2.12 | Statistical Analysis | 74 |
| 2.3 | Results | 75 |
| 2.3.1 | C-GAG Matrix Pore Structure | 75 |
| 2.3.2 | Viability of Fibroblasts on C-GAG Matrices | 75 |
| 2.3.3 | C-GAG Matrix Contraction by Fibroblasts | 76 |
| 2.3.4 | Biomechanical Properties of C-GAG Matrices with the Fibroblasts | 76 |
| 2.3.5 | Collagen Production by the Fibroblasts | 77 |
| 2.3.6 | ECM Production by Fibroblasts | 78 |
| 2.3.7 | Differentiation of Fibroblasts in the C-GAG Matrices to Myofibroblasts 78 | |
| 2.3.8 | Identification of Therapeutic Targets for HTS | 79 |
| 2.3.9 | TGF- β 1 and OPN Production by Fibroblasts | 80 |
| 2.4 | Discussion | 80 |
| 2.5 | Conclusions | 89 |
| 2.6 | Table and Figures | 90 |
| 2.7 | References | 109 |

| | |
|--|------------|
| 3 Superficial Dermal Fibroblasts Enhance Basement Membrane and Epidermal Barrier Formation in Tissue Engineered Skin: Implications for Treatment of Skin Basement Membrane Disorders..... | 119 |
| 3.1 Introduction | 119 |
| 3.2 Materials and Methods | 123 |
| 3.2.1 Preparation of C-GAG Matrices | 123 |
| 3.2.2 Preparation of Tissue Engineered Skin | 124 |
| 3.2.3 Assessment of Cell Metabolic Activity | 126 |
| 3.2.4 Immunohistochemical Analysis | 126 |
| 3.2.5 Gene Expression Studies..... | 127 |
| 3.2.6 Assessment of Barrier Function | 128 |
| 3.2.7 Statistical Analysis | 129 |
| 3.3 Results..... | 129 |
| 3.3.1 Metabolic Activity of Cells on C-GAG Matrices | 129 |
| 3.3.2 Epidermis Formation in Tissue Engineered Skin | 129 |
| 3.3.3 Basement Membrane Formation in Tissue Engineered Skin | 130 |
| 3.3.4 Proteoglycan Expression in Basement Membrane of Tissue Engineered Skin | 132 |
| 3.3.5 Epidermal Barrier Function in Tissue Engineered Skin | 133 |
| 3.4 Discussion | 133 |
| 3.5 Table and Figures | 139 |
| 3.6 References | 154 |
| 4 Keratinocytes Alter Biomechanical Characteristics and Reduce Fibrotic Remodeling of Tissue Engineered Skin made with Deep Dermal Fibroblasts.... | 163 |
| 4.1 Introduction | 163 |
| 4.2 Materials and Methods | 165 |
| 4.2.1 Preparation of C-GAG Matrices | 165 |
| 4.2.2 Preparation of Tissue Engineered Skin | 166 |
| 4.2.3 Analysis of Contraction of Tissue Engineered Skin | 167 |

| | | |
|-------|--|-----|
| 4.2.4 | Assessment of Collagen Content in Conditioned Medium of Tissue Engineered Skin | 168 |
| 4.2.5 | Immunohistochemical Analysis | 169 |
| 4.2.6 | Gene Expression Studies..... | 170 |
| 4.2.7 | Protein Expression Analysis | 171 |
| 4.2.8 | Statistical Analysis | 172 |
| 4.3 | Results..... | 172 |
| 4.3.1 | Contraction of the Different Tissue Engineered Skin | 172 |
| 4.3.2 | Collagen Production..... | 173 |
| 4.3.3 | Expression of Pro- and Anti-Fibrotic Factors and Proteoglycans | 174 |
| 4.3.4 | Myofibroblast Differentiation | 176 |
| 4.3.5 | TGF- β 1 Production | 176 |
| 4.4 | Discussion | 177 |
| 4.5 | Conclusions | 182 |
| 4.6 | Table and Figures | 183 |
| 4.7 | References | 199 |
| 5 | Conclusions and Future Avenues | 203 |
| 5.1 | Conclusions | 203 |
| 5.2 | Future Avenues | 206 |
| 5.3 | References | 209 |

List of Tables

| | |
|---|-----|
| Table 1.1: Commercially Available Skin Substitutes..... | 40 |
| Table 2.1: Primers Used in qRT-PCR for Amplification of Genes of Interest..... | 90 |
| Table 3.1: Gene Specific Primers Used in qRT-PCR for Amplification of Genes of Interest..... | 139 |
| Table 4.1: Primers Used in qRT-PCR for Amplification of Genes of Interest..... | 183 |

List of Figures

| | |
|--|-----|
| Figure 1.1: Layers of Human Skin. | 41 |
| Figure 1.2: Structure of Human Skin. | 42 |
| Figure 1.3: Relative Rates of Keratinocyte Proliferation..... | 43 |
| Figure 1.4: Preparation of CSS..... | 44 |
| Figure 2.1: Scanning Electron Micrograph of C-GAG Matrix. | 91 |
| Figure 2.2: Viability of Superficial and Deep Dermal Fibroblasts Cultured on Cross-Linked C- GAG Matrices. | 92 |
| Figure 2.3: Fibroblast-Mediated Contraction of C-GAG Matrices by Superficial and Deep Dermal Fibroblasts. | 93 |
| Figure 2.4A-B: Biomechanical Properties of C-GAG Matrices with Superficial and Deep Dermal Fibroblasts. | 95 |
| Figure 2.4C: Biomechanical Properties of C-GAG Matrices with Superficial and Deep Dermal Fibroblasts. | 97 |
| Figure 2.5A-B: Measurement of Collagen Production by Superficial and Deep Dermal Fibroblasts | 98 |
| Figure 2.6A: Hematoxylin & Eosin Staining of the Matrices for Collagen Content. | 100 |
| Figure 2.6B: Hematoxylin & Eosin Staining of the Matrices for Collagen Content. | 101 |
| Figure 2.7: Immunohistochemical Analysis of α -SMA Expression. | 102 |
| Figure 2.8A-B: Assessment of Relative Gene Expression of Superficial and Deep Dermal Fibroblasts Cultured on C-GAG Matrices by qRT-PCR..... | 103 |
| Figure 2.8C-D: Assessment of Relative Gene Expression of Superficial and Deep Dermal Fibroblasts Cultured on C-GAG Matrices by qRT-PCR..... | 105 |
| Figure 2.9A-B: Analysis of Protein Expression by Superficial and Deep Dermal Fibroblasts Cultured on C-GAG Matrices..... | 107 |

| | |
|--|-----|
| Figure 3.1: Viability of SF and DF Cultured with or without K on C-GAG Matrices. | 140 |
| Figure 3.2A: Immunofluorescent Staining of the Epidermis Formed in Tissue Engineered Skin..... | 141 |
| Figure 3.2B: Immunofluorescent Staining of the Epidermis Formed in Tissue Engineered Skin..... | 142 |
| Figure 3.3: Assessment of Relative Gene Expression of Epidermal Proteins in Tissue Engineered Skin by qRT-PCR. | 143 |
| Figure 3.4A: Immunofluorescent Staining of the Basement Membrane Formed in Tissue Engineered Skin. | 145 |
| Figure 3.4B: Immunofluorescent Staining of the Basement Membrane Formed in Tissue Engineered Skin. | 146 |
| Figure 3.5A-B: Assessment of Relative Gene Expression of Basement Membrane Proteins in Tissue Engineered Skin by qRT-PCR. | 147 |
| Figure 3.5C-D: Assessment of Relative Gene Expression of Basement Membrane Proteins in Tissue Engineered Skin by qRT-PCR. | 149 |
| Figure 3.6: Assessment of Relative Gene Expression of Basement Membrane Proteoglycans in Tissue Engineered Skin by qRT-PCR..... | 151 |
| Figure 3.7: Surface Electrical Capacitance (SEC) Measurements of Tissue Engineered Skin..... | 153 |
| Figure 4.1: Contraction of Tissue Engineered Skin made of SF or DF and K. ... | 184 |
| Figure 4.2: Measurement of Collagen Production for Tissue Engineered Skin made of SF or DF and K. | 186 |
| Figure 4.3A-B: Assessment of Relative Gene Expression of Fibrotic Marker Proteins for Tissue Engineered Skin made of SF or DF and K. | 188 |
| Figure 4.3C: Assessment of Relative Gene Expression of Fibrotic Marker Proteins for Tissue Engineered Skin made of SF or DF and K. | 190 |
| Figure 4.4A-B: Assessment of Relative Gene Expression of Proteoglycans for Tissue Engineered Skin made of SF or DF and K. | 192 |

| | |
|---|-----|
| Figure 4.4C: Assessment of Relative Gene Expression of Proteoglycans for Tissue Engineered Skin made of SF or DF and K..... | 194 |
| Figure 4.5A: Assessment of Myofibroblast Differentiation for Tissue Engineered Skin made of SF or DF and K. | 195 |
| Figure 4.5B: Assessment of Myofibroblast Differentiation for Tissue Engineered Skin made of SF or DF and K. | 196 |
| Figure 4.6: Analysis of Latent and Total TGF- β 1 Expression for Tissue Engineered Skin made of SF or DF and K. | 197 |

List of Symbols and Abbreviations

| | |
|--------------------|---------------------------------|
| α | Alpha |
| β | Beta |
| Δ | Delta; or deletion |
| γ | Gamma |
| λ | Lambda |
| μ | Micro |
| μg | Microgram(s) |
| μL | Microlitre(s) |
| μM | Micromole(s) per litre |
| 3D | Three-dimensional |
| ANG-II | Angiotensin |
| bFGF | Basic fibroblast growth factor |
| BSA | Bovine serum albumin |
| $^{\circ}\text{C}$ | Degree(s) Celsius |
| cm | Centimetre(s) |
| C-GAG | Collagen-glycosaminoglycan |
| CSS | Cultured skin substitutes |
| CT | Cycle threshold |
| CTGF | Connective tissue growth factor |
| DCN | Decorin |
| DF | Deep dermal fibroblasts |
| DHT | Dehydrothermal |

| | |
|--------|--|
| DMEM | Dulbecco's modified eagle medium |
| DMSO | Dimethyl sulfoxide |
| dNTP | Deoxynucleoside triphosphates |
| EB | Epidermolysis bullosa |
| ECM | Extracellular matrix |
| EDTA | Ethylenediaminetetraacetic acid |
| EGF | Epidermal growth factor |
| ELISA | Enzyme-linked immunosorbent assay |
| FBS | Fetal bovine serum |
| FIN | Fibronectin |
| FMOD | Fibromodulin |
| g | Gram(s); or gravity |
| GAGs | Glycosaminoglycans |
| GM-CSF | Granulocyte-macrophage colony-stimulating factor |
| h | Hour(s) |
| HCl | Hydrochloric acid |
| H & E | Hematoxylin and eosin |
| HPRT | Hypoxanthineguanine phosphoribosyl transferase |
| HSP | Heat shock protein |
| HTS | Hypertrophic scarring |
| IgG | Immunoglobulin G |
| IL | Interleukin |
| K | Keratinocyte |
| KGF | Keratinocyte growth factor |

| | |
|---------|--|
| L | Litre(s) |
| LC MS | Liquid chromatography mass spectrometry |
| M | Mole(s) per litre |
| mg | Milligram(s) |
| min | Minute(s) |
| mL | Millilitre(s) |
| mm | Millimetre(s) |
| mM | Millimole(s) per litre |
| MMP | Matrix metalloproteinase |
| MTT | 3-[4,5-dimethylthiazol-2-yl]-2,5-diphenyl tetrazolium bromide |
| NHS-EDC | N-hydroxysuccinimide-1-ethyl-3-(3-dimethyl-amino-propylcarbodiimide) |
| N | Normal |
| ng | Nanogram(s) |
| nm | Nanometre(s) |
| OPN | Osteopontin |
| PBS | Phosphate buffered saline |
| PDGF | Platelet-derived growth factor |
| P_F | Final cell population |
| P_I | Initial population |
| PPAR | Peroxisome proliferator-activated receptor |
| PBS | Phosphate buffered saline |
| PCR | Polymerase chain reaction |
| qRT-PCR | Quantitative real time polymerase chain reaction |
| rpm | Revolutions per minute |

| | |
|----------------|---|
| s | Second(s) |
| SEC | Surface electrical capacitance |
| SEM | Scanning electron microscope |
| SF | Superficial dermal fibroblasts |
| SLRPs | Small-leucine rich proteoglycans |
| SMA | Smooth muscle actin |
| | |
| T _m | Melting temperature |
| TBSA | Total body surface area |
| TGF | Transforming growth factor |
| TNF | Tumour necrosis factor |
| | |
| UTS | Ultimate tensile strength |
| | |
| vol | Volume(s) |
| VEGF | Vascular endothelial cell growth factor |
| VER | Versican |

Chapter 1

Introduction

1 Introduction

1.1 Skin

Skin, which is the largest organ of the body, plays a primary role in protecting the body from mechanical damage such as wounding. It comprises of epidermal, dermal and hypodermal layers (Fig.1.1). The barrier function of the skin is provided by its avascular epidermal layer, which is composed mainly of keratinocytes. The keratinocytes form a stratified epithelium, with proliferating basal cells at the innermost layer and the keratinized, relatively impermeable outer stratum corneum layer on the surface (1). Other non-epithelial epidermal cells include melanocytes that provide skin pigmentation; Langerhans cells that are antigen-presenting dendritic cells of immune system; and Merkel cells that are thought to function as mechanoreceptors. The dermal layer, which is the layer below the epidermis, is highly vascular, provides structural integrity and forms the bulk of the skin (1). It is composed of type I collagen with some elastin and glycosaminoglycans (GAGs), which cushion the body against mechanical injury by conferring elasticity and plasticity to the skin. Fibroblasts, the main dermal cell type, produce remodelling enzymes such as proteases and collagenases that play important roles in the wound healing process (2). There are two distinct layers of fibroblasts, the papillary fibroblasts that lie next to the basal epidermal layer and the reticular fibroblasts that lie in the deeper layers of the dermis. The other cells in the dermis include endothelial cells, smooth muscle

cells and mast cells. The dermal cells are embedded on the extracellular matrix (ECM), which serves as a scaffold to bind, integrate and support cells. ECM is a complex mixture of structural and functional proteins arranged in a unique three-dimensional ultrastructure that fills the extracellular space between cells (3, 4). ECM regulates cellular growth via two major classes of macromolecules: the GAGs, which are predominantly linked to proteins to form proteoglycans, and the fibrous proteins (5, 6). The proteoglycans can be either secreted into the extracellular environment as in the case of chondroitin sulphate and hyaluronic acid, or anchored on the plasma membrane as syndecan-1 (4). The fibrous proteins can be structural (collagen type I and elastin), adhesive (fibronectin) or de-adhesive (tenascin-C and thrombospondin) in nature (7). The ECM of basement membrane present immediately beneath epithelial cells comprises of distinctly different collections of collagenous and non-collagenous proteins including laminin, collagen type IV and entactin (8, 9). The third layer of skin, the hypodermis, contains adipose tissue that is well vascularized and contributes to both thermoregulatory and mechanical properties (1). The integrity of the three layers of skin is critical for maintenance and the proper functioning of the skin as well as survival.

1.1.1 Skin Injury from Burns

Human skin performs a wide range of functions including perception, regulation of water and temperature loss, and importantly provides a protective

barrier that is most critical for our survival. When the skin is compromised during injury as in the case of acute burn wounds or chronic wounds such as pressure and leg ulcers, the skin needs immediate coverage so as to facilitate regeneration and repair. Burn wounds are caused by damage to the skin due to heat, chemicals, electricity or radiation. Burns that result in damage to the epidermal, dermal (papillary and reticular) and hypodermal layers of the skin are referred to as first, second and third degree burns, respectively. Second and third degree burns cause fluid loss, drastic disturbances of ionic equilibrium, loss of temperature control, pain, immunosuppression, bacterial invasion and in some cases substantial or permanent disability. The annual incidence of serious burns in the United States is estimated at 70,000 with the direct cost of burn dressings alone estimated to be over \$5 billion per year (10).

The most common treatment for patients with burns and other skin wounds is the use of skin grafts. In the case of severe burn injuries, permanent wound closure currently requires grafting of autologous epithelium, wherein an area of suitable skin is separated from the tissue bed and transplanted to the recipient area on the same individual from which it should receive new blood supply. The autografts may be full-thickness, wherein a complete section of the epidermis and dermis is transplanted, or split-thickness where only part of the dermis is used (11). Use of split-thickness skin autografts is the gold standard for restoration of epidermal function of the skin in burn patients (12). However, the difficulty in the treatment of patients with extensive and deep burns is the

limited availability of sufficient donor sites for autografting. In addition, autografting generates donor sites which are not only painful during healing, but may also scar and become a cause of long-term morbidity (13). The other grafting procedures besides autografting include syngeneic, allogeneic and xenogeneic skin grafts. Syngeneic grafting is performed between genetically identical individuals such as monozygotic twins, and is taken equally well as autografts. Allogeneic grafting involves skin transplantation from non-genetically identical individuals of the same species or cadaver skin, whereas xenogeneic grafting involves transfer of skin between species. These grafts serve only as temporary treatments for full thickness burns since they require resurfacing with an autogenous epidermal layer because of immunologic rejection. Also, as opposed to autografts, both allografts and xenografts are often rejected since the antigens present in the donor tissue elicit host immune response (14). Overall, there are several limitations associated with the use of different types of grafts for treatment of patients with extensive skin loss; hence, there is an immense need to develop alternative therapeutic options.

1.1.2 Tissue Engineering of Skin

Tissue engineering was originally described by Langer and Vacanti as an interdisciplinary field that applies the principles of engineering and life sciences toward the development of biological substitutes that restore, maintain, or improve tissue function (15). Recently, it has been further defined as a field that

understands and applies the principles of tissue growth to produce functional replacement tissue for clinical use (16). Tissue engineering of skin was initially developed in the 1980s, with the primary motivation of providing coverage for extensive burn injuries in patients with insufficient sources of autologous skin for grafting. Tissue engineered skin products or skin substitutes can be cells delivered on their own, cells delivered within biomaterials, biomaterials used for replacement of dermis (with or without cells) or biomaterials used for replacement of both epidermis and dermis.

1.1.3 Wound Healing and Fibrosis

Wound healing following burns or other injuries occurs by either regeneration or fibrosis (17). Regeneration recapitulates the developmental processes that originally created the uninjured tissue, and reinstates the native tissue architecture, while fibrosis causes growth of connective tissue instead of the characteristic parenchymal tissue, resulting in the formation of dysfunctional and distorted tissue, commonly known as scar (17). In humans, wound healing by regeneration is typical during prenatal development, but this ability is retained only to a limited extent during adulthood and therefore adult wounds often heal by fibrosis. Fibrotic conditions affect most organs and may cause either cosmetic and functional problems as seen in skin fibroproliferative disorders [hypertrophic scars and keloids] or organ failure as in idiopathic pulmonary fibrosis, liver cirrhosis, cardiovascular fibrosis, systemic sclerosis, and renal fibrosis. Chronic

fibrotic diseases are a leading cause of morbidity and mortality worldwide with current health statistical estimates of 45% of all deaths in the developed world (18). Currently there are no clinically effective treatments for fibrotic diseases, thus there is an immediate need to develop innovative anti-fibrotic therapies.

In normal skin, a fine balance between synthesis and degradation of collagen, the main component of the ECM, helps maintain physiological homeostasis. However during wound healing, the equilibrium is shifted towards accelerated collagen synthesis to aid tissue repair. In the case of fibrosis, collagen homeostasis is not restored at the culmination of the wound healing process, which results in excessive accumulation of collagen, patches of fibroblasts, hypercellularity, and a disorganized ECM. Fibrosis could lead to loss of proper function of the associated organ, and can be either local (hypertrophic scars and keloids) or systemic (systemic sclerosis) (18). Hypertrophic scars, which are characterized by erythematous, raised, pruritic lesions of the healing skin, cause cosmetic and functional problems like colour mismatch, stiffness, and rough texture, in addition to itching and pain (19). Liver fibrosis interferes with drug metabolism causing accumulation of toxic metabolites, and lung fibrosis causes poor blood-gas exchange resulting in hypoxia (20). In all, fibrosis has a significant impact on the outcome of wound healing and could impose increased health-care costs.

When the integrity of skin is compromised a cascade of events including formation of granulation tissue, re-epithelialization, and contraction of the

underlying connective tissue is triggered, all of which ultimately lead to wound repair. The orchestrated tissue repair event is accompanied by recruitment of inflammatory cells to the wound site to fight possible infection. Fibrosis occurs as an aftermath of this inflammatory and connective tissue repair response to facilitate physiological repair of the body. It can be triggered by a variety of stimuli including persistent infections, autoimmune reactions, chemical insults, and tissue injury due to burns or other causes (18). The key cellular mediator of fibrosis, myofibroblast, exhibits characteristics of both fibroblasts and smooth muscle cells. Myofibroblasts can be derived from resident mesenchymal cells, epithelial and endothelial cells, or fibrocytes (18). They can be activated by a variety of mechanisms including Transforming Growth Factor (TGF)- β 1, the most extensively studied pro-fibrotic cytokine or its downstream mediator, Connective Tissue Growth Factor (CTGF) and other autocrine factors, paracrine signals derived from lymphocytes and macrophages, and molecular patterns produced by pathogens (PAMPs) (18). They are highly contractile in nature, and generate connective tissue contracture and irreversible ECM remodelling producing stiff scars. Wound healing strategies aimed at modifying the local micro-environment from pro-fibrotic to anti-fibrotic may enable us to reduce myofibroblast-mediated fibrotic remodelling and achieve regenerative wound healing.

1.2 Skin Substitutes

Skin substitutes are artificial skin replacement products that provide the protective barrier of the skin when placed over acute burn injuries or other chronic skin wounds such as cutaneous ulcers and congenital anomalies such as giant nevus (11, 21-24). Their primary objective is to work as skin equivalents, facilitate repair and regeneration, and restore the functional properties of skin. Several skin substitutes have been useful for replacement or reconstruction of one or both layers of the skin, facilitating wound healing in several different clinical settings. These skin substitutes can act as temporary wound covers or permanent skin replacements, depending on their design and composition. They reduce or remove inhibitory factors, and help in providing rapid and safe coverage. The main advantage of using skin substitutes is that they reduce or eliminate the need for donor site area, which is required for autologous split-thickness grafts. This makes skin replacement procedures available to patients contraindicated for autologous grafts such as those with over 60% of total body surface area (TBSA) burned, smoke inhalation injured, and the very young and elderly. Skin substitutes also decrease the patients' risk of infection and sepsis especially at the thin dermis of the donor site (11, 21, 24). They pose negligible risk of cross-infection, which is not the case with allografts and xenografts. Furthermore, skin substitutes reduce mortality and morbidity from scarring (both at donor and treatment sites), changes in pigmentation and patients' burden of

pain. More importantly, they may reduce the total number of surgical procedures required and patient hospitalization time (22, 23).

1.2.1 Features of Skin Substitutes

Some of the essential features of a skin substitute are that it should be sterile, provide barrier function, allow water vapor transmission similar to normal skin, evoke minimal inflammatory response in the patient, and also have no local or systemic toxicity (24). Some of the other features of a good skin substitute are that it should adhere to the wound surface in a rapid and sustained manner, have appropriate physical and mechanical properties, and undergo controlled degradation (24). It should be relatively inexpensive, easy to handle and apply onto wound sites, and also be flexible and pliable so that it could conform to irregular wound surfaces. Additionally, it should be impermeable to exogenous bacteria, resistant to linear and shear stresses, and have minimal storage requirements and an indefinite shelf life. Importantly, it should incorporate into the patient with minimal scarring and also facilitate angiogenesis (1).

1.2.2 Types of Skin Substitutes

Skin substitutes differ in complexity and can be broadly classified into two types: synthetic, which is made up of acellular materials, and natural, which is made up of cellular materials. The synthetic skin substitutes are most basic and

designed to function primarily as barriers to fluid loss and microbial contamination. The natural skin substitutes are more advanced in nature and are cultured allogeneic or autologous cell suspensions or sheets used alone or along with a dermal matrix. Alternatively, skin substitutes can also be classified into three types: those that consist of cultured epidermal cells with no dermal components, those with only dermal components, and those with a bilayer containing both dermal and epidermal components. Although each of these have their own advantages and have applications in burn treatment, none of them are ideal in all situations.

1.2.3 Commercially Available Skin Substitutes

Some of the commercially available skin substitutes that are often used in the treatment of burn injuries and chronic wounds are discussed below in detail (also see Table. 1.1). Among the synthetic acellular skin substitutes, Biobrane™, Integra™, Alloderm™ and TransCyte™ are most commonly used. Examples of frequently used natural skin substitutes with allogeneic cells include Dermagraft™, Apligraf™ and OrCel™, while those with autologous cells include Epicel™.

Biobrane™ is composed of an outer ultrathin silicone film (epidermal analog) and an inner three-dimensional irregular nylon filament (dermal analog) upon which type I collagen peptides are bonded (23). The semi-permeable silicone surface controls water vapour loss from the wound. Biobrane™ is used

as a temporary wound dressing and is removed upon wound healing or when autograft skin is available. It has been shown to be as effective as frozen human allografts and contributes to better healing, when used on excised full-thickness burns (23). In addition, Biobrane™ has been shown to reduce hospitalization time in the case of paediatric patients with second degree burn injuries.

Integra™ Dermal Regeneration Template is composed of a dermal layer made of porous bovine collagen and chondroitin-6-sulfate GAG, and an epidermal layer made of synthetic silicone polymer (25). The silicone layer provides a functional barrier that is removed upon vascularization of the dermis, and replaced by a thin layer of autograft, while the dermal layer serves as a matrix for infiltration of fibroblasts and other cells from the wound bed. As the collagen-GAG matrix is populated by these cells, it is gradually degraded and replaced by newly synthesized collagen. Integra™ is widely used for the coverage of excised burn wounds, particularly in patients with large burns and limited autograft donor sites (25).

Alloderm™, similar to Integra provides a matrix for dermal tissue remodelling (26). It is composed of human allograft skin (cadaver skin) that has been screened for transmissible pathogens and processed to remove epidermal components and all dermal cells. The dermal cells are removed by detergent treatment followed by freeze drying, which preserves the matrix in a structural form similar to that of normal human dermis. A positive aspect of Alloderm™ is that it can be grafted like a dermal autograft and subsequently covered with a

thin autograft. Also, since the allogeneic cells have been removed, it is not rejected by the immune system, which aids the regeneration of the underlying dermis. Alloderm™ has been successfully used in the resurfacing of full-thickness burn wounds in combination with an ultra-thin autograft which replaces the epidermis (1). Preclinical studies have shown that Alloderm™ can be used for the repair of soft tissue defects such as in the case of abdominal wall reconstruction (27). In addition to Alloderm™, other allogeneic skin substitutes are available as temporary wound covers, but they differ in matrix material composition and presence or absence of cells.

TransCyte™ is similar in composition to Biobrane™, and is used as a temporary cover for excised burns that await placement of autografts (28). It consists of a nylon mesh seeded with fibroblasts cultured from neonatal human foreskin, which secrete extracellular matrix components and growth factors that aid the healing process. To reduce host immune response, before grafting, the fibroblasts are destroyed by a freezing process that preserves the tissue matrix and growth factors, and hence TransCyte™ has a possible benefit for wound healing over other strictly synthetic skin substitutes (28).

Dermagraft™ is prepared using human neonatal fibroblasts similar to TransCyte™, however the fibroblasts are cryopreserved to maintain cell viability and the matrix is made of bioabsorbable polygalactin mesh (23). Dermagraft™ is used in the treatment of full-thickness foot ulcers, and functions by providing a

dermal matrix that facilitates re-epithelialization by the patient's own keratinocytes (23).

ApligrafTM is more advanced than TransCyteTM since it contains both fibroblasts and keratinocytes that are derived from neonatal foreskins (23). A gel made of bovine collagen is used as the matrix for cell growth and differentiation. ApligrafTM has been useful in the treatment of venous leg ulcers and diabetic foot ulcers, by increasing the percentage of wounds healed and decreasing time required for wound closure (29). Also, studies have reported the use of ApligrafTM for treatment of pediatric patients with various forms of epidermolysis bullosa, wherein no acute rejection reactions were observed but rather faster and less painful healing was noted compared to standard dressings (30, 31).

OrCelTM is similar to ApligrafTM since it contains both fibroblasts and keratinocytes derived from neonatal foreskin, but uses a type I collagen sponge as the matrix (32). It is used for grafting onto partial-thickness wounds, where it provides a favourable matrix for host cell migration. In a study that directly compared OrCelTM with Biobrane for the treatment of split-thickness donor site wounds, the OrCelTM-treated sites had faster rates of healing and reduced scarring (32). The improved healing was attributed to the presence of the collagen sponge, in combination with cytokines and growth factors produced by the viable allogeneic cells.

EpicelTM, also known as cultured epidermal autografts, was the first commercially available autologous skin substitute. The ability to expand

epidermal cells *in vitro* and produce autologous cultured epithelium was an important breakthrough in burn therapy (33), which led to the development of Epicel™. Epicel™ consists of sheets of autologous keratinocytes attached to a petrolatum gauze support, which is removed approximately 1 week after grafting (34). It is used on patients with full-thickness burns covering greater than 30% TBSA and on patients with giant congenital nevus. Epicel™ is extremely valuable in patients with very large (>60% TBSA) burns where the donor site availability and quality is poor. In a study involving 30 extensively burned patients, Epicel™ was observed to provide permanent coverage of a mean TBSA of 26%, which represented a relatively high average take rate of approximately 69% of the area treated (34). In another clinical study involving 28 patients with a mean TBSA of 52.2% and a mean total full thickness injury of 42.4% treated over a period of 5 years, Epicel™ had a mean take rate of 26.9% of the grafted area (35). In these patients, overall mortality, hospitalization time and number of autograft harvests were not significantly different compared to a matched control population when Epicel™ was not available, suggesting that Epicel™ is likely more useful as a temporary wound dressing. Some of the other disadvantages associated with Epicel™ are its mechanical fragility, especially during the period of maturation of the dermal-epidermal junction, hyperkeratosis, contracture and scarring.

1.2.4 Limitations of Commercially Available Skin Substitutes

The commercially available skin substitutes have several limitations such as reduced vascularization, scarring, failure to integrate, poor mechanical integrity and immune rejection (24). Skin substitutes when placed on wounds need to acquire blood supply rapidly for their long-term survival and integration into host tissue. Their inability to revascularize rapidly results in cell death and ultimate sloughing away from the host. Although some of the commercially available skin substitutes allow angiogenesis, the extent of vascularization is generally insufficient and needs to be further improved. Another important limitation is the development of scars at the graft margins after grafting, which results in a variety of functional, mechanical and aesthetic problems. Scar tissue is inferior in functional quality compared to native skin since it is less resistant to ultraviolet radiation, and does not grow back sweat glands and hair follicles unlike full thickness autografts. Furthermore, the costs associated with the use of the current skin substitutes is very high; for example, it is estimated that the cost for each 1% body surface area covered with Epicel™ is more than \$13,000 (36). These types of skin substitutes because they contain cells of allogenic origin, also pose the risk of allosensitization of the host which to date is under-recognized and its importance remains unclear.

1.3 Cultured Skin Substitutes

The commercially available skin substitutes do not provide for both the epidermal and dermal layers of the skin when placed on burn wounds. An exception to this is Epicel, a cultured epidermal autograft, which reconstructs the epidermis but does not provide for the dermis. Since the current skin substitutes do not aid the development of underlying connective tissues, the newly-formed skin lacks elasticity and mechanical stability (37). Studies have shown that replacement of connective tissue aids healing of excised full thickness burns (38). The fibrovascular connective tissue not only restores mechanical strength of the epidermis but also provides blood supply that nourishes it. Hence, repopulating the wound area with fibroblasts, endothelial and smooth muscle cells that form the connective tissue would facilitate formation of native-like skin. Cultured skin substitutes (CSS) are a promising alternative to conventional skin substitutes since they contain autologous fibroblasts and keratinocytes cultured on a scaffold. It is prepared using patient-derived fibroblasts and keratinocytes that are isolated from a split-thickness skin biopsy. CSS have been shown to effectively close full-thickness burn wounds since they provide both epidermal and dermal components that are required to achieve functional wound closure (23). Further, clinical results have shown permanent replacement of both dermal and epidermal layers in a single grafting procedure (22, 39-41). Also, CSS has been effective in treating burns of greater than 50% TBSA and giant congenital

nevi in clinical studies (22, 41, 42). The various components of CSS are discussed in detail below.

1.3.1 Scaffold

Scaffold is a three-dimensional exogenous ECM that functions analogous to native ECM of dermis, serving not only as a physical support structure but also as an insoluble regulator of biological activity thereby affecting processes such as cell migration, contraction, and cell division. ECM of native skin physically supports cells, gives tensile strength and provides a substrate for cell adhesion and migration (43). It contains a variety of growth factors including basic fibroblast growth factor (bFGF), vascular endothelial cell growth factor (VEGF), and epidermal growth factor (EGF). It affects local concentrations and biological activity of the different growth factors and cytokines by presenting them efficiently to cell surface receptors, protecting them from degradation, and modulating their synthesis (44, 45). Since ECM serves as a reservoir of growth factors and chemical cues, it contributes to regulation of diverse processes such as cell differentiation, proliferation and migration, angiogenesis and vasculogenesis, inflammation, immune responsiveness and wound healing (5, 6). ECM of skin is dynamic and plays an indispensable role in skin morphogenesis, maintenance, and reconstruction following injury, which makes it an ideal scaffold for skin repair and reconstruction (3, 46). Tissue engineering for skin regeneration and repair typically employs exogenous three-dimensional ECMs as

the scaffold to obtain new native skin from natural cells (47). The exogenous ECM mimics the native ECM and brings the desired cell types into contact in an appropriate three dimensional environment, and in addition provides mechanical support until the newly formed skin is structurally stable and specific signals begin to guide gene expression and function (48, 49). The three types of biomaterials used for preparation of scaffolds include organic polymers, inorganic materials and synthetic polymers. Organic polymers such as collagen-GAG are the most commonly used scaffolds in CSS, and are discussed in detail below.

1.3.1.1 Collagen

Collagen plays a dominant role in maintaining the biological and structural integrity of ECM and is highly dynamic, undergoing constant remodeling for proper physiological functions (43). Collagen has a distinct super-coiled triple-helical structure with three individual left handed helices wound together to form a right handed rope-like structure (50). As a result of this structure, collagen exhibits the characteristic $(\text{Gly-Xaa-Yaa})_n$ repeating sequence, wherein Yaa position is frequently occupied by 4-hydroxyproline, which stabilizes the triple-helix and contributes to the overall stability of mammalian collagen at body temperature (51). Type I collagen is the most abundant collagen that forms major tissue structures through fiber bundle networks, which are stabilized by cross-links (52). 70 to 80% of the dry weight of the dermis is mainly type I collagen which exists in the form of loosely interwoven, large, randomly oriented

bundles, each containing closely packed collagen (53, 54). Collagen types III and V have also been detected in the dermis and are primarily responsible for tensile strength. The dermal layer collagen network also contributes to the stability of the epidermis (43). In addition to providing structural stability, collagen plays an important role in the numerous interactions between cells and other molecules (52). For the preparation of scaffolds used in CSS, bovine type I collagen is commonly used since it can be readily prepared in pure form in large quantities, and also it possesses desirable hemostatic properties, low antigenicity and appropriate mechanical characteristics (55).

1.3.1.2 Glycosaminoglycans (GAGs)

GAGs are present in ECM and on cell surfaces in the form of proteoglycans. They bind a variety of proteins in the ECM and basement membrane such as fibronectin, laminin and collagen, and promote low affinity interactions with integrins (56). They also bind water and participate indirectly in collagen fibril organization. They modulate various enzymes, proteases and their inhibitors as well as cytokines. In addition, they function as co-receptors for many growth factors including FGFs and VEGF (57). Hence, GAGs play a pivotal role in the processes of cell adhesion, migration, proliferation and differentiation. Due to their significant role in skin morphogenesis and wound healing, they are often used in CSS, and the most commonly used GAG is chondroitin-6-sulphate derived from shark cartilage.

1.3.2 Design Specifications for Collagen-GAG Scaffolds

To design bioactive collagen-GAG scaffolds the following physical and structural properties need to be considered. The periodic banding of collagen fiber structure has to be selectively abolished to prevent platelet aggregation and immune response. The mean pore size of the scaffold should be within lower and upper limits. The pores need to be large enough to allow cells to migrate into it but small enough to establish a high specific surface for minimal ligand density that is required for efficient binding of a critical number of cells to the scaffold (55). Collagen-GAG scaffolds with mean pore size lower than 20 μm or higher than 120 μm have been observed to be inactive (58). The mean pore size has been shown to significantly influence cell morphology and phenotypic expression (59). Pore structure has also been observed to significantly affect cell binding and migration *in vitro*, and influence the rate and depth of cellular in-growth *in vitro* and *in vivo* (60). Cell adhesion and activity have been reported to vary considerably with scaffold composition and pore size (61). Further, the rate of degradation of the scaffold should be such that it remains insoluble for the required period of time so as to facilitate repair and regeneration (58). Lastly, the scaffolds must be non-immunogenic and free from infectious material such as prions.

1.3.3 Advantages of Using Collagen-GAG Scaffolds

The attractiveness of using collagen-GAG scaffolds for skin tissue engineering stems from the fact that collagen-GAG when used together induce more native ECM-like composition in the engineered skin than when collagen is used alone, possibly through its interactions with various growth factors (62). Collagen-GAG was also observed to increase skin growth and regeneration compared to use of collagen alone. The addition of GAG to collagen scaffold does not alter morphology, mean tensile strength, or degradation of the scaffold *in vitro* (63, 64), but *in vivo* it was observed to delay scaffold degradation, which indicates interaction between GAG and cells (65). Collagen-GAG scaffolds induce cells to retain around 60% of newly synthesized proteoglycans within the scaffold compared to only 40% of proteoglycans retained in monolayer cultures (66). The proteoglycan aggregates in the scaffold have more GAG chains compared to monolayer cultures, and hence can entrap greater volumes of water that lead to increased compressive and viscoelastic properties of the scaffold. Collagen-GAG scaffolds can be easily used in skin tissue engineering as they can be sterilized using heat or chemical procedures and manufactured with a variety of pore sizes and degradation rates (67).

1.3.4 Cells

The fundamental basis for the development of CSS for skin repair and regeneration is our ability to rapidly grow and expand cells selectively in culture. In culture, cell populations increase exponentially according to the function $(P_I)(2^n) = (P_F)$, where P_I is the initial population, n is the number of population doublings, and P_F is the final cell population. So with an approximate doubling time of 1 day or less, it is possible to generate very large populations of keratinocytes and fibroblasts within 2-3 weeks of cell culture.

1.3.4.1 Fibroblasts

Dermal fibroblasts are a heterogeneous population of cells of mesenchymal origin that synthesize and deposit ECM proteins and cytokines in a characteristic manner (68). They play an important paracrine role and produce various growth factors including members of the VEGF family, VEGF-A, -B, -C and -D, which regulate vascular and lymphatic endothelial cell proliferation (69). VEGF-A activates resident endothelial cells and endothelial progenitor cells that are capable of vasculogenesis; VEGF-B is less mitogenic for endothelial cells, while VEGF-C and -D mediate angiogenesis and lymphangiogenesis, respectively (69). Fibroblasts also contribute to the formation of basement membrane by producing collagen IV, collagen VII, laminin 5, nidogen, and cytokines that stimulate keratinocytes to produce basement membrane components (70). Fibroblasts proliferate and migrate in response to chemotactic, mitogenic and

modulatory cytokines (71). The characteristics of fibroblasts in culture and its growth curve are affected by passage number, age of donor and dermal layer subtype (reticular or papillary dermis) from which they were obtained. As opposed to younger donor skin derived fibroblasts, older donor skin fibroblasts tend to migrate more slowly, reach cell culture senescence earlier and have a prolonged cell population doubling time (72, 73). Also, fibroblasts from older donors are generally less responsive to growth factors such as platelet-derived growth factor (PDGF), EGF, dexamethasone, insulin and transferrin *in vitro* (72). Other factors that influence fibroblast behaviour in culture include antioxidants, such as vitamin C and coenzyme Q10. Irrespective of age of cells, fibroblasts treated with vitamin C ($100 \mu\text{mol L}^{-1}$) were observed to produce two-fold more collagen compared to those cultured without (72). Similarly, fibroblasts cultured with coenzyme Q10 were observed to have enhanced cell mobility and proliferation that subsequently led to increased wound healing (74).

1.3.4.1.1 Heterogeneity of dermal fibroblasts

Dermal fibroblasts are heterogeneous in nature and based on their location in the dermis are classified as superficial and deep dermal fibroblasts and hair follicle fibroblasts (Fig. 1.2). Superficial and deep dermal fibroblasts reside in the papillary and reticular dermis, respectively, whereas hair follicle fibroblasts are present in the dermal papilla region of the hair follicle and along its shaft. Fibroblasts belonging to each of these categories show different

characteristics in culture. Depending on age and anatomical location the papillary dermis is generally approximately 300-400 μm deep and extends till the rete subpapillare, the vascular plexus that marks the lower limit of the papillary dermis. The reticular dermis extends from the rete subpapillare to the rete cutaneum, a deeper vascular plexus that demarcates the dermis and the hypodermis. Superficial fibroblasts can be isolated and cultured from skin dermatomed at a depth of 0.3 mm whereas deep fibroblasts are isolated from dermal tissue below 0.7 mm depth. There are a variety of physical and biochemical differences between superficial and deep dermal fibroblasts. Compared to superficial dermal fibroblasts, deep fibroblasts are larger, they proliferate slower in culture, produce more TGF- β 1 and collagen type I but less collagenase. Deep fibroblasts also express less decorin and differentiate more into myofibroblasts. Superficial dermal fibroblasts were observed to be anti-fibrotic and behave similar to normal dermal fibroblasts, whereas deep fibroblasts were pro-fibrotic and behaved similar to hypertrophic scar fibroblasts (75). Differences between superficial and deep fibroblasts are discussed in further detail in subsequent chapters. Clinically, superficial wounds generally heal with minimum scarring, while deep wounds lead to formation of hypertrophic scars and contractures (76, 77). So, developing a better understanding of cellular and biochemical differences between superficial and deep dermal fibroblasts will enable us to gain further insight about wound repair and regeneration and

facilitate development of better therapeutics for hypertrophic scars and other fibrotic diseases.

1.3.4.2 Keratinocytes

Keratinocytes, which form the bulk of epidermis, initially exist as proliferation-competent basal layer cells that express characteristic basal-cell-associated marker proteins. These cells subsequently give rise to daughter cells that terminally differentiate and produce stacks of multiple keratinocyte layers above basal layer and form spinous, granular and cornified layers (78). During differentiation, keratinocytes in the epidermis and as well as those in culture were observed to enlarge, flatten and ultimately get released from the epithelial surface (78, 79). The principal marker for keratinocyte differentiation is the expression of keratins; proliferative basal keratinocytes express K5 and K14 keratins, whereas keratinocytes in early stages of differentiation express K1 and K10 (78). Keratinocytes produce a variety of growth factors such as transforming growth factor (TGF)- α , EGF and PDGF that not only stimulate fibroblasts but also keratinocytes themselves (80). TGF- α has an autocrine effect on keratinocytes during wound healing, and was identified in wound fluid from rats and humans. EGF has also been detected in wound fluid of paediatric burn patients and in migrating keratinocytes in a mouse burn wound model. Keratinocyte-specific inactivation of *egf* gene resulted in delayed epithelial closure in mice suggesting that EGF contributes to epithelialization by accelerating keratinocyte migration

(80). PDGF is released immediately after wounding by degranulating platelets, and is reported to signal in a paracrine manner from the epidermis to mesenchymal cells and in an autocrine manner in the granulation tissue. During culture of keratinocytes in the preparation CSS, a significant increase in their proliferation rate compared to native skin is observed (10). After confluence is achieved, the proliferation rate decreases sharply but remains greater than that of native skin. Due to finite life span of keratinocytes, their proliferation rates slowly decline to zero if the CSS remain in culture for extended periods of time. However, when grafted to wound sites keratinocytes become hyperproliferative during the wound healing process, and subsequently their proliferation rate decreases to that of native skin as the wound heals. The relative rates of proliferation of keratinocytes during preparation and grafting of CSS is shown in Fig. 1.3.

1.4 Preparation of CSS

The preparation of CSS involves fabrication of collagen-GAG scaffolds and co-culture of fibroblasts and keratinocytes on the scaffolds. A schematic representation of the preparation of CSS is shown in Fig. 1.4. Each of the steps involved are discussed in detail below.

1.4.1 Preparation of Collagen-GAG Suspension

Collagen-GAG suspension is made in 0.05 M acetic acid solution (pH 3.2) by combining type I collagen (0.5 wt %) isolated from bovine tendon and chondroitin-6-sulfate (0.05 wt %) isolated from shark cartilage (81). The suspension is mixed at 15,000 rpm using an overhead blender and the temperature of the suspension is maintained at 4°C throughout mixing to prevent heat denaturation of the collagen fibers. The suspension is then degassed under vacuum for 60 min at room temperature to remove air bubbles introduced by mixing and is stored at 4°C. Prior to use, the suspension is degassed again and allowed to equilibrate to room temperature.

1.4.2 Fabrication of Collagen-GAG Scaffolds

The degassed collagen-GAG suspension is poured into a casting apparatus made of steel plates (80 mm x 80 mm) separated by a 0.8 mm silicon gasket and placed into a circulating ethanol bath set at 20°C. The ethanol bath is cooled at a constant rate to the final freezing temperature, at which, it is held constant for 2 h to complete the freezing process. Different final temperatures of freezing (-10°C, -20°C, -30°C and -40°C) can be used to fabricate scaffolds that have a constant relative density of pores and different mean pore sizes. When the aqueous suspension is frozen, it results in a continuous, interpenetrating network of ice crystals surrounded by the collagen-GAG co-precipitate. This precipitate is an ionic complex formed by interaction between the anionic sulfate groups of the

GAG and the amino groups of collagen, which are positively charged at acidic pH. The ice crystals are then sublimated under vacuum at 0°C for 17 hours to produce highly porous collagen-GAG scaffolds, in which pores are defined by the size and shape of individual ice crystals produced during freezing (82). The formation of pores of different sizes is of biological importance since the pores need to be large enough to allow cell migration, and also different cell types have different pore size requirements. Pore volume fraction and mean pore size of the scaffolds can be controlled by modifying the volume fraction of the precipitate and the final freezing temperature, respectively. The formation of ice crystals in the collagen-GAG suspension is influenced by the ice nucleation rate and the rate of heat and protein diffusion, both of which are controlled by the final temperature of freezing and the heat transfer processes associated with freezing. The rate of ice nucleation and diffusion are mediated by the difference between the temperature of freezing and the actual temperature of the material during the freezing process, which is known as undercooling (67, 82). Solidifying the collagen-GAG suspension at a lower final freezing temperature results in larger undercooling, which increases the rate of ice crystal nucleation and the decreases rate of heat and protein diffusion relative to the point of nucleation, leading to formation of smaller ice crystals and resulting in a collagen-GAG scaffold with a smaller mean pore size. The translucent white collagen-GAG scaffolds obtained after the freeze drying process are further modified by cross-linking.

1.4.3 Cross-Linking of Collagen-GAG Scaffolds

The mechanical properties of collagen-GAG scaffolds are of critical importance in order to preserve their structural integrity and functionality for both *in vivo* implantation and long-term performance. Mechanical properties and the rate of degradation of collagen-GAG scaffolds can be improved by increasing the degree of cross-linking between amino acid side chains on collagen fibres (83). The cross-linking process increases the stiffness of collagen fibres by preventing the collagen molecules from sliding past each other under stress. Although many techniques for cross-linking of scaffolds are available, the two most commonly used are physical cross-linking by dehydrothermal (DHT) treatment and chemical cross-linking by N-hydroxysuccinimide -1-ethyl-3-(3-dimethyl amino propylcarbodiimide) (NHS-EDC) process. Both these techniques do not involve cytotoxic agents and hence do not negatively affect the quality of the scaffolds.

1.4.3.1 DHT Treatment

DHT treatment involves physical treatment of collagen-GAG scaffolds wherein they are subjected to 105-140°C under vacuum for 24-72 hours. This facilitates removal of water from the collagen molecules resulting in the formation of intermolecular cross-links through condensation reactions either by esterification or amide formation (84). Since DHT treatment involves the use of high temperatures for long exposure periods it has several advantages. The GAG

chains get grafted to collagen at high temperatures, which prevents them from getting eluted from the scaffold after *in vivo* implantation. It also helps achieve the sterilization of scaffolds (81).

In addition to forming crosslinks, the high temperatures used during DHT treatment denature collagen, wherein the collagen triple helix gets rearranged into a random-chain configuration (85). Although generally denaturation is considered undesirable since it disrupts the native conformation and banding pattern of collagen, denaturation has been shown to reduce the inflammatory response and increase cellular infiltration *in vivo* (86). Also, studies have shown that increasing the DHT treatment temperature and duration improves the mechanical properties of collagen fibers (87). Hence, increased denaturation coupled with improved mechanical properties would enhance the quality of collagen-GAG scaffolds for use in skin tissue engineering.

1.4.3.2 NHS-EDC Process

The NHS-EDC process uses N-hydroxysuccinimide and 1-ethyl-3-(3-dimethyl amino propylcarbodiimide) to cross-link the collagen-GAG scaffolds. Carbodiimides are zero-length cross-linkers that activate the carboxylic acid groups of glutamic or aspartic acid residues to react with amine groups of another chain to form amide bonds. Cross-linking with carbodiimides is attractive for biological applications since the carbodiimide does not remain in the chemical bond but is released as a substituted urea molecule. For cross-linking, the

scaffolds are immersed in a solution containing appropriate molar ratios of NHS and EDC for 30 minutes. EDC catalyzes the formation of collagen-collagen and collagen-GAG cross-links while NHS increases the efficiency of this process. The cross-link density can be modulated by altering the molar ratio of EDC:NHS:COOH, where COOH are the reactive sites on collagen. Higher amount of cross-linking can be achieved by increasing the ratios of EDC and NHS to COOH (83). Concentrations of EDC in the range of 1-5 mM have been observed to improve the biochemical stability of the collagen-GAG scaffold *in vitro*, and promote stable wound closure in nude mice (88, 89).

1.4.4 Culture Conditions

Fibroblasts and keratinocytes used for the preparation of CSS are generally derived from split thickness biopsies (250–300 µm thick) obtained from the patient. The amount of skin sample used for cell culture is based on the surgeon's estimate of the area to be covered by CSS and the number of donor sites available for autografting. The skin samples are treated with dispase to dissociate the dermis and the epidermis. Fibroblasts and keratinocytes are isolated from dermal and epidermal layers respectively. In brief, fibroblasts are isolated by digesting the dermal layer with type 1 collagenase, and cultured in Dulbecco's Modified Eagle Medium (DMEM) with 10% fetal bovine serum (FBS), while keratinocytes are isolated by trypsin-EDTA digestion of epidermal layer and cultured in calcium-free keratinocyte growth medium containing bovine pituitary

extract; both are incubated in a 5% CO₂/95% air atmosphere with saturated humidity at 37°C. After sufficient cell numbers are attained, which is generally after the third passage of cell culture, fibroblasts and keratinocytes are harvested. Fibroblasts are inoculated onto rehydrated collagen-GAG scaffolds at an approximate density of 0.5×10^6 cells/cm² and incubated for at least 18 hours to allow for cell attachment, after which keratinocytes are inoculated on top of these scaffolds at an approximate density of 1×10^6 cells/cm². The scaffolds containing the cells are then cultured for two weeks in a manner such that the keratinocytes are lifted to the air-liquid interface to stimulate formation of epidermal barrier. This method of culturing provides a polarized environment for growth, wherein medium is in contact with the scaffold, and air in contact with the keratinocytes on top (10). The keratinocytes respond to this gradient by orienting proliferating cells towards the medium and cornified cells towards air to establish the morphology of a stratified, squamous epithelium (90). In the meanwhile, fibroblasts fill the collagen-GAG scaffold and start to generate new ECM and as well begin to degrade the supporting scaffold. Basement membrane has also been observed to form at the dermal-epidermal junction in *in vitro* studies (91). After two weeks of culture, the CSS is ready for use.

1.4.5 Advantages of Co-culture of Fibroblasts and Keratinocytes

In CSS, autologous fibroblasts and keratinocytes are cocultured on the collagen-GAG scaffold to enhance wound healing. Dermal fibroblasts are known

to secrete a variety of growth factors and cytokines that have both autocrine and paracrine effects. The autocrine effects are due to transforming growth factor (TGF)- β -induced synthesis and secretion of connective tissue growth factor, which promotes collagen synthesis as well as fibroblast proliferation (92). On the other hand, the paracrine effects include keratinocyte growth and differentiation, specifically through secretion of keratinocyte growth factor (KGF), granulocyte-macrophage colony-stimulating factor, interleukin (IL)-6 and FGF-10. In response to this, keratinocytes synthesize IL-1 and parathyroid hormone-related peptide, which in turn, stimulate fibroblasts to produce KGF giving rise to a double paracrine loop (93). The keratinocytes show a relatively weak IL-1 expression when cultured alone; however when cocultured with fibroblasts, they show significantly increased expression of IL-1 and c-Jun (94). In vitro studies have shown that fibroblasts secrete soluble factors that diffuse to epidermis and influence keratinocytes (94, 95). Interestingly, dermal fibroblast heterogeneity has an effect on fibroblast-keratinocyte interactions; tissue culture plate insert co-cultures of superficial fibroblasts and keratinocytes were found to release higher levels of GM-CSF, KGF and IL-6 and form a continuous basement membrane compared to deep fibroblasts co-cultured with keratinocytes (96). Keratinocytes in monolayer cultures produce only a thin epidermal layer, and in the absence of fibroblasts undergo apoptosis after two weeks in culture. The effect of fibroblasts on growth of epidermis was investigated by seeding keratinocytes on fibroblast-embedded collagen gels, which were then submerged

in medium for several days to reach confluency, followed by culture at the air-liquid interface for two weeks. It was observed that dermal fibroblasts promoted keratinocyte proliferation and development of identifiable keratinocyte layers such as basal, prickle, granular and cornified layers (95). In all, these observations indicate that it is advantageous to co-culture fibroblasts and keratinocytes in CSS, since the paracrine interactions between keratinocytes and fibroblasts stimulate mechanisms of wound healing after application of CSS (10), and thereby enhance skin repair and regeneration.

1.5 Advantages of CSS

The main advantage of using CSS for treatment of extensive burns is the decreased requirement of donor skin autografts, which is important because there are very limited skin graft donor sites in patients with extensive burns. There is reduced short-term complications of donor site wounds and long-term problems of development of scars and chronic wounds in patients. Use of CSS has been reported to considerably decrease the length of hospitalization from the standard 1-1.5 hospital days per %TBSA full-thickness burn (97). CSS has also been used as an adjunctive treatment for chronic wounds with allogeneic fibroblasts and keratinocytes from screened human cadaveric donors (40). Another advantage is the presence of a large number of cells in CSS, which facilitates rapid reformation of functional and protective barrier in the wound area by aiding regeneration of native-like skin.

1.6 Limitations of CSS

The development of CSS is time consuming since extensive cell culture procedures are involved for the different cell types used. Cells for the epidermal and dermal components of CSS usually require two to three weeks of cell culture before they are ready for grafting. This results in an increased turn over period for production of CSS, which is a constraint for its regular use, and could be overcome, with technical advances in cell and tissue culture protocols. Although cultured skin substitutes work better than the conventional skin substitutes, they have some limitations. The currently available CSS contain only two cell types, fibroblasts and keratinocytes, and hence lack the ability to form differentiated structures such as sweat and sebaceous glands, and hair follicles. In addition, melanocytes and Langerhans cells, adipose tissue and nerve supply are absent. Hence, these substitutes are unable to provide adequate temperature control, pigmentation, immune regulation, insulation and temperature and pressure sensation (23). In order to overcome these anatomical limitations, which influence functional and cosmetic outcomes, and to increase homology to native skin, some studies have included additional cell types such as endothelial cells into CSS (98, 99). However, these studies have not been successful due to technical difficulties such as slower growth of endothelial cells compared to fibroblasts, and higher rate of endothelial cell apoptosis. Further, melanocytes have been included in CSS to overcome problems of irregular or absence of

pigmentation due to insufficiency or lack of melanocytes. Preclinical studies where human melanocytes were selectively cultivated and added to CSS showed uniform pigmentation although pigment intensity could not be regulated (100). Recent studies have incorporated melanocytes, Langerhans cells and hair follicles into CSS (101, 102). Hachiya et al. (2005) used mixed cell slurries containing keratinocytes and fibroblasts with melanocytes on the backs of severe immunodeficient mice, which gave rise to skin containing spontaneously sorted melanocytes. Zheng et al. (2005) injected a mixture of neonatal dermal cells with epidermal aggregates into the dermis of nude mice and observed normal hair morphogenesis and hair follicle cycling within 8-12 days. These studies show that it is possible to incorporate different cell types into CSS in order to increase its homology to native skin and improve functional outcomes.

Another important shortcoming of the currently used CSS is that since it is made of heterogeneous dermal fibroblasts it is prone to pro-fibrotic remodelling and formation of HTS. Superficial dermal fibroblasts are anti-fibrotic and fewer in number compared to deep dermal fibroblasts that are pro-fibrotic and larger in number in the dermis. Heterogeneity among dermal fibroblasts will have serious implications on wound repair and healing following injury.

1.7 Thesis Research Project

A lot of progress has been made in developing skin substitutes for treatment of burn injuries and chronic wounds. Skin substitutes have contributed to healing of burn and chronic wounds and revolutionized treatment options for

patients with extensive skin loss (103). Among the skin substitutes, CSS are very promising for use in treatment of burns and other injuries where loss of skin is extensive. CSS has been used by our research group to treat patients with > 85% TBSA. It increased the quality of wound healing and reduced the length of hospitalization from an average of 324.0 ± 89.9 days to 181.0 days (104).

The overall hypothesis of this research project is that the selective use of superficial dermal fibroblasts in CSS instead of the conventional heterogeneous dermal fibroblasts would result in tissue engineered skin that has anti-fibrotic characteristics and promotes dermal regeneration over dermal repair. The goals of my thesis research project were to: (i) develop CSS that has anti-fibrotic characteristics in order to employ it as a tissue engineering strategy to treat burn patients and others with extensive skin loss, (ii) further characterize superficial and deep dermal fibroblasts using C-GAG matrices, and (iii) explore new targets for treatment of hypertrophic scars using C-GAG matrices as a 3-D culture substrate. The specific aims were to: (i) optimize preparation of C-GAG matrices for development of CSS, (ii) further characterize superficial and deep dermal fibroblasts using C-GAG matrices, (iii) identify new targets for treatment of HTS using C-GAG matrices, (iv) optimize fibroblast-keratinocyte co-culture medium for CSS, and (v) assess development of basement membrane and optimal barrier formation using CSS. In order to achieve these objectives a variety of biochemical and biomechanical approaches were employed in this project, which are described in the following chapters. CSS is also referred to as tissue

engineered skin and is interchangeably used in literature; however, the term tissue engineered skin is becoming more common in recent times and better represents the use of CSS. In the subsequent chapters of this thesis CSS is referred to as tissue engineered skin.

1.8 Table and Figures

Table 1.1: Commercially Available Skin Substitutes

| Skin substitute | Composition | Comments |
|------------------------|---|---|
| Biobrane™ | Outer epidermal analog - ultrathin silicone film; inner dermal analog - 3D nylon filament with type 1 collagen peptides | Temporary wound dressing that is removed when wound is healed or when autograft skin is available |
| Integra™ | Dermal analog - bovine collagen and chondroitin-6-sulfate GAG; epidermal analog - silicone polymer | Silicone layer is removed upon vascularization of dermis, and replaced by a thin layer of autograft |
| Alloderm™ | Human allograft skin that has been screened for transmissible pathogens, with all epidermal components and dermal cells removed | Grafted like dermal autograft and covered with a thin autograft |
| TransCyte™ | Nylon mesh seeded with neonatal human foreskin fibroblasts that are destroyed before grafting | Temporary wound dressing upon which autografts are placed |
| Dermagraft™ | Bioabsorbable polygalactin mesh matrix seeded with human neonatal fibroblasts and cryopreserved | Matrix facilitates re-epithelialization by the patient's own keratinocytes |
| Apligraf™ | Bovine collagen gel seeded with neonatal foreskin fibroblasts and keratinocytes | Wound dressing with two different cell types |
| OrCel™ | Type I collagen matrix seeded with neonatal foreskin fibroblasts and keratinocytes | Wound dressing with two different cell types |
| Epiceel™ | Sheets of autologous keratinocytes attached to petrolatum gauze support | Wound dressing with autologous cells |

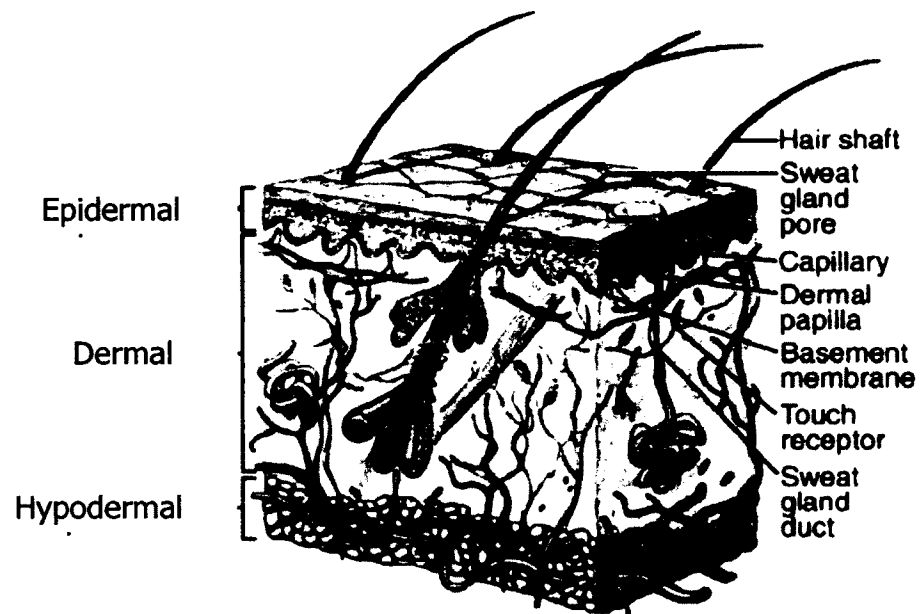


Figure 1.1: Layers of Human Skin.

Structure of human skin showing the upper epidermal layer, the thicker dermal layer and the lower hypodermal layer. Adapted from (105).

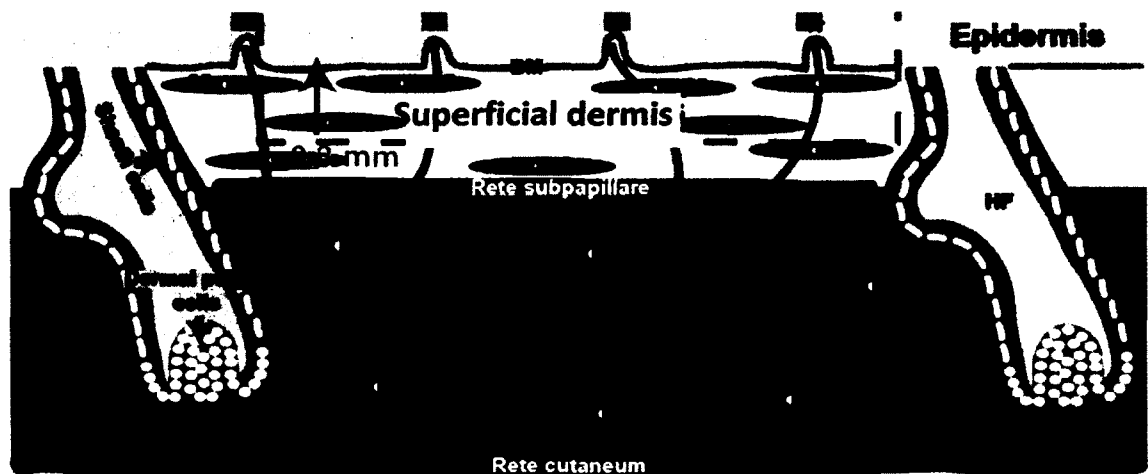


Figure 1.2: Structure of Human Skin.

Structure of human skin showing epidermis, basement membrane (BM) superficial dermis, rete pappillare, deep dermis and rete cutaneum. SF: superficial fibroblasts, DF: deep fibroblasts, HF: hair follicle. Adapted from (106).

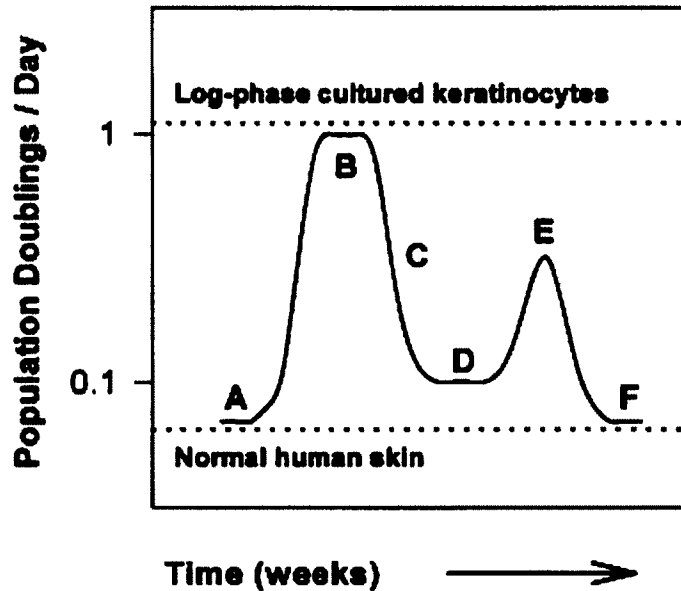


Figure 1.3: Relative Rates of Keratinocyte Proliferation.

The relative rates of proliferation of keratinocytes during preparation and grafting of CSS. (A) Basal keratinocytes in native skin divide about once in 14 days. (B) Keratinocytes cultured in growth media double about once per day during log-phase growth. (C) Confluence of keratinocyte cultures causes 'density-inhibition', and decrease of growth rates. (D) Stratified keratinocyte cultures continue slow proliferation until grafted. (E) Grafting of CSS initiates hypertrophy of transplanted keratinocytes. (F) Wound healing restores normal keratinocyte proliferation rate. Adapted from (10).

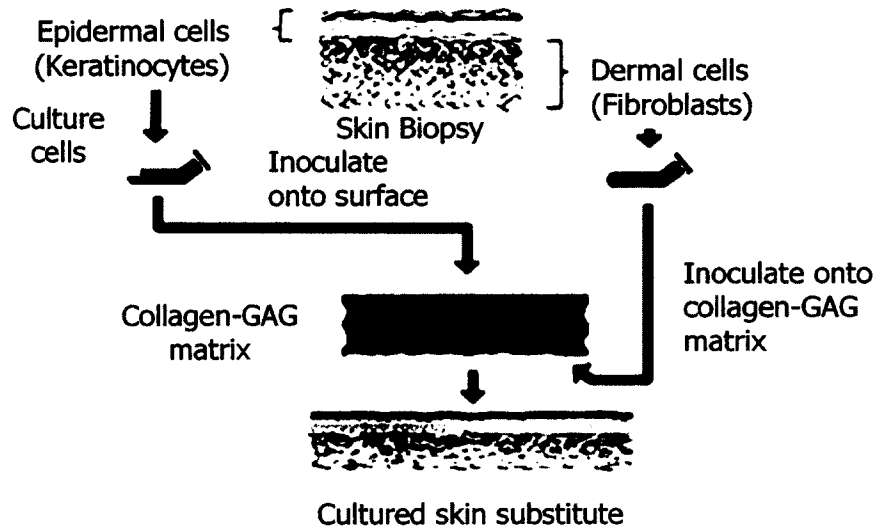


Figure 1.4: Preparation of CSS.

Schematic representation of the various stages involved in the preparation of CSS. Adapted from (10).

1.9 References

1. Metcalfe, A.D., and Ferguson, M.W. 2007. Tissue engineering of replacement skin: the crossroads of biomaterials, wound healing, embryonic development, stem cells and regeneration. *J R Soc Interface* 4:413-437.
2. Sorrell, J.M., Baber, M.A., and Caplan, A.I. 2008. Human dermal fibroblast subpopulations; differential interactions with vascular endothelial cells in coculture: nonsoluble factors in the extracellular matrix influence interactions. *Wound Repair Regen* 16:300-309.
3. Badylak, S.F. 2002. The extracellular matrix as a scaffold for tissue reconstruction. *Semin Cell Dev Biol* 13:377-383.
4. Kalluri, R. 2003. Basement membranes: structure, assembly and role in tumour angiogenesis. *Nat Rev Cancer* 3:422-433.
5. Ashkenas, J., Muschler, J., and Bissell, M.J. 1996. The extracellular matrix in epithelial biology: shared molecules and common themes in distant phyla. *Dev Biol* 180:433-444.
6. Hay, E.D. 2005. The mesenchymal cell, its role in the embryo, and the remarkable signaling mechanisms that create it. *Dev Dyn* 233:706-720.
7. Miner, J.H., and Yurchenco, P.D. 2004. Laminin functions in tissue morphogenesis. *Annu Rev Cell Dev Biol* 20:255-284.

8. Pelouch, V., and Jirmar, R. 1993. Biochemical characteristics of cardiac collagen and its role in ventricular remodelling following infarction. *Physiol Res* 42:283-292.
9. Bonewald, L.F. 1999. Regulation and regulatory activities of transforming growth factor beta. *Crit Rev Eukaryot Gene Expr* 9:33-44.
10. Boyce, S.T. 2001. Design principles for composition and performance of cultured skin substitutes. *Burns* 27:523-533.
11. Jones, I., Currie, L., and Martin, R. 2002. A guide to biological skin substitutes. *Br J Plast Surg* 55:185-193.
12. Loss, M., Wedler, V., Kunzi, W., Meuli-Simmen, C., and Meyer, V.E. 2000. Artificial skin, split-thickness autograft and cultured autologous keratinocytes combined to treat a severe burn injury of 93% of TBSA. *Burns* 26:644-652.
13. Robson, M.C., Barnett, R.A., Leitch, I.O., and Hayward, P.G. 1992. Prevention and treatment of postburn scars and contracture. *World J Surg* 16:87-96.
14. Burd, A., and Chiu, T. 2005. Allogenic skin in the treatment of burns. *Clin Dermatol* 23:376-387.
15. Langer, R., and Vacanti, J.P. 1993. Tissue engineering. *Science* 260:920-926.
16. MacArthur, B.D., and Oreffo, R.O. 2005. Bridging the gap. *Nature* 433:19.

17. Gurtner, G.C., Werner, S., Barrandon, Y., and Longaker, M.T. 2008. Wound repair and regeneration. *Nature* 453:314-321.
18. Wynn, T.A. 2008. Cellular and molecular mechanisms of fibrosis. *J Pathol* 214:199-210.
19. Bock, O., Schmid-Ott, G., Malewski, P., and Mrowietz, U. 2006. Quality of life of patients with keloid and hypertrophic scarring. *Arch Dermatol Res* 297:433-438.
20. Hold, G.L., Untiveros, P., Saunders, K.A., and El-Omar, E.M. 2009. Role of host genetics in fibrosis. *Fibrogenesis Tissue Repair* 2:6.
21. Schulz, J.T., 3rd, Tompkins, R.G., and Burke, J.F. 2000. Artificial skin. *Annu Rev Med* 51:231-244.
22. Boyce, S.T., and Warden, G.D. 2002. Principles and practices for treatment of cutaneous wounds with cultured skin substitutes. *Am J Surg* 183:445-456.
23. Supp, D.M., and Boyce, S.T. 2005. Engineered skin substitutes: practices and potentials. *Clin Dermatol* 23:403-412.
24. MacNeil, S. 2007. Progress and opportunities for tissue-engineered skin. *Nature* 445:874-880.
25. Heimbach, D.M., Warden, G.D., Luterman, A., Jordan, M.H., Ozobia, N., Ryan, C.M., Voigt, D.W., Hickerson, W.L., Saffle, J.R., DeClement, F.A., et al. 2003. Multicenter postapproval clinical trial of Integra dermal regeneration template for burn treatment. *J Burn Care Rehabil* 24:42-48.

26. Sheridan, R., Choucair, R., Donelan, M., Lydon, M., Petras, L., and Tompkins, R. 1998. Acellular allodermis in burns surgery: 1-year results of a pilot trial. *J Burn Care Rehabil* 19:528-530.
27. Menon, N.G., Rodriguez, E.D., Byrnes, C.K., Giroto, J.A., Goldberg, N.H., and Silverman, R.P. 2003. Revascularization of human acellular dermis in full-thickness abdominal wall reconstruction in the rabbit model. *Ann Plast Surg* 50:523-527.
28. Noordenbos, J., Dore, C., and Hansbrough, J.F. 1999. Safety and efficacy of TransCyte for the treatment of partial-thickness burns. *J Burn Care Rehabil* 20:275-281.
29. Curran, M.P., and Plosker, G.L. 2002. Bilayered bioengineered skin substitute (Apligraf): a review of its use in the treatment of venous leg ulcers and diabetic foot ulcers. *BioDrugs* 16:439-455.
30. Falabella, A.F., Valencia, I.C., Eaglstein, W.H., and Schachner, L.A. 2000. Tissue-engineered skin (Apligraf) in the healing of patients with epidermolysis bullosa wounds. *Arch Dermatol* 136:1225-1230.
31. Fivenson, D.P., Scherschun, L., and Cohen, L.V. 2003. Apligraf in the treatment of severe mitten deformity associated with recessive dystrophic epidermolysis bullosa. *Plast Reconstr Surg* 112:584-588.
32. Still, J., Glat, P., Silverstein, P., Griswold, J., and Mazingo, D. 2003. The use of a collagen sponge/living cell composite material to treat donor sites in burn patients. *Burns* 29:837-841.

33. Green, H., Kehinde, O., and Thomas, J. 1979. Growth of cultured human epidermal cells into multiple epithelia suitable for grafting. *Proc Natl Acad Sci U S A* 76:5665-5668.
34. Carsin, H., Ainaud, P., Le Bever, H., Rives, J., Lakhel, A., Stephanazzi, J., Lambert, F., and Perrot, J. 2000. Cultured epithelial autografts in extensive burn coverage of severely traumatized patients: a five year single-center experience with 30 patients. *Burns* 26:379-387.
35. Williamson, J.S., Snelling, C.F., Clugston, P., Macdonald, I.B., and Germann, E. 1995. Cultured epithelial autograft: five years of clinical experience with twenty-eight patients. *J Trauma* 39:309-319.
36. Rue, L.W., 3rd, Cioffi, W.G., McManus, W.F., and Pruitt, B.A., Jr. 1993. Wound closure and outcome in extensively burned patients treated with cultured autologous keratinocytes. *J Trauma* 34:662-667; discussion 667-668.
37. Wang, T.W., Sun, J.S., Wu, H.C., Tsuang, Y.H., Wang, W.H., and Lin, F.H. 2006. The effect of gelatin-chondroitin sulfate-hyaluronic acid skin substitute on wound healing in SCID mice. *Biomaterials* 27:5689-5697.
38. Boyce, S.T. 1998. Skin substitutes from cultured cells and collagen-GAG polymers. *Med Biol Eng Comput* 36:791-800.
39. Boyce, S.T., Goretsky, M.J., Greenhalgh, D.G., Kagan, R.J., Rieman, M.T., and Warden, G.D. 1995. Comparative assessment of cultured skin

substitutes and native skin autograft for treatment of full-thickness burns. *Ann Surg* 222:743-752.

40. Boyce, S.T., Glatter, R., and Kitzmiller, W.J. 1995. Case studies: treatment of chronic wounds with cultured skin substitutes. *Ostomy Wound Manage* 41:26-28, 30, 32 passim.
41. Boyce, S.T., Kagan, R.J., Meyer, N.A., Yakuboff, K.P., and Warden, G.D. 1999. The 1999 clinical research award. Cultured skin substitutes combined with Integra Artificial Skin to replace native skin autograft and allograft for the closure of excised full-thickness burns. *J Burn Care Rehabil* 20:453-461.
42. Passaretti, D., Billmire, D., Kagan, R., Corcoran, J., and Boyce, S. 2004. Autologous cultured skin substitutes conserve donor autograft in elective treatment of congenital giant melanocytic nevus. *Plast Reconstr Surg* 114:1523-1528.
43. Cen, L., Liu, W., Cui, L., Zhang, W., and Cao, Y. 2008. Collagen tissue engineering: development of novel biomaterials and applications. *Pediatr Res* 63:492-496.
44. Roberts, R., Gallagher, J., Spooncer, E., Allen, T.D., Bloomfield, F., and Dexter, T.M. 1988. Heparan sulphate bound growth factors: a mechanism for stromal cell mediated haemopoiesis. *Nature* 332:376-378.
45. Kagami, S., Kondo, S., Loster, K., Reutter, W., Urushihara, M., Kitamura, A., Kobayashi, S., and Kuroda, Y. 1998. Collagen type I modulates the

- platelet-derived growth factor (PDGF) regulation of the growth and expression of beta1 integrins by rat mesangial cells. *Biochem Biophys Res Commun* 252:728-732.
46. Laurie, G.W., Horikoshi, S., Killen, P.D., Segui-Real, B., and Yamada, Y. 1989. In situ hybridization reveals temporal and spatial changes in cellular expression of mRNA for a laminin receptor, laminin, and basement membrane (type IV) collagen in the developing kidney. *J Cell Biol* 109:1351-1362.
 47. Martins-Green, M. 2000. *Dynamics of cell-ECM interactions in Principles of Tissue Engineering.* (Ed.) Lanza, RP, Langer, R and Vacanti J, Academic Press. 33-48 pp.
 48. Putnam, A.J., and Mooney, D.J. 1996. Tissue engineering using synthetic extracellular matrices. *Nat Med* 2:824-826.
 49. Bouhadir, K.H., and Mooney, D.J. 1998. In vitro and in vivo models for the reconstruction of intercellular signaling. *Ann N Y Acad Sci* 842:188-194.
 50. Grant, M.E. 2007. From collagen chemistry towards cell therapy - a personal journey. *Int J Exp Pathol* 88:203-214.
 51. Brodsky, B., and Ramshaw, J.A. 1997. The collagen triple-helix structure. *Matrix Biol* 15:545-554.
 52. Ramshaw, J.A., Peng, Y.Y., Glattauer, V., and Werkmeister, J.A. 2008. Collagens as biomaterials. *J Mater Sci Mater Med.*

53. Waller, J.M., and Maibach, H.I. 2006. Age and skin structure and function, a quantitative approach (II): protein, glycosaminoglycan, water, and lipid content and structure. *Skin Res Technol* 12:145-154.
54. Veit, G., Kobbe, B., Keene, D.R., Paulsson, M., Koch, M., and Wagener, R. 2006. Collagen XXVIII, a novel von Willebrand factor A domain-containing protein with many imperfections in the collagenous domain. *J Biol Chem* 281:3494-3504.
55. Freyman, T.M., Yannas, I.V., Pek, Y.S., Yokoo, R., and Gibson, L.J. 2001. Micromechanics of fibroblast contraction of a collagen-GAG matrix. *Exp Cell Res* 269:140-153.
56. Pieper, J.S., van Wachem, P.B., van Luyn, M.J.A., Brouwer, L.A., Hafmans, T., Veerkamp, J.H., and van Kuppevelt, T.H. 2000. Attachment of glycosaminoglycans to collagenous matrices modulates the tissue response in rats. *Biomaterials* 21:1689-1699.
57. Lindahl, U., Kusche-Gullberg, M., and Kjellen, L. 1998. Regulated diversity of heparan sulfate. *J Biol Chem* 273:24979-24982.
58. Yannas, I.V., Lee, E., Orgill, D.P., Skrabut, E.M., and Murphy, G.F. 1989. Synthesis and characterization of a model extracellular matrix that induces partial regeneration of adult mammalian skin. *Proc Natl Acad Sci U S A* 86:933-937.

59. Kuberka, M., von Heimburg, D., Schoof, H., Heschel, I., and Rau, G. 2002. Magnification of the pore size in biodegradable collagen sponges. *Int J Artif Organs* 25:67-73.
60. van Tienen, T.G., Heijkants, R.G., Buma, P., de Groot, J.H., Pennings, A.J., and Veth, R.P. 2002. Tissue ingrowth and degradation of two biodegradable porous polymers with different porosities and pore sizes. *Biomaterials* 23:1731-1738.
61. Tsuruga, E., Takita, H., Itoh, H., Wakisaka, Y., and Kuboki, Y. 1997. Pore size of porous hydroxyapatite as the cell-substratum controls BMP-induced osteogenesis. *J Biochem* 121:317-324.
62. Hubbell, J.A. 2003. Materials as morphogenetic guides in tissue engineering. *Curr Opin Biotechnol* 14:551-558.
63. Pieper, J.S., Oosterhof, A., Dijkstra, P.J., Veerkamp, J.H., and van Kuppevelt, T.H. 1999. Preparation and characterization of porous crosslinked collagenous matrices containing bioavailable chondroitin sulphate. *Biomaterials* 20:847-858.
64. Daamen, W.F., van Moerkerk, H.T., Hafmans, T., Buttafoco, L., Poot, A.A., Veerkamp, J.H., and van Kuppevelt, T.H. 2003. Preparation and evaluation of molecularly-defined collagen-elastin-glycosaminoglycan scaffolds for tissue engineering. *Biomaterials* 24:4001-4009.

65. Ellis, D.L., and Yannas, I.V. 1996. Recent advances in tissue synthesis in vivo by use of collagen-glycosaminoglycan copolymers. *Biomaterials* 17:291-299.
66. Rong, Y., Sugumaran, G., Silbert, J.E., and Spector, M. 2002. Proteoglycans synthesized by canine intervertebral disc cells grown in a type I collagen-glycosaminoglycan matrix. *Tissue Eng* 8:1037-1047.
67. O'Brien, F.J., Harley, B.A., Yannas, I.V., and Gibson, L.J. 2005. The effect of pore size on cell adhesion in collagen-GAG scaffolds. *Biomaterials* 26:433-441.
68. Chang, H.Y., Chi, J.T., Dudoit, S., Bondre, C., van de Rijn, M., Botstein, D., and Brown, P.O. 2002. Diversity, topographic differentiation, and positional memory in human fibroblasts. *Proc Natl Acad Sci U S A* 99:12877-12882.
69. Trompezinski, S., Berthier-Vergnes, O., Denis, A., Schmitt, D., and Viac, J. 2004. Comparative expression of vascular endothelial growth factor family members, VEGF-B, -C and -D, by normal human keratinocytes and fibroblasts. *Exp Dermatol* 13:98-105.
70. Marinkovich, M.P., Keene, D.R., Rimberg, C.S., and Burgeson, R.E. 1993. Cellular origin of the dermal-epidermal basement membrane. *Dev Dyn* 197:255-267.

71. Clark, R. 1996. *Wound repair: overview and general considerations In The Molecular and Cellular Biology of Wound Repair*. New York, NY: Plenum Press. 3-35 pp.
72. Phillips, C.L., Combs, S.B., and Pinnell, S.R. 1994. Effects of ascorbic acid on proliferation and collagen synthesis in relation to the donor age of human dermal fibroblasts. *J Invest Dermatol* 103:228-232.
73. Navsaria, H.A., Myers, S.R., Leigh, I.M., and McKay, I.A. 1995. Culturing skin in vitro for wound therapy. *Trends Biotechnol* 13:91-100.
74. Woan KV, N.R.N., I Persaud 2005. Coenzyme Q10 enhances the proliferation and migration of fibroblasts and keratinocytes: a possible implication for wound healing. . *J Invest Dermatol* A57.
75. Wang, J., Dodd, C., Shankowsky, H.A., Scott, P.G., and Tredget, E.E. 2008. Deep dermal fibroblasts contribute to hypertrophic scarring. *Lab Invest* 88:1278-1290.
76. Monstrey, S., Hoeksema, H., Verbelen, J., Pirayesh, A., and Blondeel, P. 2008. Assessment of burn depth and burn wound healing potential. *Burns : journal of the International Society for Burn Injuries* 34:761-769.
77. Cubison, T.C., Pape, S.A., and Parkhouse, N. 2006. Evidence for the link between healing time and the development of hypertrophic scars (HTS) in paediatric burns due to scald injury. *Burns : journal of the International Society for Burn Injuries* 32:992-999.

78. Eckert, R.L., Efimova, T., Dashti, S.R., Balasubramanian, S., Deucher, A., Crish, J.F., Sturniolo, M., and Bone, F. 2002. Keratinocyte survival, differentiation, and death: many roads lead to mitogen-activated protein kinase. *J Invest Dermatol Symp Proc* 7:36-40.
79. Gandarillas, A. 2000. Epidermal differentiation, apoptosis, and senescence: common pathways? *Exp Gerontol* 35:53-62.
80. Werner, S., Krieg, T., and Smola, H. 2007. Keratinocyte-fibroblast interactions in wound healing. *J Invest Dermatol* 127:998-1008.
81. Yannas, I.V. 1992. Tissue regeneration by use of collagen-glycosaminoglycan copolymers. *Clin Mater* 9:179-187.
82. O'Brien, F.J., Harley, B.A., Yannas, I.V., and Gibson, L. 2004. Influence of freezing rate on pore structure in freeze-dried collagen-GAG scaffolds. *Biomaterials* 25:1077-1086.
83. Harley, B.A., Leung, J.H., Silva, E.C., and Gibson, L.J. 2007. Mechanical characterization of collagen-glycosaminoglycan scaffolds. *Acta Biomater* 3:463-474.
84. Haugh, M.G., Jaasma, M.J., and O'Brien, F.J. 2008. The effect of dehydrothermal treatment on the mechanical and structural properties of collagen-GAG scaffolds. *J Biomed Mater Res A*.
85. Yunoki, S., Suzuki, T., and Takai, M. 2003. Stabilization of low denaturation temperature collagen from fish by physical cross-linking methods. *J Biosci Bioeng* 96:575-577.

86. Koide, M., Osaki, K., Konishi, J., Oyamada, K., Katakura, T., Takahashi, A., and Yoshizato, K. 1993. A new type of biomaterial for artificial skin: dehydrothermally cross-linked composites of fibrillar and denatured collagens. *J Biomed Mater Res* 27:79-87.
87. Weadock, K.S., Miller, E.J., Bellincampi, L.D., Zawadsky, J.P., and Dunn, M.G. 1995. Physical crosslinking of collagen fibers: comparison of ultraviolet irradiation and dehydrothermal treatment. *J Biomed Mater Res* 29:1373-1379.
88. Powell, H.M., and Boyce, S.T. 2006. EDC cross-linking improves skin substitute strength and stability. *Biomaterials* 27:5821-5827.
89. Powell, H.M., and Boyce, S.T. 2007. Wound closure with EDC cross-linked cultured skin substitutes grafted to athymic mice. *Biomaterials* 28:1084-1092.
90. Supp, A.P., Wickett, R.R., Swope, V.B., Harriger, M.D., Hoath, S.B., and Boyce, S.T. 1999. Incubation of cultured skin substitutes in reduced humidity promotes cornification in vitro and stable engraftment in athymic mice. *Wound Repair Regen* 7:226-237.
91. Boyce, S.T., Supp, A.P., Swope, V.B., and Warden, G.D. 2002. Vitamin C regulates keratinocyte viability, epidermal barrier, and basement membrane in vitro, and reduces wound contraction after grafting of cultured skin substitutes. *J Invest Dermatol* 118:565-572.

92. Werner, S., and Smola, H. 2001. Paracrine regulation of keratinocyte proliferation and differentiation. *Trends Cell Biol* 11:143-146.
93. Blomme, E.A., Sugimoto, Y., Lin, Y.C., Capen, C.C., and Rosol, T.J. 1999. Parathyroid hormone-related protein is a positive regulator of keratinocyte growth factor expression by normal dermal fibroblasts. *Mol Cell Endocrinol* 152:189-197.
94. Aoki, S., Toda, S., Ando, T., and Sugihara, H. 2004. Bone marrow stromal cells, preadipocytes, and dermal fibroblasts promote epidermal regeneration in their distinctive fashions. *Mol Biol Cell* 15:4647-4657.
95. el-Ghalbzouri, A., Gibbs, S., Lamme, E., Van Blitterswijk, C.A., and Ponec, M. 2002. Effect of fibroblasts on epidermal regeneration. *Br J Dermatol* 147:230-243.
96. Sorrell, J.M., Baber, M.A., and Caplan, A.I. 2004. Site-matched papillary and reticular human dermal fibroblasts differ in their release of specific growth factors/cytokines and in their interaction with keratinocytes. *Journal of cellular physiology* 200:134-145.
97. Boyce, S.T., Kagan, R.J., Yakuboff, K.P., Meyer, N.A., Rieman, M.T., Greenhalgh, D.G., and Warden, G.D. 2002. Cultured skin substitutes reduce donor skin harvesting for closure of excised, full-thickness burns. *Ann Surg* 235:269-279.

98. Supp, D.M., Wilson-Landy, K., and Boyce, S.T. 2002. Human dermal microvascular endothelial cells form vascular analogs in cultured skin substitutes after grafting to athymic mice. *Faseb J* 16:797-804.
99. Sahota, P.S., Burn, J.L., Heaton, M., Freedlander, E., Suvarna, S.K., Brown, N.J., and Mac Neil, S. 2003. Development of a reconstructed human skin model for angiogenesis. *Wound Repair Regen* 11:275-284.
100. Swope, V.B., Supp, A.P., Cornelius, J.R., Babcock, G.F., and Boyce, S.T. 1997. Regulation of pigmentation in cultured skin substitutes by cytometric sorting of melanocytes and keratinocytes. *J Invest Dermatol* 109:289-295.
101. Hachiya, A., Sriwiriyanont, P., Kaiho, E., Kitahara, T., Takema, Y., and Tsuboi, R. 2005. An in vivo mouse model of human skin substitute containing spontaneously sorted melanocytes demonstrates physiological changes after UVB irradiation. *J Invest Dermatol* 125:364-372.
102. Zheng, Y., Du, X., Wang, W., Boucher, M., Parimoo, S., and Stenn, K. 2005. Organogenesis from dissociated cells: generation of mature cycling hair follicles from skin-derived cells. *J Invest Dermatol* 124:867-876.
103. Ehrenreich, M., and Ruszczak, Z. 2006. Update on dermal substitutes. *Acta Dermatovenerol Croat* 14:172-187.
104. Shankowsky, H. 2008. Statistics for use of CSS in Burns Unit, University of Alberta.
105. <http://www.nlm.nih.gov/medlineplus/skincancer.html>

106. Sorrell, J.M., and Caplan, A.I. 2004. Fibroblast heterogeneity: more than skin deep. *Journal of cell science* 117:667-675.

Chapter 2

Differential Collagen-Glycosaminoglycan Matrix Remodeling by Superficial and Deep Dermal Fibroblasts: Potential Therapeutic Targets for Hypertrophic Scar*

*Parts of this chapter have been published as: Varkey M, Ding J, Tredget EE. (2011) Differential collagen-glycosaminoglycan matrix remodeling by superficial and deep dermal fibroblasts: Potential therapeutic targets for hypertrophic scar. *Biomaterials*. 32:7581-91.

2 Differential Collagen-Glycosaminoglycan Matrix Remodeling by Superficial and Deep Dermal Fibroblasts: Potential Therapeutic Targets for Hypertrophic Scar

2.1 Introduction

Skin protects the body from exogenous substances and trauma, and acts as a barrier to temperature and water loss. During skin loss due to burns or other causes split-thickness skin autografts are often used to treat patients. However, in the case of extensive skin loss due to deep dermal or full-thickness wounds as in third-degree burns suitable donor sites for autografts are not available and therefore skin substitutes are the preferred treatment option for wound closure. Of the skin substitutes, cultured skin substitutes (CSS) containing autologous fibroblasts and keratinocytes seeded on an artificial extracellular matrix (ECM) made of collagen-glycosaminoglycan (C-GAG) are very promising for use in skin repair since favourable clinical results for wound coverage and pliability have been reported [1].

A significant negative outcome of post-burn skin wound healing is hypertrophic scarring (HTS), a fibroproliferative disorder characterized by erythematous lesions that compromise the appearance of the healing skin and cause scar contractures that limit movement and function [2]. Excessive

deposition of ECM that has an altered organization and composition compared to normal dermis contributes to the characteristic features observed in HTS. Two-thirds of patients suffering from skin burn injuries develop HTS that often results in prolonged and uncomfortable rehabilitation periods especially for those who have survived second and third degree burns [3]. The degree and extent of HTS has been clinically observed to be related to the depth of injury. Superficial wounds are generally observed to heal with minimum HTS without surgical intervention while deep wounds are more prone to HTS and scar contracture and need surgical intervention [4, 5]. Recently, Dunkin *et al.* using a novel jigsaw scratch/incision approach determined that there is a threshold depth of dermal injury at which HTS occurs [6]. The molecular basis of HTS and the differences in biomechanical milieu at different depths of the dermis that contribute to HTS are not clearly understood.

The primary cells that mediate skin wound healing and HTS, the dermal fibroblasts, are heterogeneous and consist of three sub-populations that exhibit distinct characteristics when cultured separately [7]. Two of these fibroblast sub-populations reside in the papillary and reticular dermis, while the third group is associated with hair follicles. The papillary and reticular fibroblasts are also known as superficial and deep dermal fibroblasts, respectively; the latter nomenclature will be used hereafter in this paper. Superficial and deep dermal fibroblasts when cultured, exhibit differences in physical and biochemical characteristics including size, packing density, rate of proliferation, growth

kinetics, production of collagenase and type I and III procollagen [8-11].

Recently our research group demonstrated that deep fibroblasts compared to superficial fibroblasts produce more Transforming Growth Factor (TGF)- β 1, the most extensively studied pro-fibrotic cytokine [12], type I collagen and more of the large proteoglycan, versican (VER), but less of the small proteoglycan, decorin (DCN) [13]. Interestingly, it was observed that superficial dermal fibroblasts may be similar to normal dermal fibroblasts while deep dermal fibroblasts may be similar to fibroblasts found in HTS [13].

To minimize post-burn HTS it is important to decipher the different factors that contribute to wound healing following superficial and deep dermal injury. Differences in biomechanical properties of the dermis at different depths of the skin are not known. A clear understanding of the role of superficial and deep dermal fibroblasts in anti-fibrotic and pro-fibrotic healing will enable us to develop strategies and therapies for prevention and effective treatment of HTS. This motivated us to explore whether superficial and deep dermal fibroblasts differentially remodel C-GAG matrices. It is even more important to assess differences between superficial and deep fibroblasts especially since current cultured skin substitutes are prepared using a mixed population of dermal fibroblasts on C-GAG matrices. In this study, matrices independently containing superficial and deep fibroblasts were analyzed to understand the molecular basis of biochemical and functional differences of the fibroblasts and their possible differential contribution to HTS. Differences in biomechanical properties of the

ECM remodelled by superficial and deep dermal fibroblasts were investigated. To the best of our knowledge, biomechanical differences in matrices remodelled by superficial and deep dermal fibroblasts have not been reported before. Collagen production, expression of specific genes and protein levels were also analyzed. Superficial and deep fibroblasts grown on C-GAG matrices were also examined for differences in gene expression of connective tissue growth factor (CTGF), TGF- β 1, heat shock protein(HSP)-47, matrix metalloproteinase (MMP)-1, osteopontin (OPN), angiotensin (ANG)-II, tumour necrosis factor (TNF)- α , peroxisome proliferator-activated receptor (PPAR)- α , PPAR- β/δ , PPAR- γ , VER, DCN and fibromodulin (FMOD).

2.2 Materials and Methods

2.2.1 Preparation of C-GAG Matrices

Acellular C-GAG matrices were prepared by freeze-drying a co-precipitate of type I collagen and chondroitin-6-sulfate. Briefly, collagen powder (0.5 wt %; Devro Pty. Ltd., Bathurst, NSW, Australia) was solubilized in 0.5 M acetic acid and co-precipitated with chondroitin-6-sulfate (0.05 wt %; Sigma, St. Louis, MO, USA). The co-precipitate was mixed (15,000 rpm, 4°C, 4 h) with an overhead blender (IKA, Wilmington, NC, USA) and subsequently degassed under vacuum (2 h, room temperature). The degassed C-GAG suspension was then cast between steel plates and frozen to -40°C at a constant rate in a refrigerated

circulating ethanol bath (Haake Phoenix II, Thermo Scientific, USA) and held at that temperature for 1 h. The frozen casting apparatus was opened and the C-GAG matrices were freeze-dried (FreeZone⁶Plus, Labconco, Kansas City, MI, USA) for 17 h to produce highly porous matrices.

The matrices obtained were cut into 30 mm discs and cross-linked by dehydrothermal treatment at 140°C under vacuum for 24 h in a drying oven (APT.Line VD, Binder GmbH, Germany). Following cross-linking, the matrix discs were rinsed with phosphate buffered saline (PBS; twice, 15 min each) and subsequently with cell culture medium (DMEM, 10% FBS, 1% Antibiotic-antimycotic; twice, 15 min each).

2.2.2 Determination of Pore Structure and Sizes of C-GAG

Matrices

The cross-linked C-GAG matrices were sputter-coated with gold for 2 min at 15 mA and viewed at 20 kV using a LEO 1430 scanning electron microscope (SEM) at 250× and 500× magnifications. Pore structure of the matrices was examined and the pore sizes were determined by NIH Image J. The pore size of at least 50 pores was determined for each matrix.

2.2.3 Isolation of Fibroblasts and Cell Culture

The protocols for human tissue sampling used in this study were approved by the University of Alberta Hospital's Health Research Ethics Board. The superficial and deep dermal fibroblasts used here were isolated from lower abdominal tissue obtained from three patients who underwent elective abdominoplasty surgery following informed consent. The tissue samples were horizontally sectioned into five dermal layers (referred to as layers 1 to 5) using a dermatome (Padgett Instruments, Plainsboro, NJ, USA) set approximately at 0.5 mm. The superficial dermal layer (layer 1; L1) was treated overnight with 25 U/mL dispase (Gibco, Grand Island, NY, USA) at 4°C to remove the epidermis. Subsequently, the superficial dermal layer and the deep dermal layer (layer 5; L5) were separately treated with 455.3 U/mL collagenase (Gibco Grand Island, NY, USA) for 18 hours at 37°C, 60 rpm to isolate the superficial (SF) and deep (DF) dermal fibroblasts, respectively. The cell suspensions were passed through 100 µm cell strainers and centrifuged at 800 rpm for 10 minutes. The cell pellet was then re-suspended in cell culture medium (DMEM, 10% FBS, 1% Antibiotic-antimycotic) and seeded in tissue culture flasks. The required number of superficial and deep dermal fibroblasts was obtained by serial expansion of fibroblasts. Passage 4 superficial and deep dermal fibroblasts were seeded onto cross-linked C-GAG discs at a density of 0.5×10^6 cells/cm² and cultured (at 37°C, 5% CO₂) for upto 21 days. The matrices with fibroblasts were used at different time points in the assays described below.

2.2.4 Assessment of Cell Viability on C-GAG Matrices

From the fibroblast-populated C-GAG matrices, 5 mm punch biopsies were collected on days 4, 7, 14 and 21 of culture and placed into separate wells in a 24-well microtitre plate. A standard 3-[4,5-dimethylthiazol-2-yl]-2,5-diphenyl tetrazolium bromide (MTT) assay was performed to assess viability of cells in the matrices. Briefly, the punch biopsies were incubated with 250 μ l of tissue culture medium containing MTT substrate (5 mg/mL) for 4 hours at 37°C. The obtained MTT-formazan product was dissolved in 200 μ l of dimethyl sulfoxide and quantified at 570 nm using a microplate reader (THERMOmax, Molecular Devices, Sunnyvale, CA, USA). The values are shown as mean optical density \pm standard error.

2.2.5 Analysis of Contraction of C-GAG Matrices with Fibroblasts

To determine the extent of fibroblast-mediated matrix contraction, C-GAG matrices populated with superficial or deep dermal fibroblasts were photographed on days 4, 7, 14 and 21, and the images were analyzed using NIH image J. The values are reported as mean percentage contraction \pm standard error.

2.2.6 Biomechanical Testing of C-GAG Matrices with Fibroblasts

The biomechanical properties of C-GAG matrices containing fibroblasts were determined by subjecting them to tensile testing. Briefly, C-GAG matrices were cut into dog-bone shaped pieces (gauge length of 50 mm and width of 15 mm) and were cross-linked, and subsequently superficial and deep dermal fibroblasts were separately cultured on these matrices. On day 11 of culture, the matrices were mounted onto the grips of an Insight tensile tester (MTS systems corporation, Eden Prairie, MN, USA) connected to a 500 N load cell and were tested at a strain rate of 2 mm/min. Tensile strength assessment of the matrices was done on day 11 of culture based on results from our previous studies (unpublished data). The tensile tests were set up such that all the samples were strained to failure and at the time of rupture of the samples the tests were stopped. C-GAG matrices without cells were used as controls. The ultimate tensile strength (UTS; kPa) and stiffness (mN/mm) values were calculated and are reported as mean \pm standard error.

2.2.7 Assessment of Collagen Content in Fibroblast-Populated C-GAG Matrices and Conditioned Medium

The total collagen content of C-GAG matrices containing superficial or deep dermal fibroblasts and the corresponding conditioned medium (DMEM, 2% FBS, 50 μ g/mL ascorbic acid, 50 μ g/mL β -amino propionitrile, 0.1 mM proline)

was determined by hydroxyproline assay. The amount of hydroxyproline, a major component of collagen protein, was quantified on days 4, 7, 14 and 21 of culture. C-GAG matrices without cells were used as controls. Briefly, acetonitrile was added to the matrices and the conditioned medium to precipitate collagen. The samples were centrifuged for 15 min at 4°C and the precipitates were hydrolyzed using 6N HCl at 110°C overnight. A known amount of N-methyl-proline was added to the hydrolysate after drying, to obtain the N-butyl ester derivative of hydroxyproline. The samples were then subjected to liquid chromatography/ mass spectrometry using a HP 1100 Liquid Chromatograph linked to a HP 1100 Mass Selective detector and the ions 186 (N-butyl ester of N-methyl-proline) and 188 (N-butyl ester of 4-hydroxyproline) were monitored. Each sample was analyzed with respect to a standard curve of 4-hydroxyproline (generated under identical conditions) and the results are presented as mean \pm standard error.

2.2.8 Histological Analysis

From C-GAG matrices containing superficial or deep dermal fibroblasts, 5 mm punch biopsies were collected at days 4, 7, 14 and 21 of culture for histological analysis. C-GAG matrices without cells were used as controls. The samples were fixed with 4% paraformaldehyde for 12 h and 70% ethanol for 12 h, embedded in paraffin, sectioned at 5 μ m and mounted on microscope slides. The slides were then stained with hematoxylin and eosin (H & E), and were

viewed by light microscopy at 100× and 200× magnification and photographed. DAPI staining was also performed in order to assess viable cells on the matrices.

2.2.9 Immunohistochemical Analysis

5 mm punch biopsies were collected from C-GAG matrices containing superficial or deep dermal fibroblasts at days 4, 7, 14 and 21 of culture for immunohistochemical staining of α -Smooth Muscle Actin (α -SMA), a marker for myofibroblasts. C-GAG matrices without cells were used as controls. Briefly, the samples were fixed with 4% paraformaldehyde (12 h) and 70% ethanol (12 h), paraffin embedded and sectioned at 5 μ m and mounted on microscope slides. The sections were then deparaffinized with xylene and rehydrated in descending series of ethanol, and subsequently blocked with 10% BSA in PBS for 60 min to avoid non-specific protein binding. The sections were incubated overnight at 4°C with 1:25 dilution of primary mouse anti- α -SMA antibody (Dako, Denmark), and were washed three times with PBS for 5 min each. Non-immune human IgG at 1:25 dilution was used as the negative control. Endogenous peroxide activity was quenched with 0.3% H₂O₂ (15 min) and subsequently the sections were incubated for 60 min at room temperature with 1:150 dilution of secondary goat anti-mouse IgG antibody conjugated with horseradish peroxidase (Sigma Aldrich, Oakville, ON, Canada). The bound secondary antibody was detected by incubation with 3,3'-diaminobenzidine substrate, and the sections were then counterstained with haematoxylin. The stained sections were dehydrated,

mounted, and viewed by light microscopy at 100× and 200× magnification and photographed.

2.2.10 Gene Expression Studies

C-GAG matrices with superficial or deep dermal fibroblasts were treated with Trizol reagent (Invitrogen, Carlsbad, CA, USA) on days 4, 7, 14 and 21 of culture and the obtained supernatant was stored at -80°C. On a later date, total RNA was extracted from all the supernatants using RNeasy Mini Kit (Qiagen, Mississauga, ON, Canada) following manufacturer's instructions, and was quantified using a spectrophotometer at 260 nm. RNA extract of each sample (0.5 µg) was used for first-strand cDNA synthesis using M-MLV Reverse Transcriptase (Invitrogen, Carlsbad, CA, USA) by incubation at three different conditions, 25°C for 10 min followed by 37°C for 50 min and 70°C for 15 min. The resulting cDNA was used as a template for quantitative Real Time Polymerase Chain Reaction (qRT-PCR) amplification of genes of interest. The gene specific primers used in qRT-PCR were designed using Primer Express 3.0 and are listed in Table 2.1. qRT-PCR was done using Power Sybr Green™ PCR master mix (ABI, Foster, CA, USA) in a total reaction volume of 25 µl containing 5 µl of a 1:10 dilution of cDNA product from the first-strand reaction and 1 µM gene-specific forward and reverse primers on a StepOne Plus qRT-PCR system (ABI, Foster, CA, USA). The amplification conditions included initial denaturation at 95°C for 3 min followed by 40 cycles of denaturation at 95°C for 15 sec and

annealing and primer extension at 60°C for 30 sec. The amplification of genes was measured in terms of cycle threshold (CT) values, and the obtained CT values were normalized with the CT value of a house-keeping gene. Gene expression levels are shown as mean fold change \pm standard error.

2.2.11 Protein Expression Analysis

The corresponding conditioned medium from superficial or deep dermal fibroblast culture on C-GAG matrices were collected on days 4, 7, 14 and 21 and stored at -80°C to analyze TGF- β 1 and OPN protein expression using Enzyme-linked immunosorbent assay (ELISA). For analysis of TGF- β 1, briefly, 48 h before collecting conditioned medium at the respective time points the culture medium was changed from 10% FBS-DMEM to 0.2% FBS-DMEM and cells were allowed to grow. To quantify latent TGF- β 1 200 μ l of conditioned medium was directly used, while for active TGF- β 1 conditioned medium was first acidified (1 N HCl, 10 min) and neutralized (1.2 N NaOH, 0.5 M HEPES, 1 min) and then used. In both cases, samples along with TGF- β 1 standards were diluted in assay buffer (0.1% BSA, 0.1% Tween 20, 150 mM NaCl, 100 mM Tris) and added to 96-well microtitre plates coated overnight with 2 μ g/mL of TGF- β 1 mouse monoclonal antibody (R&D Systems, Minneapolis, MN, USA) and incubated for 2 h at 37°C. Subsequently chicken anti-TGF- β 1 antibody (R&D Systems, Minneapolis, MN, USA) was added and the plates were incubated for 1 h at 37°C. Alkaline phosphatase conjugated rabbit anti-chicken IgG (Jackson ImmunoResearch,

West Grove, PA, USA) was then added at a dilution of 1:5000 and incubated for 1 h at 37°C followed by addition of *p*-nitrophenyl phosphate substrate solution (1 mg/ml in diethanolamine buffer). The resulting colored product was quantified at 405 nm using a microplate reader (THERMOmax, Molecular Devices, Sunnyvale, CA, USA).

For analysis of OPN, 200 µl of conditioned medium was directly used in a Quantikine OPN ELISA kit (R&D Systems, Minneapolis, MN, USA) assay following the manufacturer's instructions. The resulting colored product was quantified as described above.

2.2.12 Statistical Analysis

Experiments were conducted in triplicates and data are expressed as mean ± standard error. Statistical analysis was done using paired t-tests for means with significance set at $P < 0.05$, $P < 0.01$ and $P < 0.001$ using Microsoft Excel 8.0.

2.3 Results

2.3.1 C-GAG Matrix Pore Structure

Acellular C-GAG matrices were prepared by freeze-drying a co-precipitate of type I collagen and chondroitin-6-sulfate, and were subsequently cross-linked by dehydrothermal treatment. The resulting C-GAG matrices were examined by SEM, and were found to have heterogeneous pore structures and sizes (Fig. 2.1). The pore sizes were determined to be $43\pm 17\ \mu\text{m}$ in all of the matrices.

2.3.2 Viability of Fibroblasts on C-GAG Matrices

Fibroblasts were separately isolated from superficial or deep dermal layers of lower abdominal tissue from three abdominoplasty patients and serially expanded. Passage 4 superficial and deep dermal fibroblasts were then independently cultured on cross-linked C-GAG matrices and subsequently assayed at different time points for viability using MTT assay. C-GAG matrices without cells were used as controls. Both superficial and deep fibroblasts were found to be viable on the matrices, with no significant differences observed in viability among fibroblasts (Fig. 2.2).

2.3.3 C-GAG Matrix Contraction by Fibroblasts

C-GAG matrices cultured independently with superficial or deep fibroblasts were analyzed at different time points to determine the degree of fibroblast-mediated contraction. The percentage of contraction of matrices was calculated by determining the change in area of the matrices at each time point with respect to the original area; the original area of the matrix before seeding the fibroblasts was considered as 100%. C-GAG matrices without cells were used as controls. At all time points, matrices with fibroblasts contracted while those without fibroblasts did not contract (Fig. 2.3). Further, deep fibroblasts contracted the matrices more than the superficial fibroblasts with the extent of contraction progressively increasing from day 4 to 21. The difference in matrix contraction by superficial and deep fibroblasts was significant on days 7, 14 and 21 of culture.

2.3.4 Biomechanical Properties of C-GAG Matrices with the Fibroblasts

C-GAG matrices cultured independently with superficial or deep fibroblasts were assessed at day 11 of culture for their stiffness and UTS using a tensile tester to the point just before they failed mechanically. It was observed that C-GAG matrices with deep fibroblasts were significantly stiffer than the matrices containing superficial fibroblasts (Fig. 2.4A), whereas those with superficial

fibroblasts had significantly higher UTS than the matrices containing deep fibroblasts (Fig. 2.4B). Control matrices lacking fibroblasts had significantly lower stiffness and UTS compared to matrices with fibroblasts. Representative stress-strain curves indicate the mode of deformation of matrices containing superficial and deep fibroblasts (Fig. 2.4C).

2.3.5 Collagen Production by the Fibroblasts

The amount of collagen produced by fibroblasts was determined at different time points by quantifying hydroxyproline present in matrices and in conditioned medium by mass spectrometry. The conditioned medium taken from matrices with deep fibroblasts had higher amounts of hydroxyproline than that obtained from matrices with superficial fibroblasts (Fig. 2.5A), which was significant at days 14 and 21 of culture. Similarly, matrices with deep fibroblasts had higher hydroxyproline level than matrices with superficial fibroblasts (Fig. 2.5B), which was significant on days 4 and 14 of culture. Compared to the control matrices lacking fibroblasts, matrices with fibroblasts and the respective conditioned media had significantly higher hydroxyproline levels at all time points.

2.3.6 ECM Production by Fibroblasts

Histological analysis of matrices showed that the matrices with deep fibroblasts stained significantly darker with hematoxylin than those with superficial fibroblasts (Fig. 2.6) indicating the presence of higher amounts of ECM. The intensity of hematoxylin staining was also found to increase with time. Control matrices showed significantly lower hematoxylin staining than matrices with fibroblasts.

2.3.7 Differentiation of Fibroblasts in the C-GAG Matrices to Myofibroblasts

Myofibroblasts mediate wound contraction that occurs during tissue repair and healing, and are characterized by the presence of α -SMA. In order to examine the extent of fibroblast differentiation to myofibroblasts the matrices were subjected to α -SMA staining at the different time points of culture. α -SMA staining was found to be maximum at day 14 for both matrices with superficial fibroblasts and matrices with deep fibroblasts. However, matrices containing deep fibroblasts had significantly more α -SMA staining than matrices with superficial fibroblasts (Fig. 2.7). At the other time points, matrices with deep fibroblasts were generally observed to have more α -SMA staining than matrices with superficial fibroblasts (data not shown). These results suggest that more of

the deep fibroblasts differentiated into myofibroblasts compared to superficial fibroblasts.

2.3.8 Identification of Therapeutic Targets for HTS

To understand the molecular basis of the role of superficial and deep dermal fibroblasts in HTS, expression of 13 different genes was analyzed by qRT-PCR. Genes coding for OPN, HSP-47, TNF- α , ANG-II, MMP-1, TGF- β 1, CTGF, the proteoglycans DCN, VER, and FMOD, and the PPAR isoforms PPAR- α , PPAR- β/δ , PPAR- γ were examined. The obtained gene expression data was normalized with respect to the house-keeping gene Hypoxanthineguanine phosphoribosyl transferase (HPRT). Deep fibroblasts had significantly higher expression of CTGF, TGF- β 1 and HSP-47 compared to superficial fibroblasts, while superficial fibroblasts had significantly higher MMP-1 expression compared to deep fibroblasts (Fig. 2.8A). These results are similar to those found in our previous study [13]. Deep fibroblasts were found to have significantly higher expression of OPN and ANG-II, and lower expression of TNF- α compared to superficial fibroblasts (Fig. 2.8B). In addition, deep fibroblasts had higher expression of PPAR- α but lower expression of PPAR- β/δ and PPAR- γ compared to superficial fibroblasts (Fig. 2.8C). In the case of proteoglycans, deep fibroblasts had higher levels of the large proteoglycan versican, but lower levels of the small proteoglycans decorin and fibromodulin compared to the superficial fibroblasts (Fig. 2.8D).

2.3.9 TGF- β 1 and OPN Production by Fibroblasts

TGF- β 1, one of the most important pro-fibrotic factors involved in wound healing, has been reported to be over-expressed in deep dermal fibroblasts [13] and in HTS [14]. In order to determine the amount of TGF- β 1 protein produced by the superficial and deep dermal fibroblasts in the matrices, their respective conditioned media were analyzed by ELISA. Deep fibroblasts produced significantly more latent TGF- β 1 as well as total TGF- β 1 compared to superficial fibroblasts (Fig. 2.9A). OPN has been reported to play an important role in the fibrosis of lung, kidney and heart [15-17]. To assess whether OPN is differentially expressed in superficial and deep fibroblasts, the level of OPN protein in their respective conditioned media was analyzed. Deep fibroblasts were found to produce more OPN compared to superficial fibroblasts (Fig. 2.9B).

2.4 Discussion

In the case of extensive skin loss as in third-degree burns, CSS are the preferred treatment modality to facilitate rapid wound coverage, tissue repair and healing. Currently preparation of CSS involves the culture of a heterogeneous population of fibroblasts obtained from the dermis on C-GAG matrices [18, 19]. To develop CSS with enhanced functionality that could provide improved outcomes for burn patients it is critical to understand whether superficial and deep dermal fibroblast populations differentially remodel the C-

GAG matrices. A major negative outcome of post-burn skin wound healing is HTS, which affects about two-thirds of burn patients and impacts their complete recovery. Deciphering the anti-fibrotic and pro-fibrotic role of superficial and deep dermal fibroblasts in HTS will enable the development of therapeutic strategies that would reduce the occurrence of post-burn HTS. This study aimed to determine whether superficial and deep dermal fibroblasts differentially remodel C-GAG matrices, and examine if these fibroblast sub-populations differentially contribute to HTS.

In order to limit variability of superficial and deep dermal fibroblasts used in this study, all of the fibroblasts were obtained from lower abdominal tissue of female abdominoplasty patients close in age (29, 32 and 47 years). The cells were seeded on cross-linked C-GAG matrices at a density similar to that reported in literature [20], and the matrices were then assessed for differences in biomechanical properties, collagen synthesis, and gene and protein expression. SEM analysis revealed that the cross-linked C-GAG matrices had heterogeneous pore structures, which made them suitable to support the growth of cells of different sizes (Fig. 2.1). The viability of both superficial and deep fibroblasts on the matrices progressively increased till day 14 of culture and thereafter there was a slight decrease on day 21 possibly due to fibroblast apoptosis (Fig. 2.2). This pattern was also observed on the DAPI stained matrices, with no significant differences between superficial and deep fibroblasts at all time points (data not shown). Day 14 DAPI analysis of matrices with superficial and deep fibroblasts

revealed that cell numbers of superficial and deep fibroblasts on the matrices were similar (Fig. 2.6B). A similar trend has been observed *in vivo* during cutaneous healing, wherein the fibroblasts initially proliferate at a rapid rate and colonize the granulation tissue, later some differentiate into myofibroblasts, and then during the late stages of wound healing some of these fibroblasts and myofibroblasts undergo apoptosis [21, 22]. Apoptosis of fibroblasts has also been reported when cultured in collagen gels [23], although the stimuli that trigger the process are not clearly understood. The initiation of apoptosis is thought to be cell density dependent [24]. By the end of 14 days of culture the matrices have very high fibroblast densities, and therefore it is possible that the high cell density triggers apoptosis. Reduction in mechanical tension has also been proposed to initiate apoptosis of fibroblasts [25]. The observed reduction in mechanical tension after day 14 of culture, which coincides with the end of the matrix contraction phase (Fig. 2.3), also possibly stimulates fibroblast apoptosis.

C-GAG matrices with deep fibroblasts were found to be significantly more contracted than matrices with superficial fibroblasts at days 7, 14 and 21 of culture (Fig. 2.3), which likely is due to differences in matrix remodelling by the superficial and deep fibroblasts. Remodelling of the C-GAG matrices could be compared to that described for the floating collagen lattice model [26], wherein matrix remodelling occurs as a result of motile activity of fibroblasts migrating through the matrix. The high density of fibroblasts on the C-GAG matrices likely results in extensive migration of fibroblasts through the collagen fibrils causing

matrix contraction. Further, the difference in contraction of the matrices by superficial and deep fibroblasts is due to differences in biomechanical properties of the respective remodelled matrices. Tensile strength assessment of the matrices at day 11 of culture revealed that matrices with deep dermal fibroblasts were significantly stiffer (Fig. 2.4A) and had significantly lower UTS compared to matrices with superficial fibroblasts (Fig. 2.4B). Based on our results of contraction, stiffness and UTS of the matrices we conclude that the superficial and deep dermal fibroblasts differentially remodel the C-GAG matrices by selectively altering the biomechanical properties of the respective matrices. Interestingly, in HTS it has been observed that the scar tissue has different biomechanical properties compared to normal skin; HTS tissue is stiffer and has lower UTS compared to normal tissue [27, 28]. We therefore propose that deep dermal fibroblasts play a critical role in the formation of HTS.

Homeostasis of collagen in the skin is normally maintained by the fine balance between the synthesis and degradation pathways. However, in the case of thermal and other skin injuries this balance is disturbed causing abnormalities in collagen metabolism. This leads to accumulation of collagen in the ECM, which is characteristic of HTS and other fibroproliferative diseases [29-31]. Such alterations in ECM composition are responsible for the compromised appearance and functionality of the scar tissue observed in HTS. To determine the amount of collagen produced by superficial and deep dermal fibroblasts, the respective matrices and conditioned media were analyzed for the presence of

hydroxyproline. The conditioned media of the deep fibroblasts had significantly higher hydroxyproline levels than that of the superficial fibroblasts on days 14 and 21 of culture (Fig. 2.5A). Also, matrices populated by deep fibroblasts had significantly higher levels of hydroxyproline than those by superficial fibroblasts on days 4 and 14 of culture (Fig. 2.5B). These results clearly indicate that deep dermal fibroblasts contribute to the formation of HTS by producing excessive amounts of collagen.

The higher amount of collagen produced by deep fibroblasts contributes to the observed increased stiffness of the matrices. Differences in proteoglycan expression by superficial and deep fibroblasts could be the reason for observed differences in UTS. The increased stiffness in turn stimulates differentiation of fibroblasts to myofibroblasts since substrate stiffness has been previously reported to stimulate differentiation of fibroblasts to myofibroblasts [21]. Also, cell substrate stiffness and mechanical tension from cell adhesion to the substrate have been found to be critical for differentiation of cells in culture [32-34]. Recently Li *et al.* demonstrated that matrix substrate stiffness regulates *in vitro* differentiation of rat hepatic stellate cells and portal fibroblasts to myofibroblasts [35]. Mechanical tension has also been identified to contribute to the release of active TGF- β 1 from the ECM, which gives rise to an environment conducive for differentiation and maintenance of myofibroblasts [36]. Further, Georges *et al.* found that increased stiffness of liver precedes myofibroblast activation and ECM deposition in a rat model of liver fibrosis [37]. Myofibroblasts

are characterized by an increased contractile ability and have higher expression of α -SMA and collagen [38]. To determine the extent of fibroblast differentiation in the matrices, immunohistochemical analysis of the matrices was done to examine the expression of α -SMA. Matrices with deep dermal fibroblasts showed higher number of myofibroblasts compared to those with superficial fibroblasts on day 14 of culture (Fig. 2.7), which coincided with the end of the matrix contraction phase (see Fig. 2.3). Increased activation of myofibroblasts in matrices containing deep dermal fibroblasts explains the observed increased contraction of these matrices. The presence of higher number of myofibroblasts in the matrices with deep dermal fibroblasts may also be due to decreased apoptosis of the myofibroblasts since increased ECM stiffness has been correlated to down-regulation of myofibroblast apoptosis in HTS and other fibrotic disorders [39].

In order to understand the molecular basis of functional differences between superficial and deep dermal fibroblasts, and determine their anti-fibrotic and pro-fibrotic roles, expression of 13 genes and two proteins was analyzed. Relative gene expression of CTGF, TGF- β 1, HSP-47, MMP-1, OPN, ANG-II, TNF- α , PPAR- α , PPAR- β/δ , PPAR- γ , VER, DCN and FMOD was examined on days 4, 7, 14 and 21 of culture. CTGF, TGF- β 1 and HSP-47 were up-regulated while MMP-1 was down-regulated in the deep fibroblasts (Fig. 2.8A), similar to that previously reported [13]. Analysis of TGF- β 1 protein levels on days 4, 7, 14 and 21 of culture revealed a progressive increase in TGF- β 1 over time in both superficial

and deep fibroblasts, with deep fibroblasts having significantly more TGF- β 1 at days 7, 14 and 21 compared to superficial fibroblasts (Fig. 2.9A). TGF- β 1 plays a critical role in wound healing and is known to be over-expressed in HTS fibroblasts compared to normal dermal fibroblasts [14, 40]. Of the known factors implicated in wound healing and fibrosis, TGF- β 1 is considered important since it directly mediates collagen synthesis at the wound site. Development of HTS and other fibrotic diseases is linked to over-expression of TGF- β 1 and its downstream mediator CTGF [31, 40, 41]. HSP-47 is a heat shock protein that functions as a chaperone for type I collagen, and therefore is a marker for the observed increase in type I collagen production during HTS [42]. Further, HTS fibroblasts are known to express significantly less MMP-1 than normal fibroblasts obtained from the same patients [43]. Taken together, increased TGF- β 1, CTGF, HSP-47 and decreased MMP-1 expression contributes to excess accumulation of collagen on matrices with deep fibroblasts, which is similar to that observed in the case of HTS.

OPN and ANG-II expression was up-regulated, while TNF- α was down-regulated in the deep fibroblasts (Fig. 2.8B). Analysis of OPN protein levels on days 4, 7, 14 and 21 of culture showed that it peaks at day 7 and gradually decreases thereafter, with significantly higher levels observed for deep fibroblasts as opposed to superficial fibroblasts (Fig. 2.9B). OPN has been suggested to be essential for TGF- β 1 and type I collagen expression in lung fibrosis [15], and for α -SMA and CTGF expression in cardiac fibrosis [17].

Further, depletion of OPN levels at wound sites was recently found to accelerate skin wound healing, reduce granulation tissue formation and subsequent fibrosis [44]. Increased OPN production by deep fibroblasts therefore suggests a pro-fibrotic role for deep fibroblasts in HTS. ANG-II has been previously reported to be involved in triggering fibrosis in other organs such as lungs, heart and kidney by increasing TGF- β 1 expression and collagen production [45-47]. The reduced expression of TNF- α in deep fibroblasts observed in this study is consistent with the decreased level of TNF- α reported for HTS tissue [48]. TNF- α is a potent inflammatory cytokine with antagonistic activity towards TGF- β 1; it inhibits ECM synthesis and activates matrix metalloproteinases [49, 50]. Additionally, it was recently identified to inhibit α -SMA expression and subsequent myofibroblast differentiation in human dermal fibroblasts [51].

Interestingly, expression of PPAR- α was elevated, whereas that of PPAR- β/δ and PPAR- γ was reduced in deep fibroblasts compared to the superficial fibroblasts (Fig. 2.8C). PPARs are ligand-activated transcription factors that have recently been identified to be important in organ fibrosis [31]. Among the PPARs, PPAR- γ plays an active role in the regulation of cell cycle, inflammation and immune responses, and is a promising candidate for development of anti-fibrotic therapeutics. It is also known to have an antagonistic function with respect to TGF- β 1 [52]. PPAR- γ -based strategies have been employed to inhibit fibrosis in organs such as liver, pancreas, lungs and kidney [53-56]. Natural PPAR- γ ligands like 15-deoxy- Δ 12,14-prostaglandin J2 or synthetic ligands like thiazolidinedione

compounds were found to inhibit TGF- β 1 and significantly reduce myofibroblast differentiation and collagen production in hepatic and pancreatic stellate cells, and pulmonary and kidney fibroblasts. PPAR- α and PPAR- β/δ have been studied to a relatively lesser extent in the context of fibrosis compared PPAR- γ . Use of PPAR- α and PPAR- β/δ ligands have been reported to prevent ANG-II-induced myocardial fibrosis in rats [57, 58]. The observed differential expression of PPAR- α , PPAR- β/δ and PPAR- γ by deep fibroblasts suggests a role for these fibroblasts in HTS and the potential of using PPAR ligands to treat HTS.

Expression of small-leucine rich proteoglycans (SLRPs), DCN and FMOD, was low and that of the large proteoglycan, VER, was high in the deep fibroblasts compared to superficial fibroblasts (Fig. 2.8D). The observed differential expression of DCN and VER is consistent with that previously reported for different dermal fibroblast sub-populations and fibroblasts from post-burn HTS [13, 59, 60]. DCN and FMOD are involved in regulation of TGF- β 1 activity and collagen fibrillogenesis [61], and VER is a hyaluronan-binding proteoglycan involved in cell adhesion, migration and proliferation [62]. Adenoviral over-expression of FMOD reduced scar formation in a rabbit skin wound healing model and suppressed expression of pro-fibrotic TGF- β 1 and TGF- β 2, and increased expression of anti-fibrotic TGF- β 3 in cultured fibroblasts [63]. Interestingly, FMOD expression was found to decrease during transition from fetal to adult wound repair in rat skin wounds [64]. Up-regulation of the SLRPs could therefore

be a useful strategy to inhibit the pro-fibrotic activity of TGF- β 1 and reduce scar formation during wound repair.

2.5 Conclusions

In this study superficial and deep dermal fibroblasts were found to differentially remodel C-GAG matrices; deep fibroblasts contracted and stiffened the matrices significantly more and decreased their ultimate tensile strength compared to superficial fibroblasts. Deep fibroblasts were also found to express significantly more OPN, ANG-II and PPAR- α , and significantly less TNF- α , PPAR- β/δ , PPAR- γ and FMOD compared to superficial fibroblasts. The newly identified molecular targets described above interact with the critical regulator, TGF- β 1, and therefore are ideal candidates to develop strategies to control HTS and promote regenerative healing of the skin. Further, results from this study indicate that the use of a specific sub-population of dermal fibroblasts such as superficial fibroblasts in CSS rather than a heterogeneous population of fibroblasts may be more beneficial for wound healing and minimizing post-burn HTS.

2.6 Table and Figures

Table 2.1: Primers Used in qRT-PCR for Amplification of Genes of Interest

| Gene | Forward Primer | Reverse Primer |
|--|------------------------------|------------------------------|
| Versican | GCAGCTGAACGGGAATGC | CGTGAGACAGGATGCTTG TGA |
| Decorin | TGTCATAGAACTGGGCACCA AT | GGAAAGCCCCATTTTCAA TTC |
| Fibromodulin | TTTTATCATCGTTCTGCCTT CATG | TGTTTGCGGGACCTTAGG AA |
| TGF- β 1 | GGGAAATTGAGGGCTTTTCG | AGTGTGTTATCCCTGCTG TCACA |
| MMP-1 | CCTCGCTGGGAGCAAACA | TTGGCAAATCTGGCGTGT AA |
| HSP47 | TGAAGATCTGGATGGGGAA G | CTTGTCAATGGCCTCAGT CA |
| CTGF | TCCACCCGGGTTACCAATG | CAGGCGGCTCTGCTTCTC TA |
| TNF- α | TGCTCCTCACCCACACCAT | GGAGGTTGACCTTGGTCT GGTA |
| Angiotensin II | CCCGTGACCAAGTCCTGAA | AGCAAATGATGAAGGCCA GAA |
| Osteopontin | TGAGCATTCCGATGTGATTG A | TGTGGAATTCACGGCTGA CTT |
| PPAR- α | AACATCCAAGAGATTTTCGCA ATC | CCGTAAAGCCAAAGCTTC CA |
| PPAR- β/δ | AGCATCCTCACCGGCAAA | CGATGTCGTGGATCACAA AGG |
| PPAR- γ | TCAGGGCTGCCAGTTTCG | GCTTTTGGCATACTCTGT GATCTC |
| Hypoxanthine guanine phospho- ribosyl transferase (House-keeping gene) | GACCAGTCAACAGGGGACA | ACACTTCGTGGGGTCCTT TT |

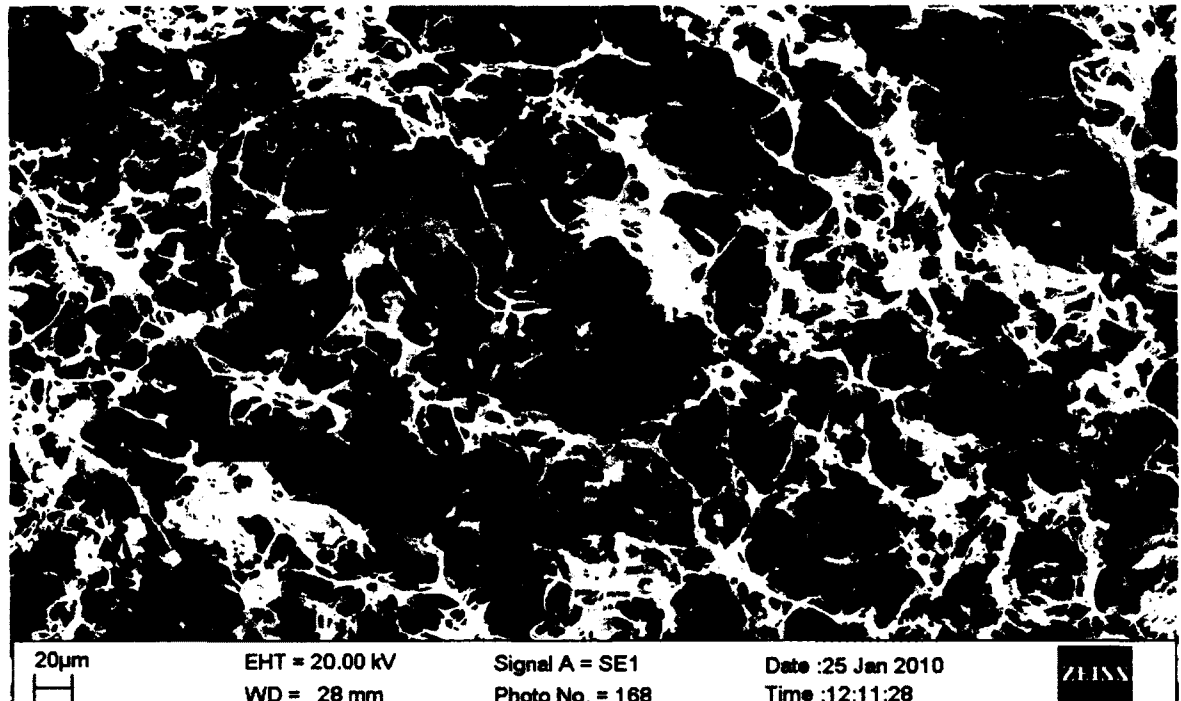


Figure 2.1: Scanning Electron Micrograph of C-GAG Matrix.

Scanning electron micrograph of a representative dehydrothermally cross- linked C-GAG matrix at 500× magnification showing heterogeneous pore structures and sizes. Scale bar = 20 µm.

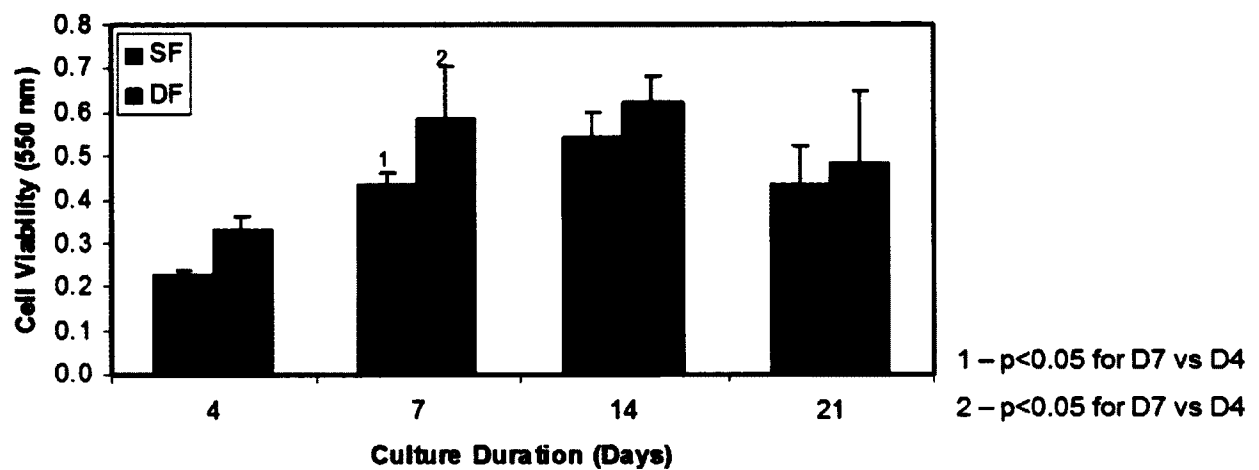


Figure 2.2: Viability of Superficial and Deep Dermal Fibroblasts Cultured on Cross-Linked C- GAG Matrices.

Superficial and deep dermal fibroblasts were cultured on C-GAG matrices and their viability on days 4, 7, 14 and 21 was assessed by MTT assay. Each bar represents Mean \pm SE (standard error) Cell Viability (n = 3 abdominoplasty patients). Significant increase in viability of superficial ($*p < 0.05$) and deep dermal fibroblasts ($*p < 0.05$) was observed on day 7 compared to day 4.

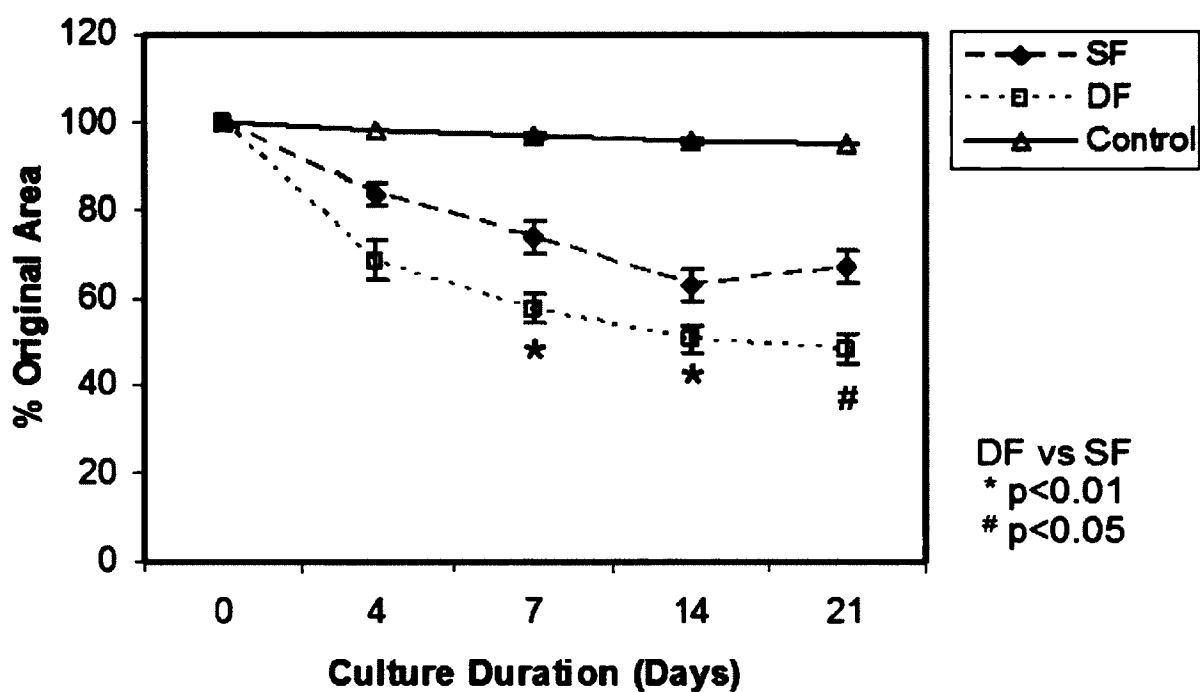


Figure 2.3: Fibroblast-Mediated Contraction of C-GAG Matrices by Superficial and Deep Dermal Fibroblasts.

Superficial and deep dermal fibroblasts were independently cultured on C-GAG matrices for 21 days. Digital photographs of the matrices were taken before the fibroblasts were seeded and on days 4, 7, 14 and 21 of culture and the extent of contraction was measured using NIH Image J. Each data point represents Mean

± SE Contraction (n = 3 abdominoplasty patients). Significant differences in contraction were observed between deep and superficial dermal fibroblasts on days 7 (**p<0.01), 14 (**p<0.01), and 21 (*p<0.05).

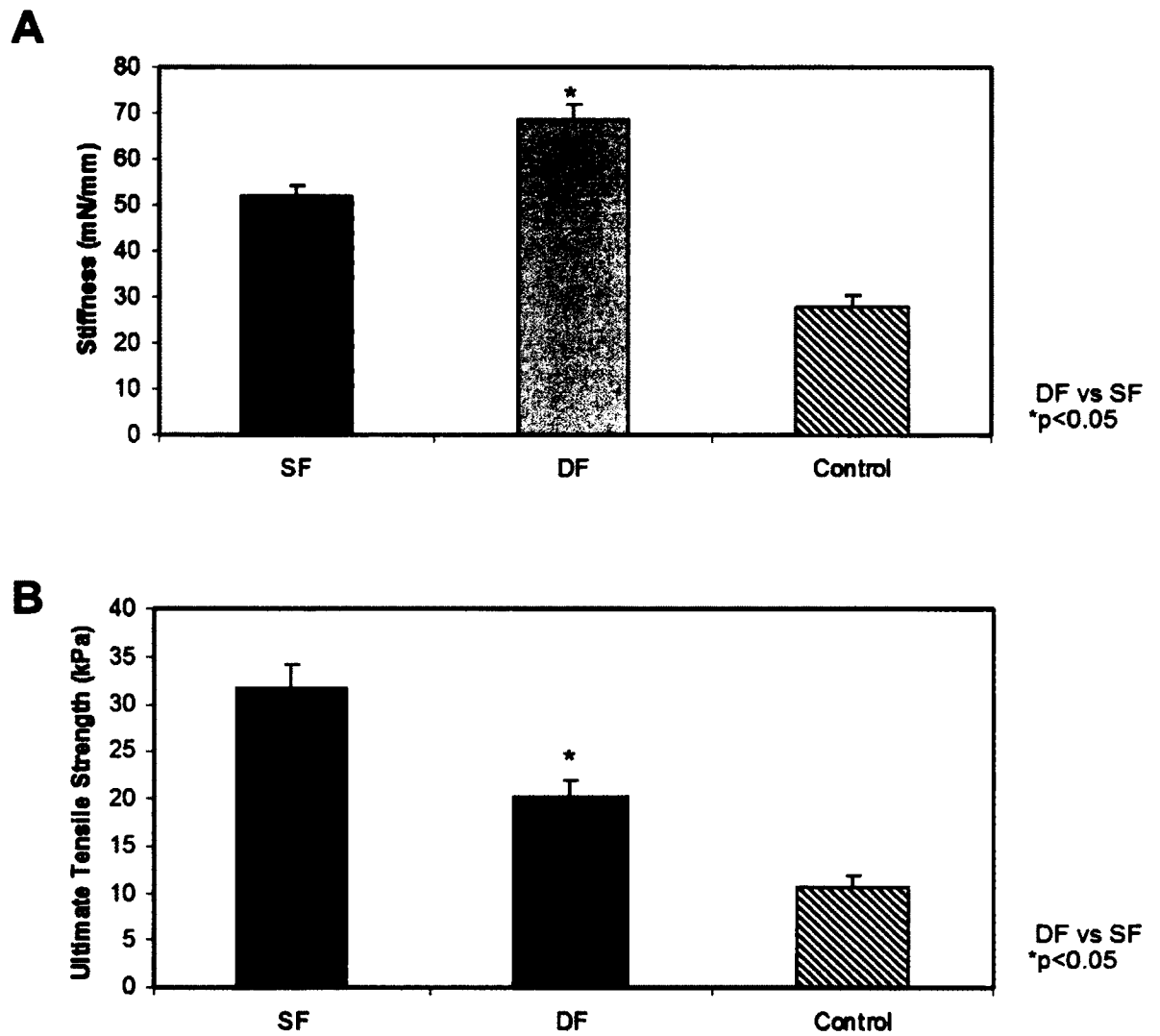


Figure 2.4A-B: Biomechanical Properties of C-GAG Matrices with Superficial and Deep Dermal Fibroblasts.

The biomechanical properties of the C-GAG matrices with superficial and deep dermal fibroblasts were assessed on day 11 of culture using MTS tensile tester.

A. The stiffness of C-GAG matrices with superficial and deep dermal fibroblasts.

Each bar represents Mean \pm SE Stiffness (n = 3 abdominoplasty patients).

Significant differences in matrix stiffness were observed between deep and

superficial fibroblasts (*p<0.05). **B.** The UTS of C-GAG matrices with superficial

and deep dermal fibroblasts. Each bar represents Mean \pm SE UTS (n = 3

abdominoplasty patients). Significant differences in matrix UTS were observed

between deep and superficial fibroblasts (*p<0.05).

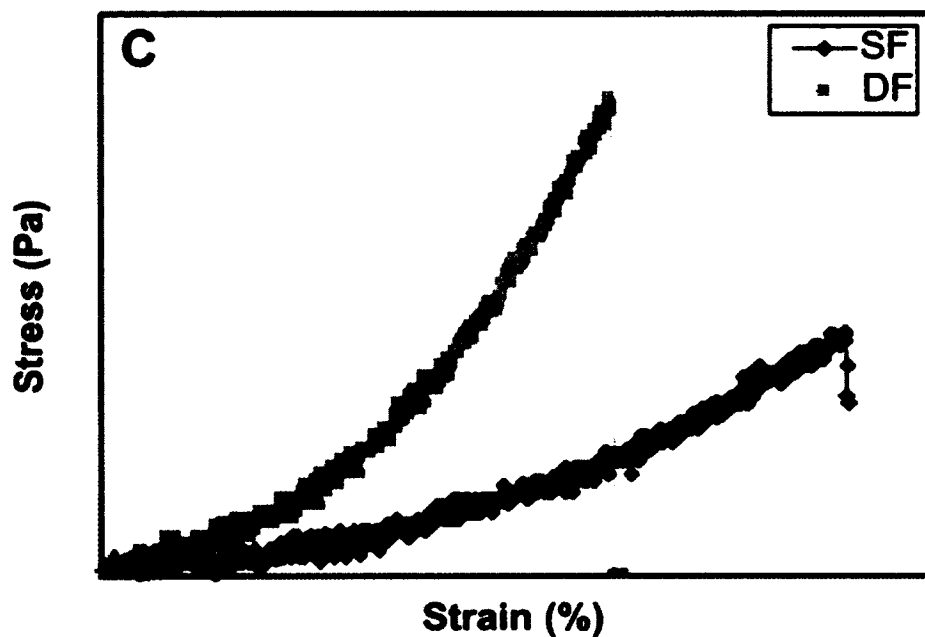


Figure 2.4C: Biomechanical Properties of C-GAG Matrices with Superficial and Deep Dermal Fibroblasts.

The biomechanical properties of the C-GAG matrices with superficial and deep dermal fibroblasts were assessed on day 11 of culture using MTS tensile tester. C. Representative stress-strain curve for matrices with superficial and deep dermal fibroblasts.

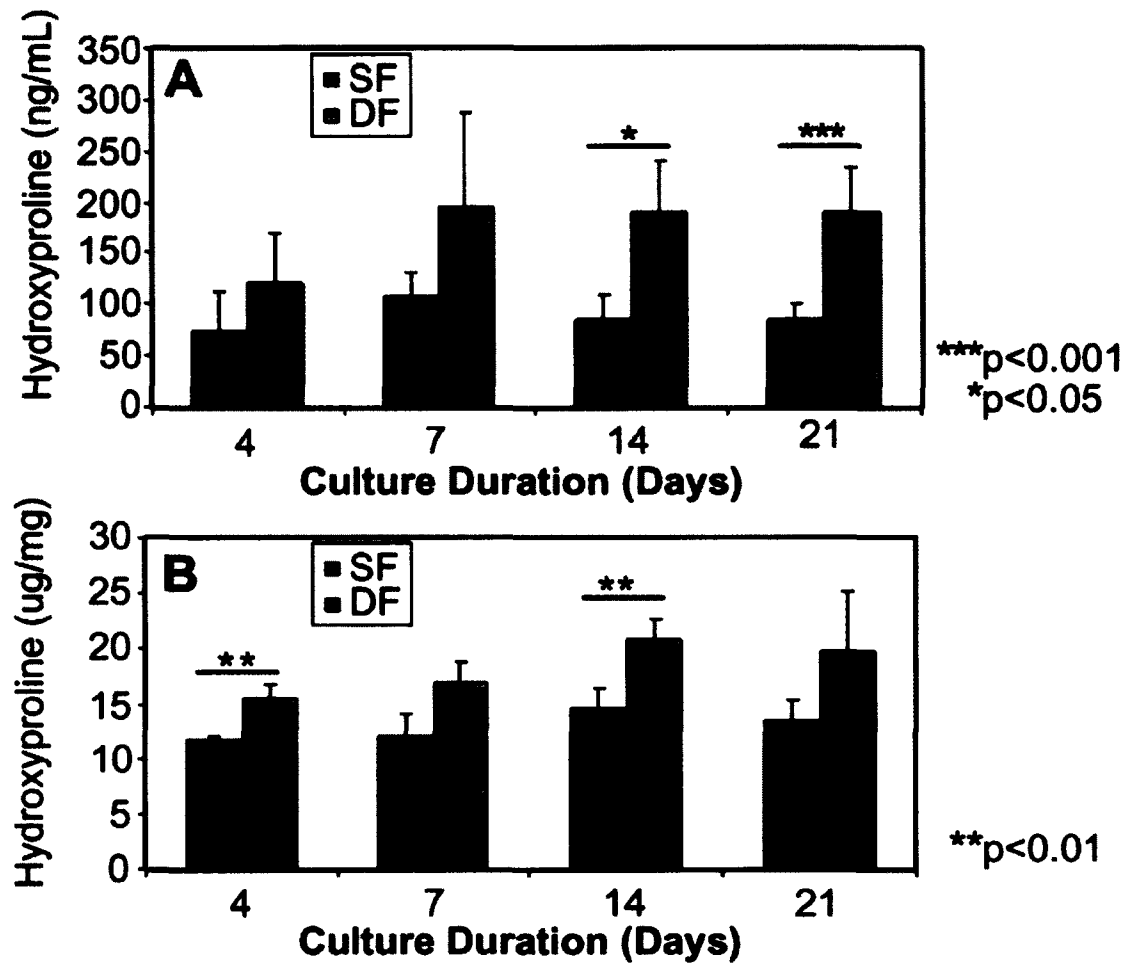


Figure 2.5A-B: Measurement of Collagen Production by Superficial and Deep Dermal Fibroblasts

Collagen production by superficial and deep dermal fibroblasts was assessed by LC/MS measurement of hydroxyproline on days 4, 7, 14 and 21 of culture. Each bar represents Mean \pm SE Hyp (n = 3 abdominoplasty patients). **A.** Superficial and deep dermal fibroblasts were grown in 10% FBS/DMEM and 48 h before each time point the medium was changed to 2% FBS/DMEM. The supernatants were collected and assessed by LC/MS. Significant differences were observed in level of hydroxyproline in conditioned media of deep and superficial dermal fibroblasts on days 14 (*p<0.05) and 21 (**p<0.001). **B.** The matrices were freeze-dried, weighed, hydrolyzed and subsequently subjected to LC/MS analysis. Significant differences were observed in level of hydroxyproline in C-GAG matrix that contained deep and superficial dermal fibroblasts on days 4 (**p<0.01) and 14 (**p<0.01).

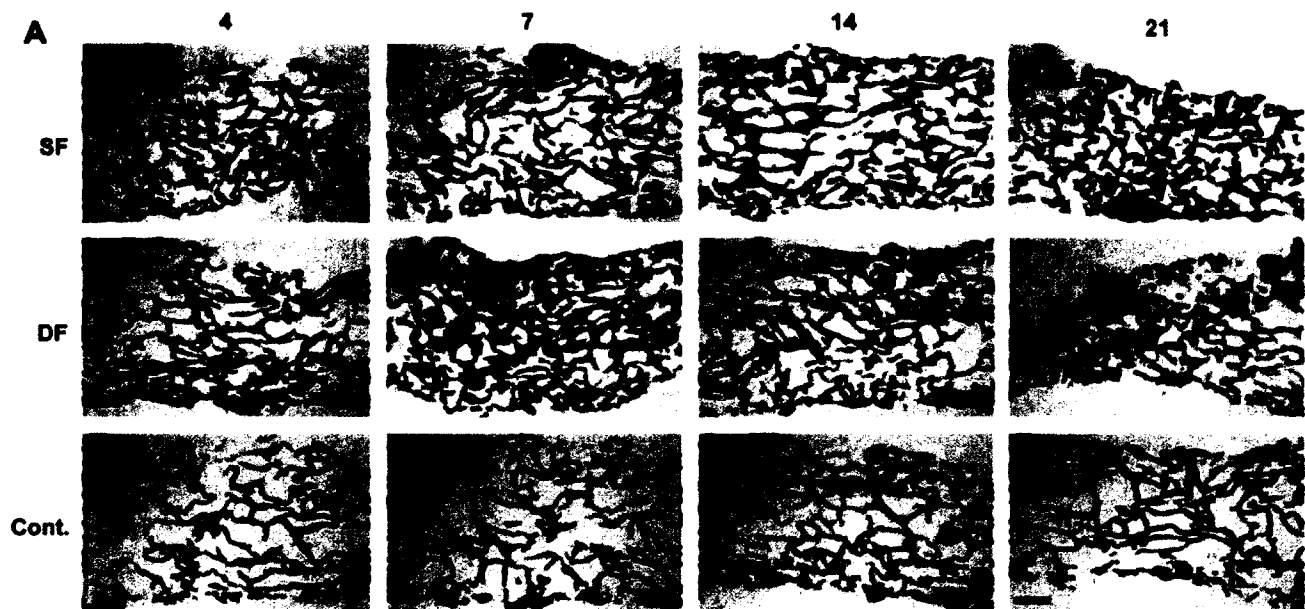


Figure 2.6A: Hematoxylin & Eosin Staining of the Matrices for Collagen Content.

A. Hematoxylin & Eosin staining of the matrices with and without the dermal fibroblasts for collagen content at a magnification of 100 \times . Scale bar = 100 μ m.

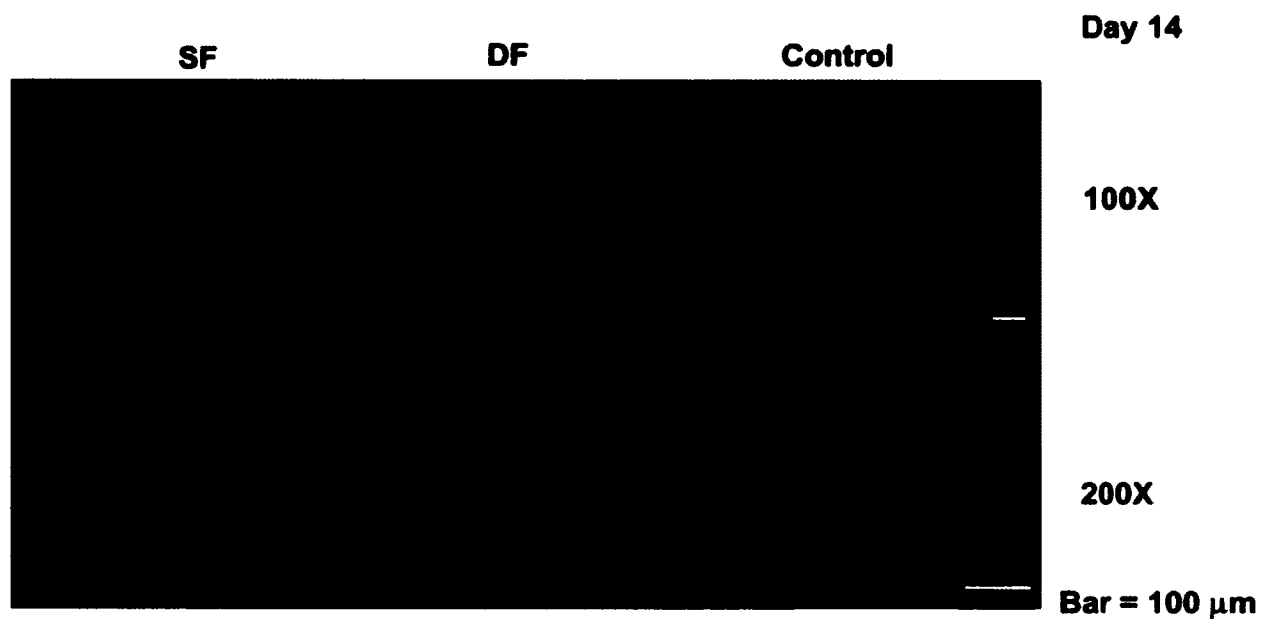


Figure 2.6B: DAPI Staining of the Matrices.

Hematoxylin & Eosin staining of the matrices with and without the dermal fibroblasts was done to assess collagen content. **B.** Blue indicates DAPI staining for nuclei on matrices containing superficial and deep dermal fibroblasts on day 14 of culture. Magnification of upper panel is 100 \times , while magnification of lower panel is 200 \times . Scale bar = 100 μm .

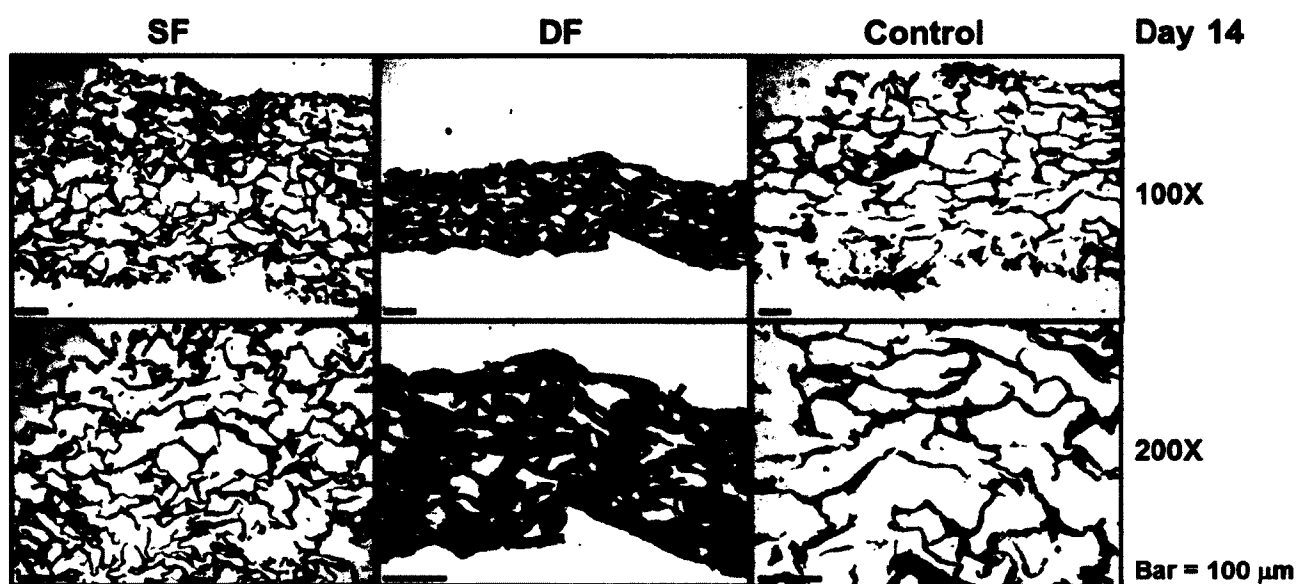


Figure 2.7: Immunohistochemical Analysis of α -SMA Expression.

Immunohistochemical analysis of α -SMA expression was done on matrices containing superficial and deep dermal fibroblasts on day 14 of culture.

Magnification of upper panel is 100 \times , while magnification of lower panel is 200 \times .

Scale bar = 100 μ m.

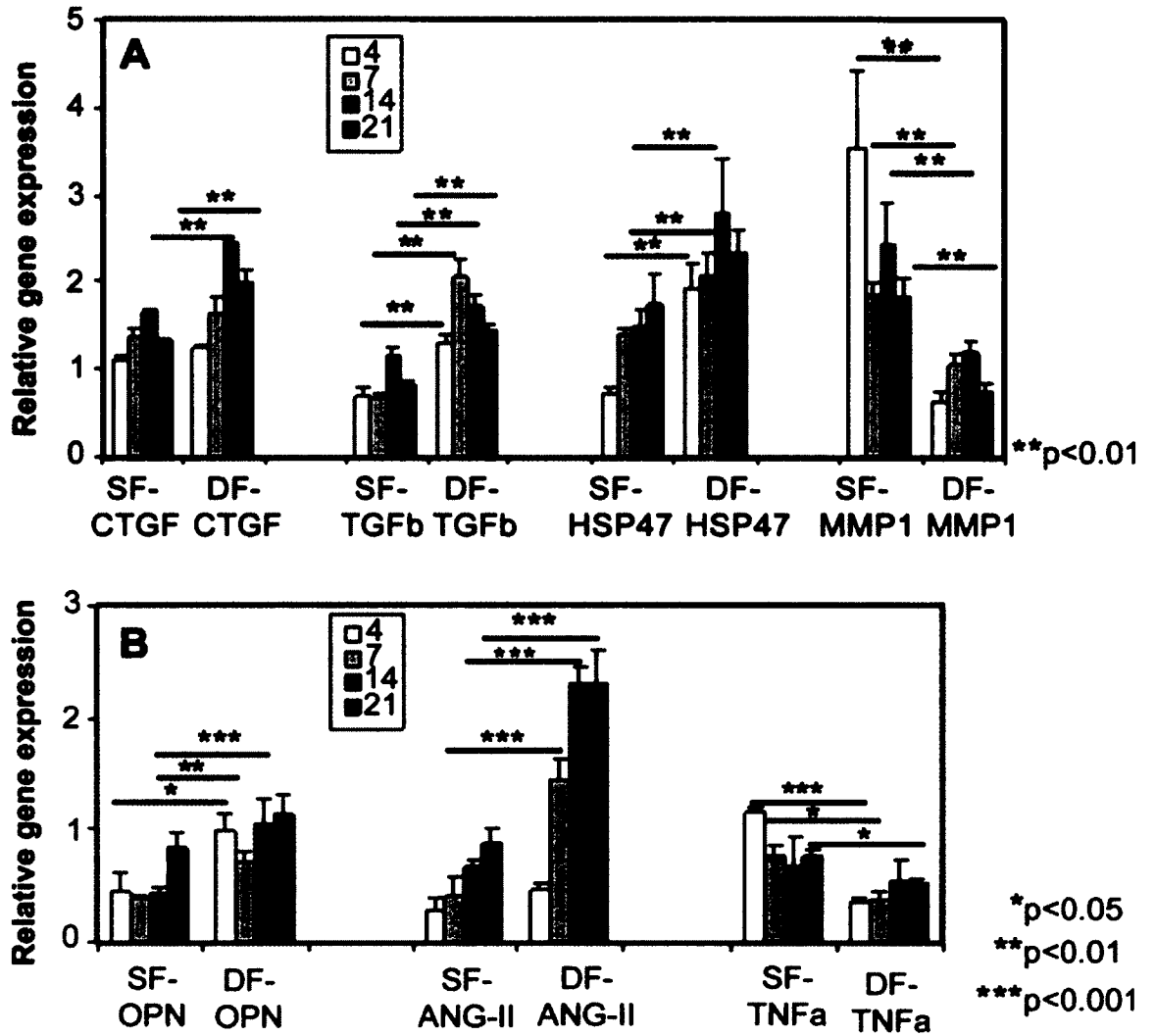


Figure 2.8A-B: Assessment of Relative Gene Expression of Superficial and Deep Dermal Fibroblasts Cultured on C-GAG Matrices by qRT-PCR.

mRNA was isolated from cultures of superficial and deep dermal fibroblasts on days 4, 7, 14 and 21 and reverse transcribed using specific primers for the genes of interest. cDNA was amplified and relative gene expression was analyzed by qRT-PCR. Each bar represents Mean \pm SE Relative gene expression (n = 3 abdominoplasty patients). **A.** Relative gene expression for CTGF, TGF- β 1, HSP-47 and MMP-1. Significant differences between deep and superficial dermal fibroblasts were observed for: CTGF on days 7, 14 and 21 (**p<0.01), TGF- β 1 on days 4,7, 14 and 21 (**p<0.01), HSP-47 on days 4,7 and 14 (**p<0.01), and MMP-1 on days 4, 7, 14 and 21 (**p<0.01). **B.** Relative gene expression for OPN, ANG-II and TNF- α . Significant differences between deep and superficial dermal fibroblasts were observed for: OPN on days 4 (**p<0.001), 7 (**p<0.01) and 14(**p<0.001), ANG-II on days 7 (**p<0.001), 14 (*p<0.05) and 21(*p<0.05), TNF- α on days 4 (**p<0.001), 7(*p<0.05) and 21(*p<0.05).

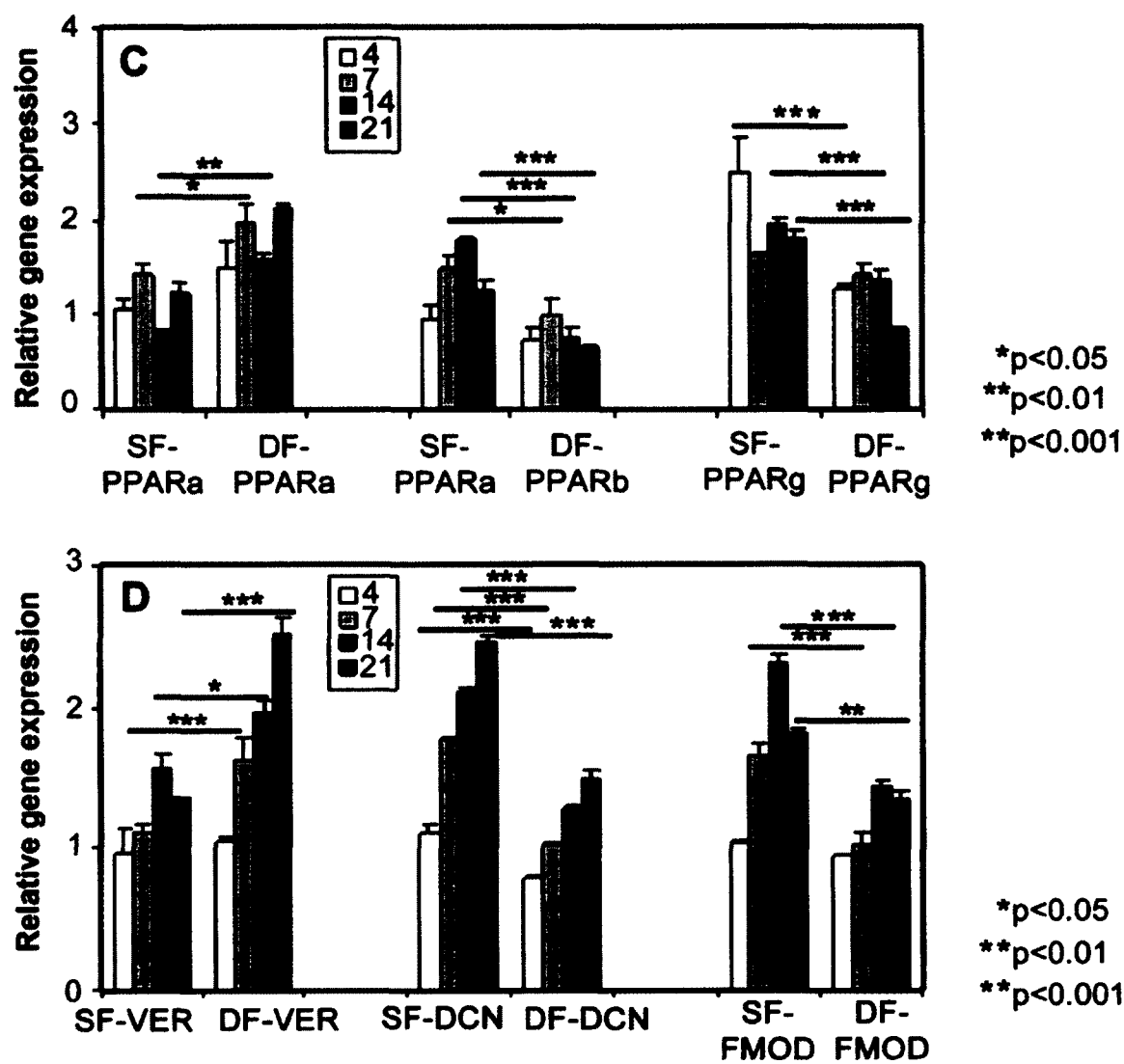


Figure 2.8C-D: Assessment of Relative Gene Expression of Superficial and Deep Dermal Fibroblasts Cultured on C-GAG Matrices by qRT-PCR.

mRNA was isolated from cultures of superficial and deep dermal fibroblasts on days 4, 7, 14 and 21 and reverse transcribed using specific primers for the genes of interest. cDNA was amplified and relative gene expression was analyzed by qRT-PCR. Each bar represents Mean \pm SE Relative gene expression (n = 3 abdominoplasty patients). **C.** Relative gene expression for PPAR- α , PPAR- β/δ , and PPAR- γ . Significant differences between deep and superficial dermal fibroblasts were observed for: PPAR- α on days 7 (***p<0.001), 14 (***p<0.001) and 21(**p<0.01), PPAR- β/δ on days 7 (**p<0.01), 14 (***p<0.001) and 21(**p<0.01), PPAR- γ on days 4 (***p<0.001), 14 (***p<0.001) and 21(***p<0.001). **D.** Relative gene expression for VER, DCN and FMOD. Significant differences between deep and superficial dermal fibroblasts were observed for: VER on days 7 (***p<0.001), 14 (*p<0.05) and 21(***p<0.001), DCN on days 4, 7, 14 and 21 (all ***p<0.001), FMOD on days 7(***p<0.001), 14 (***p<0.001) and 21 (**p<0.01).

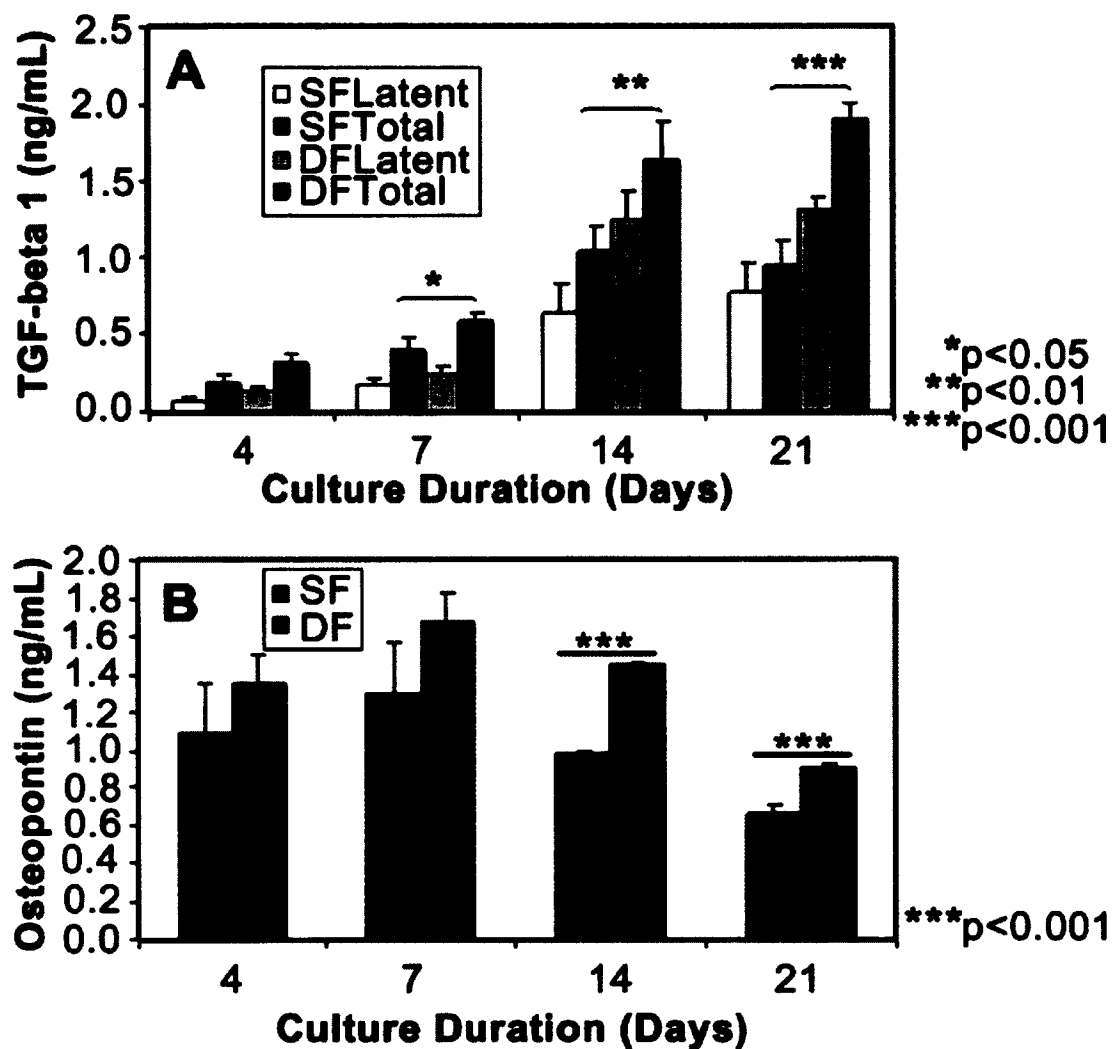


Figure 2.9A-B: Analysis of Protein Expression by Superficial and Deep Dermal Fibroblasts Cultured on C-GAG Matrices.

Analysis of protein expression by superficial and deep dermal fibroblasts cultured on C-GAG matrices was done using ELISA on days 4, 7, 14 and 21 of culture. **A.** Latent and total TGF- β 1 in conditioned media from matrices with superficial and deep dermal fibroblasts. 48 h before each time point, media was changed from 10% FBS/DMEM to 0.2% FBS/DMEM. Conditioned media was directly used in the assay to quantify latent TGF- β 1, while to quantify active TGF- β 1 the conditioned media was acidified and then neutralized before use in assay. Total TGF- β 1 includes latent and active TGF- β 1. Each bar represents Mean \pm SE TGF- β 1 (n = 3 abdominoplasty patients). Significant differences were observed in total TGF- β 1 content of deep and superficial dermal fibroblasts on days 7 (*p<0.05), 14 (**p<0.01) and 21 (**p<0.001). **B.** OPN in conditioned media from matrices with superficial and deep dermal fibroblasts. Each bar represents Mean \pm SE OPN (n = 3 abdominoplasty patients). Significant differences were observed in OPN content of deep and superficial dermal fibroblasts on days 14 (**p<0.001) and 21 (**p<0.001).

2.7 References

- [1] Boyce ST, Kagan RJ, Yakuboff KP, Meyer NA, Rieman MT, Greenhalgh DG, et al. Cultured skin substitutes reduce donor skin harvesting for closure of excised, full-thickness burns. *Ann Surg.* 2002;235:269-79.
- [2] Scott PG, Ghahary A, Tredget EE. Molecular and cellular aspects of fibrosis following thermal injury. *Hand Clin.* 2000;16:271-87.
- [3] Bombaro KM, Engrav LH, Carrougher GJ, Wiechman SA, Faucher L, Costa BA, et al. What is the prevalence of hypertrophic scarring following burns? *Burns.* 2003;29:299-302.
- [4] Monstrey S, Hoeksema H, Verbelen J, Pirayesh A, Blondeel P. Assessment of burn depth and burn wound healing potential. *Burns.* 2008;34:761-9.
- [5] Cubison TC, Pape SA, Parkhouse N. Evidence for the link between healing time and the development of hypertrophic scars (HTS) in paediatric burns due to scald injury. *Burns.* 2006;32:992-9.
- [6] Dunkin CS, Pleat JM, Gillespie PH, Tyler MP, Roberts AH, McGrouther DA. Scarring occurs at a critical depth of skin injury: precise measurement in a graduated dermal scratch in human volunteers. *Plast Reconstr Surg.* 2007;119:1722-32; discussion 33-4.
- [7] Sorrell JM, Caplan AI. Fibroblast heterogeneity: more than skin deep. *J Cell Sci.* 2004;117:667-75.
- [8] Schafer IA, Pandey M, Ferguson R, Davis BR. Comparative observation of fibroblasts derived from the papillary and reticular dermis of infants and adults:

growth kinetics, packing density at confluence and surface morphology. *Mech Ageing Dev.* 1985;31:275-93.

[9] Azzarone B, Macieira-Coelho A. Heterogeneity of the kinetics of proliferation within human skin fibroblastic cell populations. *J Cell Sci.* 1982;57:177-87.

[10] Sorrell JM, Baber MA, Caplan AI. Site-matched papillary and reticular human dermal fibroblasts differ in their release of specific growth factors/cytokines and in their interaction with keratinocytes. *J Cell Physiol.* 2004;200:134-45.

[11] Ali-Bahar M, Bauer B, Tredget EE, Ghahary A. Dermal fibroblasts from different layers of human skin are heterogeneous in expression of collagenase and types I and III procollagen mRNA. *Wound Repair Regen.* 2004;12:175-82.

[12] Armour A, Scott PG, Tredget EE. Cellular and molecular pathology of HTS: basis for treatment. *Wound Repair Regen.* 2007;15 Suppl 1:S6-17.

[13] Wang J, Dodd C, Shankowsky HA, Scott PG, Tredget EE. Deep dermal fibroblasts contribute to hypertrophic scarring. *Lab Invest.* 2008;88:1278-90.

[14] Wang R, Ghahary A, Shen Q, Scott PG, Roy K, Tredget EE. Hypertrophic scar tissues and fibroblasts produce more transforming growth factor-beta1 mRNA and protein than normal skin and cells. *Wound Repair Regen.* 2000;8:128-37.

[15] Berman JS, Serlin D, Li X, Whitley G, Hayes J, Rishikof DC, et al. Altered bleomycin-induced lung fibrosis in osteopontin-deficient mice. *Am J Physiol Lung Cell Mol Physiol.* 2004;286:L1311-8.

- [16] Persy VP, Verhulst A, Ysebaert DK, De Greef KE, De Broe ME. Reduced postischemic macrophage infiltration and interstitial fibrosis in osteopontin knockout mice. *Kidney Int.* 2003;63:543-53.
- [17] Lenga Y, Koh A, Perera AS, McCulloch CA, Sodek J, Zohar R. Osteopontin expression is required for myofibroblast differentiation. *Circ Res.* 2008;102:319-27.
- [18] Boyce ST, Kagan RJ, Greenhalgh DG, Warner P, Yakuboff KP, Palmieri T, et al. Cultured skin substitutes reduce requirements for harvesting of skin autograft for closure of excised, full-thickness burns. *J Trauma.* 2006;60:821-9.
- [19] Swope VB, Boyce ST. Differential expression of matrix metalloproteinase-1 in vitro corresponds to tissue morphogenesis and quality assurance of cultured skin substitutes. *J Surg Res.* 2005;128:79-86.
- [20] Powell HM, Boyce ST. EDC cross-linking improves skin substitute strength and stability. *Biomaterials.* 2006;27:5821-7.
- [21] Tomasek JJ, Gabbiani G, Hinz B, Chaponnier C, Brown RA. Myofibroblasts and mechano-regulation of connective tissue remodelling. *Nat Rev Mol Cell Biol.* 2002;3:349-63.
- [22] Desmouliere A, Redard M, Darby I, Gabbiani G. Apoptosis mediates the decrease in cellularity during the transition between granulation tissue and scar. *Am J Pathol.* 1995;146:56-66.

- [23] Fluck J, Querfeld C, Cremer A, Niland S, Krieg T, Sollberg S. Normal human primary fibroblasts undergo apoptosis in three-dimensional contractile collagen gels. *J Invest Dermatol.* 1998;110:153-7.
- [24] Miller CC, Godeau G, Lebreton-DeCoster C, Desmouliere A, Pellat B, Dubertret L, et al. Validation of a morphometric method for evaluating fibroblast numbers in normal and pathologic tissues. *Exp Dermatol.* 2003;12:403-11.
- [25] Grinnell F, Zhu M, Carlson MA, Abrams JM. Release of mechanical tension triggers apoptosis of human fibroblasts in a model of regressing granulation tissue. *Exp Cell Res.* 1999;248:608-19.
- [26] Jiang H, Rhee S, Ho CH, Grinnell F. Distinguishing fibroblast promigratory and procontractile growth factor environments in 3-D collagen matrices. *Faseb J.* 2008;22:2151-60.
- [27] Dunn MG, Silver FH, Swann DA. Mechanical analysis of hypertrophic scar tissue: structural basis for apparent increased rigidity. *J Invest Dermatol.* 1985;84:9-13.
- [28] Clark JA, Cheng JC, Leung KS. Mechanical properties of normal skin and hypertrophic scars. *Burns.* 1996;22:443-6.
- [29] Rudolph R. Wide spread scars, hypertrophic scars, and keloids. *Clin Plast Surg.* 1987;14:253-60.
- [30] Cohen IK. Can collagen metabolism be controlled: theoretical considerations. *J Trauma.* 1985;25:410-2.

- [31] Wynn TA. Cellular and molecular mechanisms of fibrosis. *J Pathol.* 2008;214:199-210.
- [32] Engler AJ, Griffin MA, Sen S, Bonnemann CG, Sweeney HL, Discher DE. Myotubes differentiate optimally on substrates with tissue-like stiffness: pathological implications for soft or stiff microenvironments. *J Cell Biol.* 2004;166:877-87.
- [33] Georges PC, Miller WJ, Meaney DF, Sawyer ES, Janmey PA. Matrices with compliance comparable to that of brain tissue select neuronal over glial growth in mixed cortical cultures. *Biophys J.* 2006;90:3012-8.
- [34] McDaniel DP, Shaw GA, Elliott JT, Bhadriraju K, Meuse C, Chung KH, et al. The stiffness of collagen fibrils influences vascular smooth muscle cell phenotype. *Biophys J.* 2007;92:1759-69.
- [35] Li Z, Dranoff JA, Chan EP, Uemura M, Sevigny J, Wells RG. Transforming growth factor-beta and substrate stiffness regulate portal fibroblast activation in culture. *Hepatology.* 2007;46:1246-56.
- [36] Wipff PJ, Rifkin DB, Meister JJ, Hinz B. Myofibroblast contraction activates latent TGF-beta1 from the extracellular matrix. *J Cell Biol.* 2007;179:1311-23.
- [37] Georges PC, Hui JJ, Gombos Z, McCormick ME, Wang AY, Uemura M, et al. Increased stiffness of the rat liver precedes matrix deposition: implications for fibrosis. *Am J Physiol Gastrointest Liver Physiol.* 2007;293:G1147-54.

- [38] Hinz B, Phan SH, Thannickal VJ, Galli A, Bochaton-Piallat ML, Gabbiani G. The myofibroblast: one function, multiple origins. *Am J Pathol.* 2007;170:1807-16.
- [39] Aarabi S, Bhatt KA, Shi Y, Paterno J, Chang EI, Loh SA, et al. Mechanical load initiates hypertrophic scar formation through decreased cellular apoptosis. *Faseb J.* 2007;21:3250-61.
- [40] Tredget EE. Pathophysiology and treatment of fibroproliferative disorders following thermal injury. *Ann N Y Acad Sci.* 1999;888:165-82.
- [41] Brigstock DR. The CCN family: a new stimulus package. *J Endocrinol.* 2003;178:169-75.
- [42] Nagata K. Hsp47: a collagen-specific molecular chaperone. *Trends Biochem Sci.* 1996;21:22-6.
- [43] Ghahary A, Shen YJ, Nedelec B, Wang R, Scott PG, Tredget EE. Collagenase production is lower in post-burn hypertrophic scar fibroblasts than in normal fibroblasts and is reduced by insulin-like growth factor-1. *J Invest Dermatol.* 1996;106:476-81.
- [44] Mori R, Shaw TJ, Martin P. Molecular mechanisms linking wound inflammation and fibrosis: knockdown of osteopontin leads to rapid repair and reduced scarring. *J Exp Med.* 2008;205:43-51.
- [45] Marshall RP, Gohlke P, Chambers RC, Howell DC, Bottoms SE, Unger T, et al. Angiotensin II and the fibroproliferative response to acute lung injury. *Am J Physiol Lung Cell Mol Physiol.* 2004;286:L156-64.

- [46] Berk BC, Fujiwara K, Lehoux S. ECM remodeling in hypertensive heart disease. *J Clin Invest.* 2007;117:568-75.
- [47] Mezzano SA, Ruiz-Ortega M, Egido J. Angiotensin II and renal fibrosis. *Hypertension.* 2001;38:635-8.
- [48] Peruccio D, Castagnoli C, Stella M, D'Alfonso S, Momigliano PR, Magliacani G, et al. Altered biosynthesis of tumour necrosis factor (TNF) alpha is involved in postburn hypertrophic scars. *Burns.* 1994;20:118-21.
- [49] Singer AJ, Clark RA. Cutaneous wound healing. *N Engl J Med.* 1999;341:738-46.
- [50] Abraham DJ, Shiwen X, Black CM, Sa S, Xu Y, Leask A. Tumor necrosis factor alpha suppresses the induction of connective tissue growth factor by transforming growth factor-beta in normal and scleroderma fibroblasts. *J Biol Chem.* 2000;275:15220-5.
- [51] Goldberg MT, Han YP, Yan C, Shaw MC, Garner WL. TNF-alpha suppresses alpha-smooth muscle actin expression in human dermal fibroblasts: an implication for abnormal wound healing. *J Invest Dermatol.* 2007;127:2645-55.
- [52] Ghosh AK, Bhattacharyya S, Wei J, Kim S, Barak Y, Mori Y, et al. Peroxisome proliferator-activated receptor-gamma abrogates Smad-dependent collagen stimulation by targeting the p300 transcriptional coactivator. *Faseb J.* 2009;23:2968-77.
- [53] Burgess HA, Daugherty LE, Thatcher TH, Lakatos HF, Ray DM, Redonnet M, et al. PPARgamma agonists inhibit TGF-beta induced pulmonary myofibroblast

differentiation and collagen production: implications for therapy of lung fibrosis.

Am J Physiol Lung Cell Mol Physiol. 2005;288:L1146-53.

[54] Zafiriou S, Stanners SR, Saad S, Polhill TS, Poronnik P, Pollock CA.

Pioglitazone inhibits cell growth and reduces matrix production in human kidney fibroblasts. *J Am Soc Nephrol.* 2005;16:638-45.

[55] Galli A, Crabb DW, Ceni E, Salzano R, Mello T, Svegliati-Baroni G, et al.

Antidiabetic thiazolidinediones inhibit collagen synthesis and hepatic stellate cell activation in vivo and in vitro. *Gastroenterology.* 2002;122:1924-40.

[56] Masamune A, Kikuta K, Satoh M, Sakai Y, Satoh A, Shimosegawa T. Ligands of peroxisome proliferator-activated receptor-gamma block activation of pancreatic stellate cells. *J Biol Chem.* 2002;277:141-7.

[57] Diep QN, Benkirane K, Amiri F, Cohn JS, Endemann D, Schiffrin EL. PPAR alpha activator fenofibrate inhibits myocardial inflammation and fibrosis in angiotensin II-infused rats. *J Mol Cell Cardiol.* 2004;36:295-304.

[58] Zhang H, Pi R, Li R, Wang P, Tang F, Zhou S, et al. PPARbeta/delta activation inhibits angiotensin II-induced collagen type I expression in rat cardiac fibroblasts. *Arch Biochem Biophys.* 2007;460:25-32.

[59] Scott PG, Dodd CM, Ghahary A, Shen YJ, Tredget EE. Fibroblasts from post-burn hypertrophic scar tissue synthesize less decorin than normal dermal fibroblasts. *Clin Sci (Lond).* 1998;94:541-7.

- [60] Sayani K, Dodd CM, Nedelec B, Shen YJ, Ghahary A, Tredget EE, et al. Delayed appearance of decorin in healing burn scars. *Histopathology*. 2000;36:262-72.
- [61] Hildebrand A, Romaris M, Rasmussen LM, Heinegard D, Twardzik DR, Border WA, et al. Interaction of the small interstitial proteoglycans biglycan, decorin and fibromodulin with transforming growth factor beta. *Biochem J*. 1994;302 (Pt 2):527-34.
- [62] Wight TN. Versican: a versatile extracellular matrix proteoglycan in cell biology. *Curr Opin Cell Biol*. 2002;14:617-23.
- [63] Stoff A, Rivera AA, Mathis JM, Moore ST, Banerjee NS, Everts M, et al. Effect of adenoviral mediated overexpression of fibromodulin on human dermal fibroblasts and scar formation in full-thickness incisional wounds. *J Mol Med*. 2007;85:481-96.
- [64] Soo C, Hu FY, Zhang X, Wang Y, Beanes SR, Lorenz HP, et al. Differential expression of fibromodulin, a transforming growth factor-beta modulator, in fetal skin development and scarless repair. *Am J Pathol*. 2000;157:423-33.

Chapter 3

Superficial Dermal Fibroblasts Enhance Basement Membrane and Epidermal Barrier Formation in Tissue Engineered Skin: Implications for Treatment of Skin Basement Membrane Disorders*

*Parts of this chapter are being published as: Varkey M, Ding J, Tredget EE. (2013) Superficial dermal fibroblasts enhance basement membrane and epidermal barrier formation in tissue engineered skin: Implications for treatment of skin basement membrane disorders. Manuscript to be submitted.

3 Superficial Dermal Fibroblasts Enhance Basement Membrane and Epidermal Barrier Formation in Tissue Engineered Skin: Implications for Treatment of Skin Basement Membrane Disorders

3.1 Introduction

The basement membrane is a highly dynamic and specialized adhesive structure at the dermal-epithelial junction that binds the epidermis to the underlying dermis and provides resilience to the skin. It functions as an exchange zone between epidermal keratinocytes and dermal fibroblasts, and serves as a reservoir of growth factors and cytokines. The basement membrane contains laminin, nidogen, collagen types IV and VII, and the proteoglycans, perlecan and collagen XVIII [1, 2], in addition to the extracellular matrix proteins collagen type I and III, tenascin and fibrillin-1. Both keratinocytes and fibroblasts contribute to the formation of the basement membrane [3-5]. The basement membrane and the underlying dermis play critical roles in the maturation and function of skin by regulating keratinocyte growth and terminal differentiation. The barrier property of the epidermis is due to the presence of tight junctions and lipids such as ceramides, cholesterol esters and free fatty acids that accumulate during epidermal differentiation. Regulation of epidermal

differentiation may either be through fibroblast-derived diffusible factors that act on keratinocytes in a paracrine manner or interactions of keratinocytes with basement membrane proteins [6, 7].

Dermal fibroblasts are heterogeneous, they consist of superficial, deep and hair follicle fibroblasts, each of which exhibit distinct characteristics when cultured independently [8]. Superficial and deep dermal fibroblasts differ in physical and biochemical characteristics such as production of collagenase, procollagen type I and III, TGF- β 1 and proteoglycans such as decorin, versican and fibromodulin [9, 10]. Further, recently our research showed that superficial fibroblasts are anti-fibrotic while deep fibroblasts are pro-fibrotic and both differentially remodel collagen-glycosaminoglycan (C-GAG) matrices [9, 10]. Also, compared to superficial wounds, deep dermal wounds were found to express lower amounts of the anti-fibrotic molecules decorin, fibromodulin, TGF- β ₃ and Thy-1, but higher TGF- β type II receptors [11]. Furthermore, studies in 2-D culture showed that site- matched superficial and deep dermal fibroblasts differ in production of certain cytokines and in their interactions with keratinocytes; superficial fibroblasts release higher levels of GM-CSF, KGF and IL-6, and form a continuous basement membrane compared to deep fibroblasts [8]. Epidermal growth and differentiation is influenced by dermal fibroblasts; however, the specific effects superficial and deep dermal fibroblasts have on keratinocytes in a 3-D microenvironment are not understood.

In the basement membrane, collagen type IV, laminin-5, nidogen and perlecan form a network that functions as a barrier between epidermis and dermis. Collagen type VII, another essential component of the basement membrane, forms fibrils that anchor the basement membrane to the underlying dermis. Disruption of the basement membrane results in skin fragility, and blistering of the skin and mucous membranes, which is a serious problem in children with epidermolysis bullosa (EB), a family of severe life-threatening congenital skin basement membrane disorders [12]. Some forms of EB such as the junctional form are lethal at the neonatal stage, while the dystrophic form results in years of severely painful blistering and repeated wounding in children. These wounds typically heal with fibrosis and scarring; the newly formed epidermis poorly adheres to the underlying dermis, and therefore the skin blisters and disadheres at the slightest trauma. This lack of adherence is due to defects in basement membrane proteins such as laminin-5 and collagen type VII [13]; mutations in genes encoding laminin-5 lead to severe blistering as seen in Herlitz' junctional EB [14]. Mutations or deficiency of collagen type VII as in bullous systemic lupus erythematosus or dystrophic forms of EB [15] results in a paucity of collagen type VII anchoring collagen fibrils [16] leading to skin fragility and extensive blistering. Patients with skin basement membrane disorders constantly suffer from severe blisters and recurring wounds throughout the body, and associated infections. In addition to experiencing excruciating pain, they are

prone to fatal sepsis and therefore need on-going wound care, hospitalization and health care support.

Skin basement disorders such as EB are devastating and currently there are no clinically proven therapies for effective management and treatment of the disease. Existing treatment options are mainly palliative and include surgical debridement, analgesia, and bandaging most of the body surface to protect from friction and prevent infection. Studies in animal models of EB have attempted delivery of wild-type collagen VII to wound sites by direct injection of either recombinant protein or cells that have mini-genes or are gene-modified using retroviral, lentiviral, transposon, ϕ C31-based integrase vectors, but have had limited success [17-19]. Treatment of collagen type VII knock out mouse models of EB with bone marrow derived cells have shown improvements in some symptoms of the disease [20, 21]. However, for clinical realization of gene therapy and stem cell-based approaches, technical and safety issues such as oncogenic potential of the vectors or cells need to be addressed [22]. Fibroblast therapy has been proposed as an alternative to circumvent these problems; recently, use of fibroblasts in a collagen VII-hypomorphic mouse model for recessive dystrophic EB showed that small increases in collagen VII significantly stabilized the skin against shearing forces and reduced the disease phenotype, suggesting that full restoration of collagen VII may not be critical for improvement in function and quality of life of EB patients [23].

There is an urgent need to develop new therapeutic strategies for effective wound management and cure of EB and other skin basement membrane disorders. We propose the use of tissue engineered skin as a promising approach, since it not only would provide effective coverage at wound sites but also promote healing and adherence of newly-formed skin due to the presence of exogenous fibroblasts and keratinocytes. Moreover, the use of tissue engineered skin to treat burn patients has yielded favourable clinical outcomes for wound coverage and pliability [24]. Currently available tissue engineered skin consists of a heterogeneous population of dermal fibroblasts with keratinocytes; however, recent studies have shown differences in fibrotic characteristics and cytokine expression in the different subpopulations of dermal fibroblasts [8, 10, 25]. The aim of this study therefore was to assess differences in basement membrane, epidermis formation and barrier function of tissue engineered skin containing superficial and deep dermal fibroblasts independently co-cultured with keratinocytes.

3.2 Materials and Methods

3.2.1 Preparation of C-GAG Matrices

Acellular C-GAG matrices were prepared by freeze-drying a co-precipitate of type I collagen and chondroitin-6-sulfate as reported previously [10]. Briefly, collagen powder (0.5 wt %; Devro Pty. Ltd., Bathurst, NSW, Australia) was co-

precipitated with chondroitin-6-sulfate (0.05 wt %; Sigma, St. Louis, MO, USA) in 0.5 M acetic acid, degassed under vacuum (2 h, room temperature), cast into sheets, frozen to -40°C and freeze-dried (FreeZone⁶Plus, Labconco, Kansas City, MI, USA) to produce highly porous matrices. The matrices obtained were cut into 30 mm discs and cross-linked by dehydrothermal treatment under vacuum (140°C , 48 h) in a drying oven (APT.Line VD, Binder GmbH, Germany). Thereafter, the matrix discs were rinsed with phosphate buffered saline (PBS; twice, 15 min each) and subsequently with cell culture medium (DMEM, 10% FBS, 1% Antibiotic-antimycotic; twice, 15 min each).

3.2.2 Preparation of Tissue Engineered Skin

Tissue engineered skin was prepared by culturing superficial or deep dermal fibroblasts and keratinocytes on dehydrothermal-treated C-GAG matrices. The cells were obtained from lower abdominal tissue of patients ($n = 3$) who underwent elective abdominoplasty surgery following informed consent. The protocols for human tissue sampling used in this study were approved by the University of Alberta Hospital's Health Research Ethics Board. Superficial and deep dermal fibroblasts and keratinocytes were isolated as reported previously [10]; briefly, tissue samples were horizontally sectioned into five layers (referred to as layers 1 to 5) using a dermatome (Padgett Instruments, Plainsboro, NJ, USA) set approximately at 0.5 mm. The superficial dermal layer (layer 1) was treated overnight with 25 U/mL dispase (Gibco, Grand Island, NY, USA) at 4°C to

remove the epidermis, which was digested with trypsin to isolate keratinocytes. On the other hand, the superficial dermal layer and the deep dermal layer (layer 5) were separately treated with 455.3 U/mL collagenase (Gibco Grand Island, NY, USA) for 18 hours at 37°C, 60 rpm to isolate the superficial (SF) and deep (DF) dermal fibroblasts, respectively. The keratinocyte (K) and fibroblast cell suspensions were passed through 100 µm cell strainers and centrifuged at 800 rpm for 10 minutes. The epidermal and dermal cell pellets were then re-suspended in the respective cell culture media and serially expanded in tissue culture flasks till the desired number of K, SF and DF were obtained. Passage 4 SF or DF were seeded onto cross-linked C-GAG discs at a density of 0.5×10^6 cells/cm² and cultured (at 37°C, 5% CO₂). Two days later, K were seeded on top of the fibroblast-populated matrices at a density of 1.0×10^6 cells/cm² and medium was replaced with co-culture medium containing serum (DMEM-HG and nutrient mixture F-12 Ham (3:1), 2 nM triiodothyronine, 5% FBS, 0.5% insulin–transferrin–selenium-G supplement, 1 nM cholera toxin, 10 ng/ml EGF, 0.4 µg/ml hydrocortisone, 5 µg/ml transferrin, 1% antibiotic-antimycotic; [26]). Matrices with fibroblasts alone were used as controls, wherein the number of cells was adjusted so as to make the number of cells on the matrices comparable to those with K. The submerged culture was continued for 5 additional days and then lifted to the air-liquid interface on a steel platform to enable epidermal stratification. The tissue engineered skin and the respective controls were used in assays at different time points as described below.

3.2.3 Assessment of Cell Metabolic Activity

5 mm punch biopsies were collected at days 7, 14 and 21 of culture and placed in separate wells in a 24-well microtitre plate; C-GAG matrices without cells were used as controls. A standard 3-[4,5-dimethylthiazol-2-yl]-2,5-diphenyl tetrazolium bromide (MTT) assay was performed to assess activity in the matrices. Briefly, the punch biopsies were incubated with 250 μ l of tissue culture medium containing MTT substrate (5 mg/mL) for 4 h at 37°C, and the obtained MTT-formazan product was dissolved in 200 μ l of DMSO and quantified at 570 nm using a microplate reader (THERMOmax, Molecular Devices, Sunnyvale, CA, USA). The values are shown as mean optical density \pm standard error.

3.2.4 Immunohistochemical Analysis

For immunohistochemical staining of cytokeratin and laminin-5, 5 mm punch biopsies were collected at days 7, 14 and 21 of culture; keratinocyte-free C-GAG matrices were included as one of the controls. Briefly, the samples were fixed with 4% paraformaldehyde (12 h) and 70% ethanol (12 h), paraffin embedded, sectioned at 5 μ m, and mounted on microscope slides. The sections were then deparaffinized with xylene and rehydrated in descending series of ethanol, and boiled in citrate buffer (10 mmol/L, pH 6.0) for 20 minutes for epitope retrieval. Subsequently, the sections were blocked with 10% BSA in PBS for 60 min to avoid non-specific protein binding, and incubated overnight at 4°C with primary mouse anti-cytokeratin or laminin-5 antibodies (1:50 dilution; Dako,

Denmark), and then washed with PBS (3×, 5 min each); non-immune human IgG (1:50 dilution) was used as negative control. Endogenous peroxidase activity was quenched with 0.3% H₂O₂ (15 min) and the sections were incubated with fluorescent secondary goat anti-mouse Alexa Fluor 488 antibody (1:500 dilution, 60 min, 25°C; Invitrogen, Oakville, ON, Canada). The stained sections were then mounted with ProLong^R Gold antifade reagent containing DAPI (Invitrogen, Eugene, OR), and viewed by fluorescent microscopy at 100× and 200× magnifications and photographed.

3.2.5 Gene Expression Studies

For gene expression analysis, 5 mm punch biopsies were collected at days 7, 14 and 21 of culture, and snap frozen in liquid nitrogen; C-GAG matrices with fibroblasts but no K were used as controls. The frozen samples were homogenized (2000 rpm, 2 min; Mikro-Dismembrator S, B. Braun Biotech International) and treated with Trizol reagent (Invitrogen, Carlsbad, CA, USA); the resultant supernatant was stored at -80°C. Total RNA was then extracted from all the supernatants using RNeasy Mini Kit (Qiagen, Mississauga, ON, Canada) following manufacturer's instructions, and quantified using Nano Drop 1000 spectrophotometer (Thermo Fisher Scientific, Wilmington, DE). RNA extracts (0.5 µg) from the samples were used for first-strand cDNA synthesis using M-MLV Reverse Transcriptase (Invitrogen, Carlsbad, CA, USA) by incubation at three different conditions (25°C for 10 min followed by 37°C for 50

min and 70°C for 15 min). The resulting cDNA was used as a template for quantitative Real Time Polymerase Chain Reaction (qRT-PCR) amplification of genes of interest; the gene specific primers were designed using Primer Express 3.0 (Table 3.1). qRT-PCR was done using Power Sybr Green™ PCR master mix (ABI, Foster, CA, USA) in a total reaction volume of 25 µl containing 5 µl of a 1:10 dilution of cDNA product from the first-strand reaction and 1 µM gene-specific forward and reverse primers on a StepOne Plus qRT-PCR system (ABI, Foster, CA, USA). The amplification conditions included denaturation at 95°C for 3 min followed by 40 cycles of denaturation at 95°C for 15 sec and annealing and primer extension at 60°C for 30 sec. Amplification of genes was measured in terms of cycle threshold (C_T) values; the obtained C_T values were normalized with the C_T value of the house-keeping gene, hypoxanthineguanine phosphoribosyl transferase (HPRT). Gene expression levels are shown as mean fold change \pm standard error. Quantitation was performed in the linear range of amplification as per standard procedure.

3.2.6 Assessment of Barrier Function

Epidermal barrier function was assessed by measuring surface electrical capacitance of the C-GAG matrices on days 7, 14 and 21 of culture, using a Nova Dermal Phase Meter (DPM 9003, NOVA Technology Corporation, Portsmouth, NH). The measurements were taken at four different sites on each of the matrices, and expressed as mean DPM units \pm standard error.

3.2.7 Statistical Analysis

All experiments were conducted in triplicate and data are expressed as mean \pm standard error. Statistical analysis was done using ANOVA with significance set at $P < 0.05$, $P < 0.01$ and $P < 0.001$ using Microsoft Excel 8.0.

3.3 Results

3.3.1 Metabolic Activity of Cells on C-GAG Matrices

SF, DF and K were isolated from lower abdominal tissue of three abdominoplasty patients and serially expanded. Passage 4 SF and DF were then independently cultured or co-cultured with K on cross-linked C-GAG matrices, and assayed at different time points for activity. C-GAG matrices with SF or DF alone were used as controls for fibroblasts, while matrices without any cells were used as cell-free controls. Cell metabolic activity was observed to be significantly higher for matrices with SF and K, DF and K, and SF, DF and K compared to those with SF and DF alone at days 14 and 21 ($p < 0.001$). Metabolic activity was not significantly different for SF and K, DF and K, and SF, DF and K (Fig. 3.1).

3.3.2 Epidermis Formation in Tissue Engineered Skin

Tissue engineered skin containing SF and K, DF and K, and SF, DF and K were assessed at different time points for formation of epidermis by

immunofluorescence staining for cytokeratin, a marker for keratinocytes. At all time points, epidermis for tissue engineered skin with SF and K was observed to be continuous, better defined and thinner compared to that with DF and K, which was intermittently broken (Fig. 3.2 A, B; day 7 data not shown). To further understand differences in epidermis formation, gene expression of the specific epithelial proteins, E-cadherin and keratin-5, was examined at days 7, 14 and 21, by qRT-PCR. Tissue engineered skin with SF and K expressed more E-cadherin than that with DF and K, which was significant ($p < 0.01$) on days 14 and 21 (Fig. 3.3 A). Tissue engineered skin with SF, DF and K had similar expression of E-cadherin compared to that with SF and K. Matrices with fibroblasts alone did not express E-cadherin. The trend was similar for keratin-5, tissue engineered skin with SF and K expressed more keratin-5 than that with DF and K, which was significant ($p < 0.01$) on days 14 and 21 (Fig. 3.3 B). Tissue engineered skin with SF, DF and K had slightly higher expression of keratin-5 compared to that with SF and K, but this was not significant. Matrices with fibroblasts alone did not express keratin-5.

3.3.3 Basement Membrane Formation in Tissue Engineered Skin

Tissue engineered skin containing SF and K, DF and K, and SF, DF and K were assessed at different time points for formation of basement membrane by immunofluorescence staining for laminin-5, a critical basement membrane protein. At all time points, laminin-5 for tissue engineered skin with SF and K was

more compared to that with DF and K (Fig. 3.4 A, B; day 7 data not shown). Tissue engineered skin with SF, DF and K had similar levels of laminin-5 compared to that with SF and K. Matrices with fibroblasts alone did not have laminin-5. To further investigate differences in basement membrane formation, gene expression of four different basement membrane proteins, laminin-5, nidogen, collagen type VII and IV, was examined at days 7, 14 and 21, by qRT-PCR. Tissue engineered skin with SF and K expressed more laminin-5 than that with DF and K, which was significant ($p < 0.01$, $p < 0.05$) at all time-points (Fig. 3.5 A). Matrices with fibroblasts alone did not express laminin-5. Tissue engineered skin with SF and K expressed higher nidogen than that with DF and K, which was significant ($p < 0.01$) at all time-points (Fig. 3.5 B). Matrices with fibroblasts alone expressed low levels of nidogen, which was significantly lower than that expressed by SF or DF cultured with K ($p < 0.001$). Tissue engineered skin with SF, DF and K had similar expression of nidogen compared to that with SF and K. For collagen type VII, tissue engineered skin with SF and K had higher expression compared to that with DF and K, which was significant ($p < 0.01$) at all time-points (Fig. 3.5 C). Tissue engineered skin with SF, DF and K had lower expression of collagen type VII compared to that with SF and K, which was significant at days 7 and 14 ($p < 0.05$). Matrices with fibroblasts alone expressed significantly lower collagen type VII than those with SF and DF cultured with K ($p < 0.001$). Tissue engineered skin with SF and K had lower expression of collagen type IV than that with DF and K, which was significant on days 14

($p < 0.01$) and 21 ($p < 0.001$; Fig. 3.5 D). Matrices with fibroblasts alone express very little collagen type IV. Tissue engineered skin with SF, DF and K had similar expression of collagen type IV compared to that with SF and K, with no significant differences.

3.3.4 Proteoglycan Expression in Basement Membrane of Tissue Engineered Skin

To investigate possible differences in proteoglycan expression in the basement membrane of tissue engineered skin with fibroblasts and K, gene expression of the proteoglycans, perlecan and collagen type XVIII, was examined. Tissue engineered skin with SF and K expressed less perlecan than that with DF and K, which was significant ($p < 0.01$) at all time-points (Fig. 3.6 A). Matrices with fibroblasts alone did not express perlecan. Tissue engineered skin with SF, DF and K expressed slightly lower perlecan than that with DF and K, which was significant only at day 7 ($p < 0.05$). For collagen type XVIII, tissue engineered skin with SF and K had lower expression compared to that with DF and K, which was significant ($p < 0.001$) at all time points (Fig. 3.6 B). Tissue engineered skin with SF, DF and K had higher expression of collagen type XVIII compared to that with SF and K, which was significant on days 7 and 14 ($p < 0.001$). Matrices with fibroblasts alone did not express collagen type XVIII.

3.3.5 Epidermal Barrier Function in Tissue Engineered Skin

The barrier function of the epidermis is due to the semi-permeable stratum corneum layer in the upper epidermis. In human skin, a water gradient exists across the stratum corneum; hydration is lowest on the surface of the skin and highest within the distal layers. Surface electrical capacitance (SEC) can be used to directly measure surface hydration of skin, which then can be correlated to the barrier function of the epidermis [27]. SEC was monitored for tissue engineered skin with fibroblasts and K at different time points; as the skin matured at the air-liquid interface, its surface was observed to dry out due to keratinization of the epidermis and formation of an epidermal barrier layer, and therefore the SEC decreased with time. For tissue engineered skin with SF and K, SEC values were lower than that with DF and K, which was significant ($p < 0.01$) on days 14 and 21 (Fig. 3.7). SEC values for tissue engineered skin with SF, DF and K were lower than that with DF and K, but higher than that with SF and K.

3.4 Discussion

In this study, SF or DF were independently co-cultured with K on C-GAG matrices, which provided a true 3-D micro-environment for cellular cross-talk, and the resulting tissue engineered skin was assessed for differences in basement membrane, epidermis formation and barrier function. To the best of our knowledge, this is the first study to investigate the use of selective sub-

population of dermal fibroblasts to make tissue engineered skin, and examine its functional characteristics. SF, DF and K were obtained from the same patients to control for cell source variability. The C-GAG matrices were conducive for the growth of cells as was evident from cell viability and DAPI staining. Matrices with K had higher cell metabolic activity compared to those with fibroblasts alone; possibly due to differences in rates of proliferation of K or due to specific proteins produced by K that support survival and proliferation of fibroblasts. Fibroblast secreted-keratinocyte growth factor and keratinocyte-secreted epidermal growth factor (EGF) could be potential factors contributing to the observed differences in metabolic activity. Also, it is possible that cells secreted EGF induces keratinocytes and dermal fibroblasts to overexpress TGF- β 1, which could act in a negative feedback autocrine and/or paracrine manner for keratinocytes proliferation. The epidermis formed in the tissue engineered skin with SF and K was significantly thinner and had better overall integrity compared to that with DF and K, or SF, DF and K. These differences in epidermal characteristics are likely due to differential interaction of SF and DF with K; our previous studies have found that DF behave similar to hypertrophic scar fibroblasts and contribute to skin fibrosis [9]. The observed increased epidermal thickness in tissue engineered skin with DF and K is consistent with our previous finding that human hypertrophic scars have a thicker epithelium compared to normal skin [28]. An extended phase of re-epithelialization due to prolonged activation of K even after completion of epithelialization is believed to cause a thicker epidermis in

hypertrophic scars [29, 30]; our current results suggest that DF may have a role in this activation. Interestingly, differences in expression of epidermal proteins were also observed with the different types of tissue engineered skin especially that with SF and K had higher levels of keratin-5 and E-cadherin that likely contributed to better epidermis formation.

The basement membrane orchestrates growth factor-mediated extracellular communication, cellular adhesion, migration and differentiation [31], and is therefore critical. Tissue engineered skin with SF and K, or DF and K showed distinct expression profiles for the different basement membrane components. Interestingly, tissue engineered skin with SF and K produced more laminin-5 compared to that with DF and K as was evident from gene and protein expression levels. Laminin-5 mediates adhesion of basal keratinocytes [32, 33], and is indispensable for keratinocyte migration in wounded monolayers and epidermal wound healing [34-36]. Tissue engineered skin with SF and K also expressed significantly more nidogen and collagen type VII compared to that with DF and K, or SF, DF and K. Extremely low levels of nidogen expression observed for SF and DF cultured alone further confirmed previous findings [37, 38] that fibroblast-keratinocyte interaction is essential for optimal nidogen expression. Nidogen interacts with other basement membrane components, perlecan, laminin-5 and collagen type IV, and stabilises networks formed by laminin and collagen type IV [39-41]. Deficiency of nidogen results in accelerated epidermal maturation and affects deposition of laminin-5, laminin-10, perlecan,

and collagen type IV in the basement membrane [38], and is therefore a key fibroblast-derived factor [42]. On the other hand, collagen type VII is secreted by both fibroblasts and keratinocytes, and it self-assembles into anchoring fibrils that extend from the lamina densa of the epidermal basement membrane into the dermis and secure the epidermal-dermal junction. Paucity of collagen type VII anchoring fibrils results in separation of the epidermis from the dermis and thus leads to the pathogenesis of EB [43, 44]. Further, tissue engineered skin with SF and K expressed less collagen type IV compared to that with DF and K, or SF, DF and K. Collagen type IV is an essential collagenous glycoprotein in the basement membrane [45]. Extremely low levels of collagen type IV and VII expression observed for SF and DF cultured alone further confirmed previous findings [37] that fibroblast-keratinocyte interaction is necessary for their optimal expression.

Interestingly, differences in the expression profile of the basement membrane proteoglycans, perlecan and collagen XVIII, were observed; tissue engineered skin with SF and K expressed less perlecan than that with DF and K, but had similar levels as that with SF, DF, and K. Perlecan is a large heparin-sulfate proteoglycan that plays an important role in binding several growth factors and their receptors, cell migration, proliferation and differentiation [46, 47]. It is critical for keratinocyte survival and epidermis formation, and its deficiency results in thinner epidermis [48]. Tissue engineered skin with SF and K expressed less collagen type XVIII compared to that with DF and K, or SF, DF,

and K. Collagen type XVIII, another heparan sulphate proteoglycan, is critical for maintenance of basement membrane structural integrity; low levels have been observed to result in a thicker basement membrane [49] and enhanced wound healing due to increased vascularization of the wound bed and reduced wound area [50].

For the development of a structured and organized epidermis, continuous interaction of the epidermal cells with the underlying dermal fibroblasts is essential [6]. It is possible that depending on the composition of the underlying dermal fibroblasts (superficial versus deep) there would be differences in the microenvironment the keratinocytes are continuously exposed to, which in turn would affect epidermal morphogenesis and regeneration. To evaluate functional differences in keratinocyte growth and differentiation when the underlying dermal fibroblasts are different, we monitored SEC of the tissue engineered skin as a measure of epidermal barrier function. The SEC probe detects a phase shift created in an alternating current as it is passed through the tissue engineered skin. This phase shift is caused by water which accumulates between the tissue engineered skin surface and the probe during the sampling period. A greater degree of surface hydration generates a larger dielectric constant which is detected as a greater capacitance. Tissue engineered skin with SF and K had better epidermal barrier function than that with DF and K, and was comparable to that with SF, DF and K. Further, the expression of E-cadherin, which is essential for tight junction formation in the epidermis [51-53], was up-regulated

in tissue engineered skin with SF and K compared to that with DF and K; this likely contributed to the better epidermal barrier observed in the case of the former. Moreover, increased keratin-5 expression observed for tissue engineered skin with SF and K compared to that with DF and K suggests better epidermal stratification and therefore enhanced epidermal barrier function, since keratin-5 is essential for the intermediate filament network formation required for epidermal stratification [54]. Differences in barrier function may also be due to differences in the inter-cellular lipid component of the cells which plays a role in the barrier function of the skin also facilitates the water-holding capacity of the stratum corneum.

Taken together, our results demonstrate that tissue engineered skin with SF and K forms better basement membrane with higher expression of dermo-epidermal adhesive and anchoring proteins, and superior epidermis with enhanced barrier function compared to that with DF and K, or SF, DF and K. The selective use of SF in tissue engineered skin may therefore be more beneficial for treatment of patients with basement membrane disorders such as EB and other skin blistering diseases. Further work in animal models is necessary for effective translation of this treatment modality to the clinic.

3.5 Table and Figures

Table 3.1: Gene Specific Primers Used in qRT-PCR for Amplification of Genes of Interest

| Gene | Forward Primer | Reverse Primer |
|--|------------------------------|-------------------------------|
| Keratin-5 | GCTGAGAGCCGAGAT TGACAA | TCCGCAATGGCGTTC TG |
| E-cadherin | CAGTGAACAACGATG GCATTTT | ACTGCTGCTTGGCCT CAAA |
| Nidogen | AAGGTGAAAGGAAGG ATCTTTGTG | ACGTAAGAGTGGAGG TCAGTGTTCT |
| Collagen type IV | TGCCAGGCGCAATGA TAAA | GGCTGACGGGCATCA TG |
| Collagen type VII | CTGAGGAGCTGAAGC GAGTTG | CCTCAAGATGCTGAA GTCATTGA |
| Laminin-5 | GCTCCTGAGGACTGA AGTGAAAAC | AGACTCCCGTGGCAT TGC |
| Perlecan | ATTCCCGGAGACCAG GTTGT | CTTCCGAGCCCACAT CCA |
| Collagen type XVIII | GGGCCAGATGCCAAC AGT | GCAGTGAGAAGTCAC GGAAGAA |
| Hypoxanthine guanine phospho- ribosyl transferase (House-keeping gene) | GACCAGTCAACAGGG GACA | ACACTTCGTGGGGTC CTTTT |

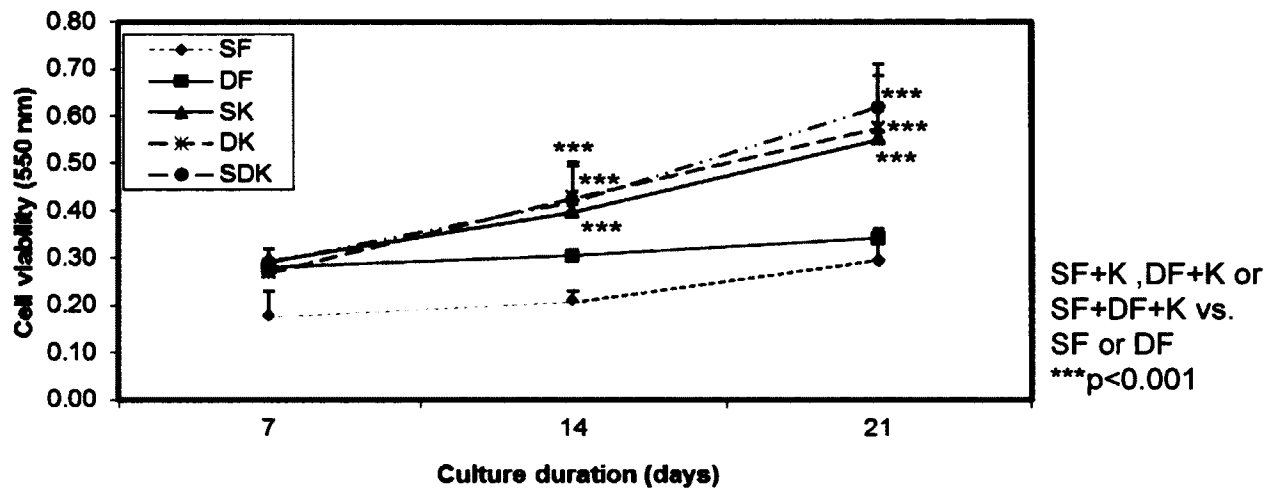


Figure 3.1: Metabolic activity of SF and DF Cultured with or without K on C-GAG Matrices.

SF and DF were cultured for 21 days with or without K on cross-linked C-GAG matrices, and their metabolic activity was assessed by MTT assay on days 7, 14 and 21. Each bar represents Mean \pm standard error cell viability (n = 3 abdominoplasty patients). Significant differences in cell metabolic activity for matrices with SF and K, DF and K, and SF, DF and K compared to those with SF and DF alone at days 14 and 21 ($p < 0.001$).

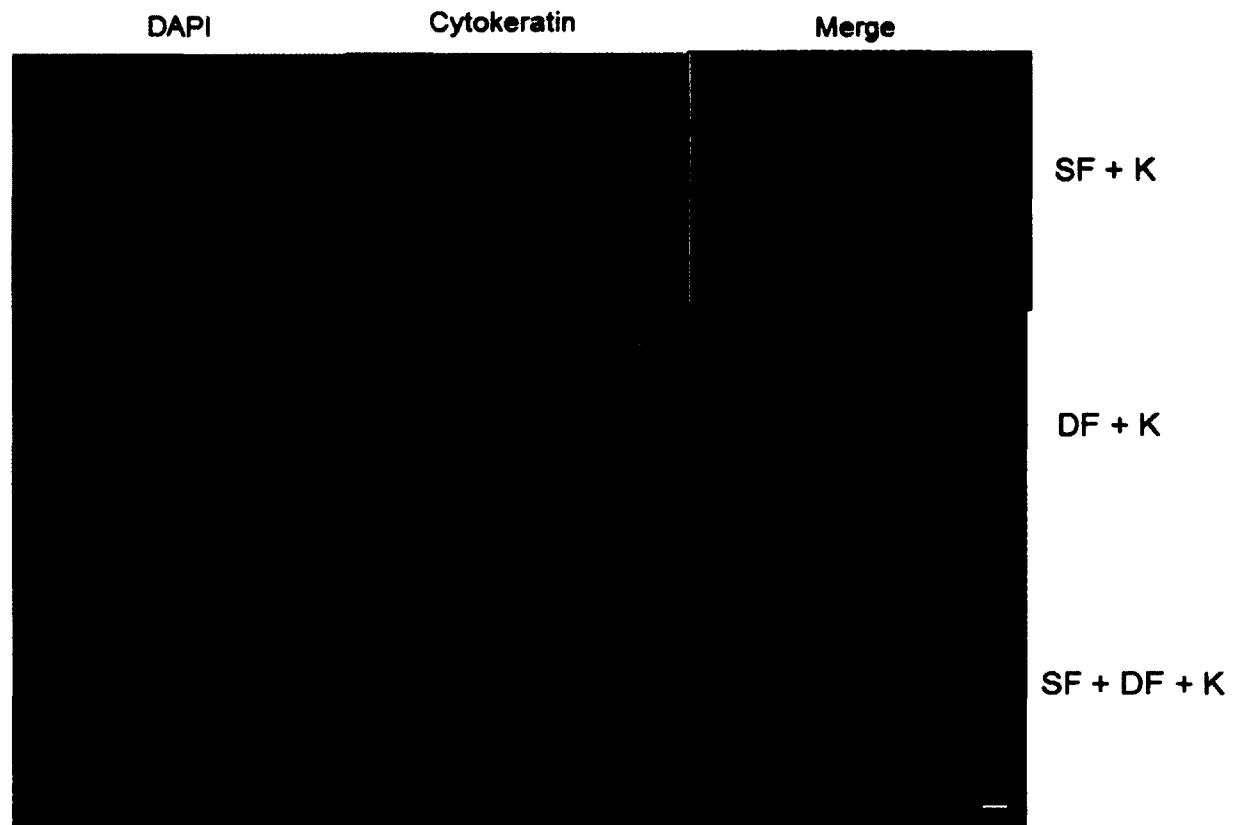


Figure 3.2A: Immunofluorescent Staining of the Epidermis Formed in Tissue Engineered Skin.

DAPI and cytokeratin staining were done, and then the images were merged. **A.** Week 2 staining for tissue engineered skin with SF and K, DF and K, or SF, DF and K at 100× magnification. Scale bar = 100 μm. Blue indicates DAPI staining of nuclei on matrices while green indicates presence of cytokeratin.

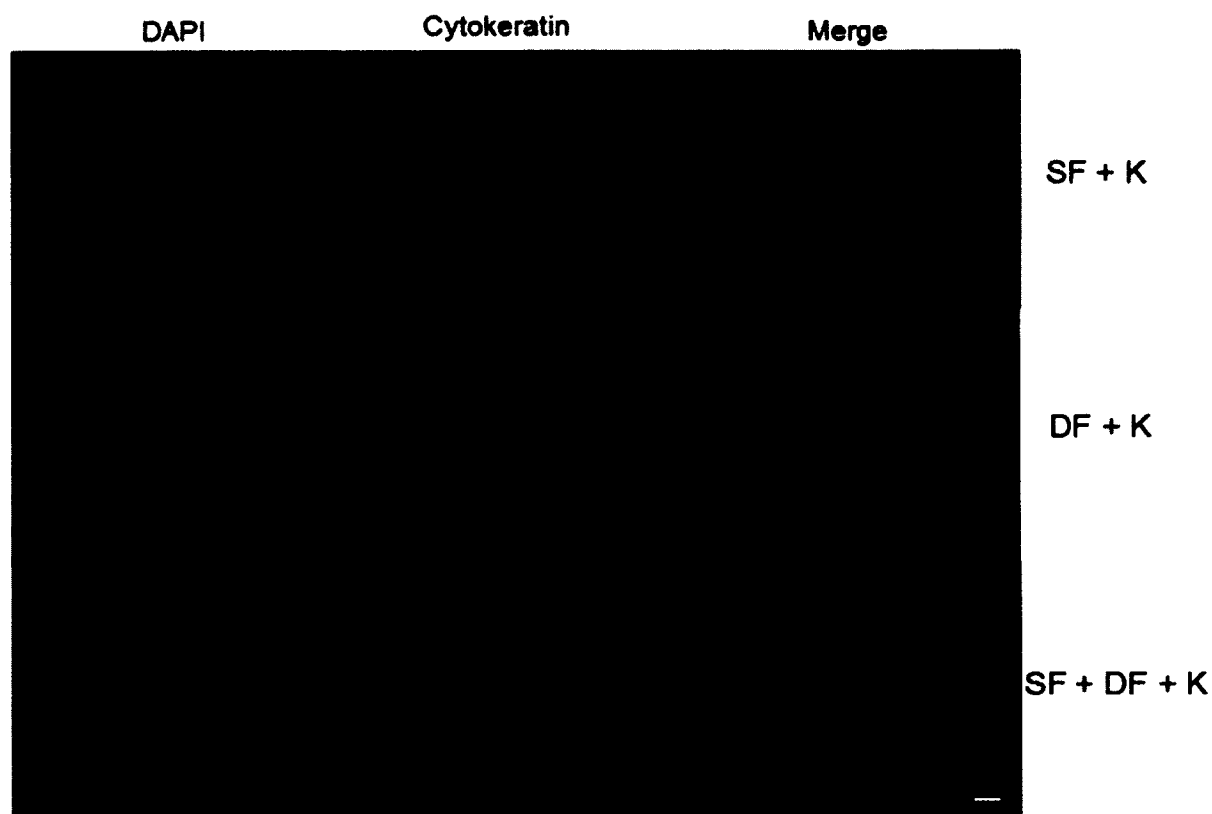


Figure 3.2B: Immunofluorescent Staining of the Epidermis Formed in Tissue Engineered Skin.

DAPI and cytokeratin staining were done, and then the images were merged. **B.** Week 3 staining for tissue engineered skin with SF and K, DF and K, or SF, DF and K at 100× magnification. Scale bar = 100 μm. Blue indicates DAPI staining of nuclei on matrices while green indicates presence of cytokeratin.

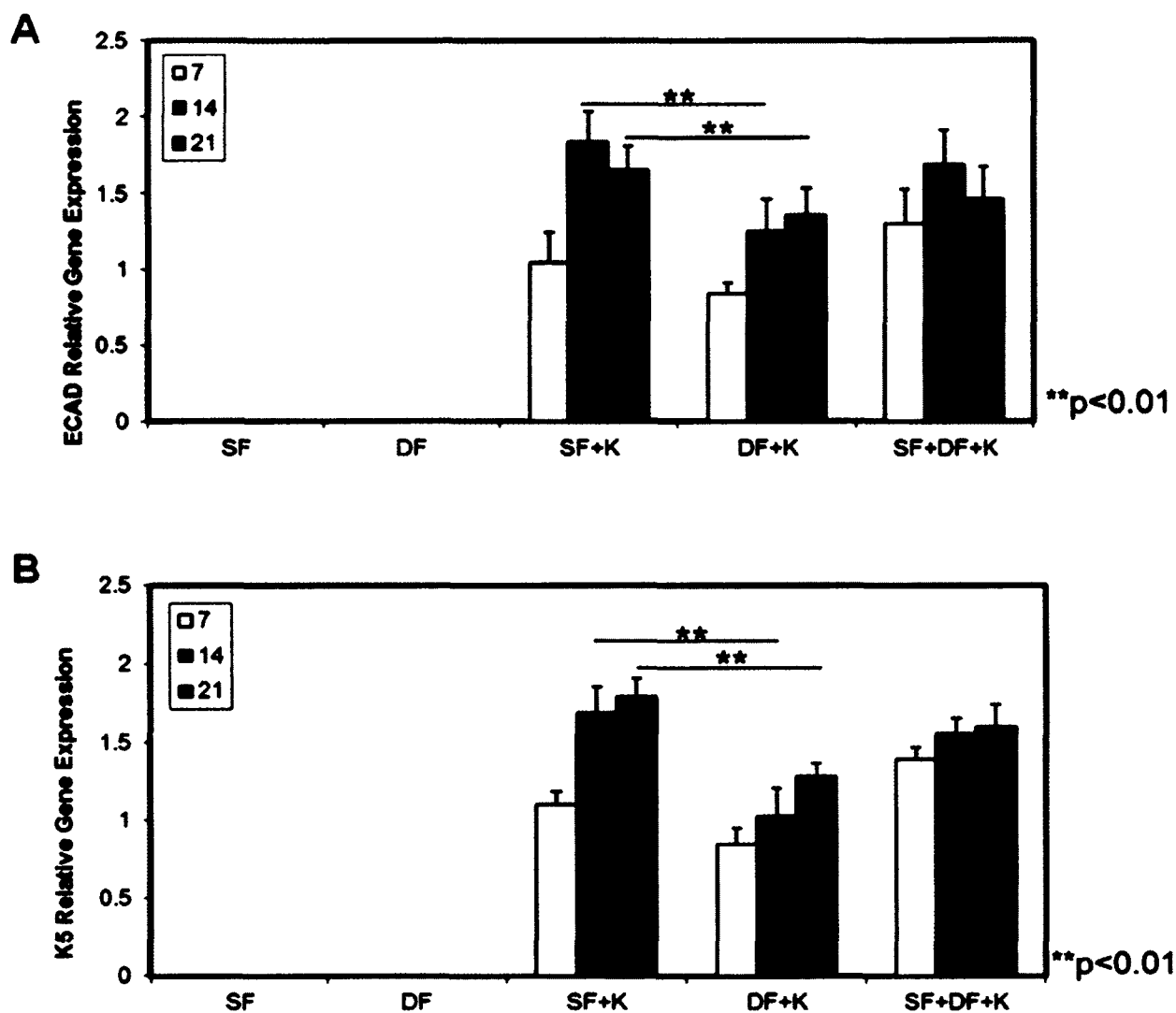


Figure 3.3: Assessment of Relative Gene Expression of Epidermal Proteins in Tissue Engineered Skin by qRT-PCR.

mRNA was isolated on days 7, 14 and 21, and reverse transcribed using specific primers (Table 3.1). cDNA was subsequently amplified and relative gene

expression was analyzed by qRT-PCR. Each bar represents Mean \pm standard error relative gene expression (n = 3 abdominoplasty patients). **A.** Relative gene expression for E-Cadherin (ECAD). Significant differences between tissue engineered skin with SF and K, DF and K, or SF, DF and K on days 14 and 21 ($p < 0.01$). **B.** Relative gene expression for Keratin-5 (K5). Significant differences between tissue engineered skin with SF and K, DF and K, or SF, DF and K on days 14 and 21 ($p < 0.01$).

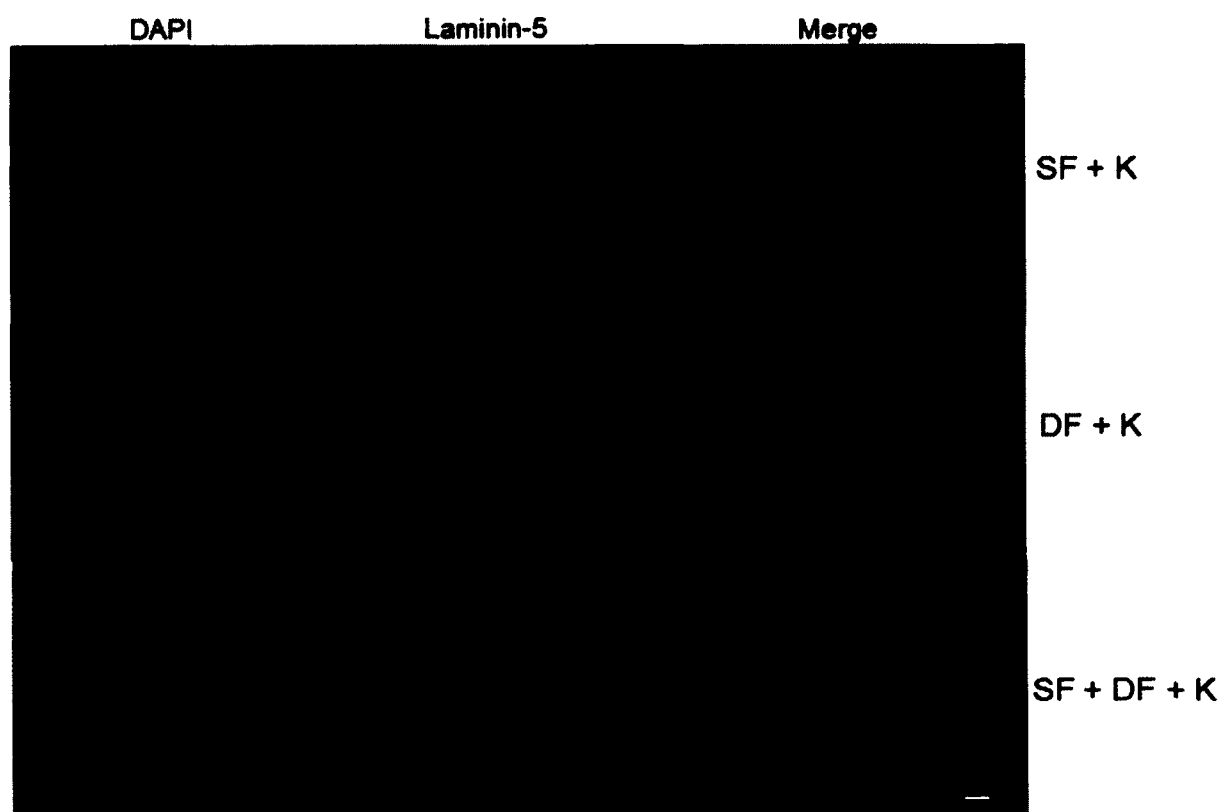


Figure 3.4A: Immunofluorescent Staining of the Basement Membrane Formed in Tissue Engineered Skin.

DAPI and laminin-5 staining were done, and then the images were merged. **A.** Week 2 staining for tissue engineered skin with SF and K, DF and K, or SF, DF and K at 100× magnification. Scale bar = 100 μm. Blue indicates DAPI staining of nuclei on matrices while green indicates presence of laminin-5.

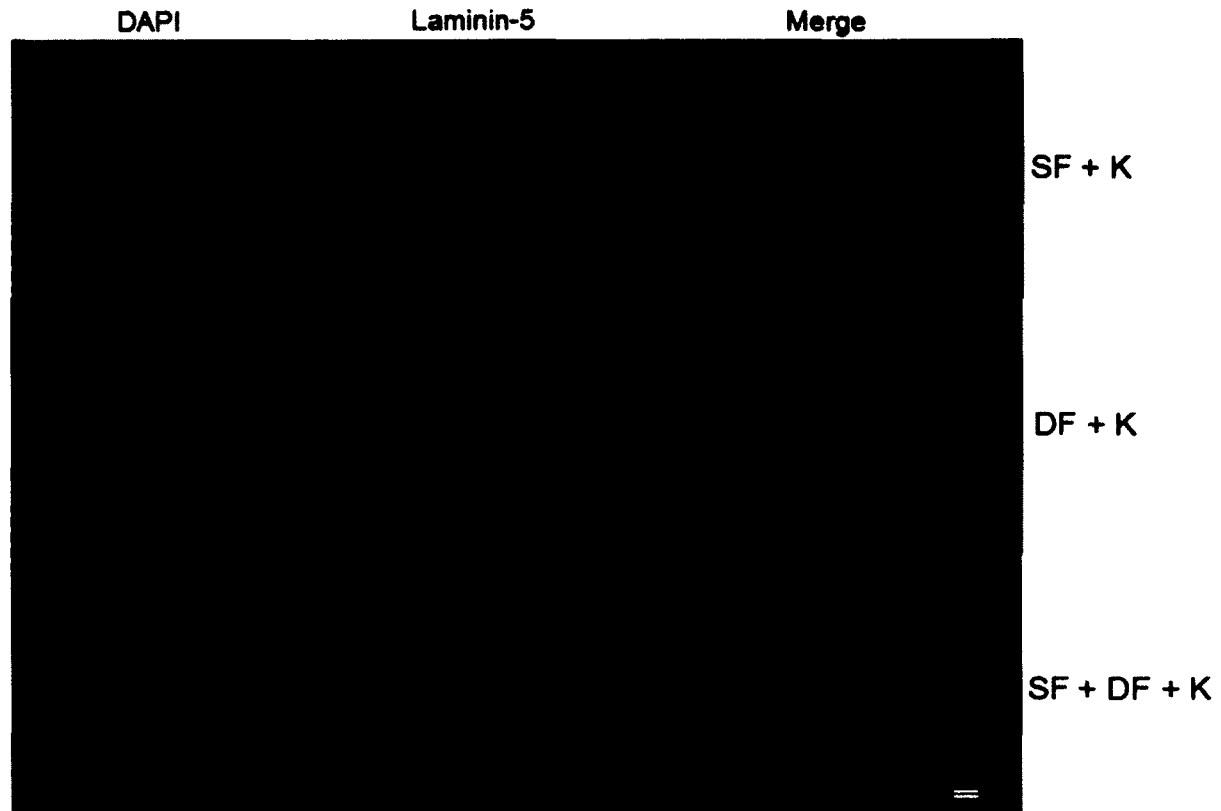


Figure 3.4B: Immunofluorescent Staining of the Basement Membrane Formed in Tissue Engineered Skin.

DAPI and laminin-5 staining were done, and then the images were merged. **B.** Week 3 staining for tissue engineered skin with SF and K, DF and K, or SF, DF and K at 100× magnification. Scale bar = 100 μm. Blue indicates DAPI staining of nuclei on matrices while green indicates presence of laminin-5.

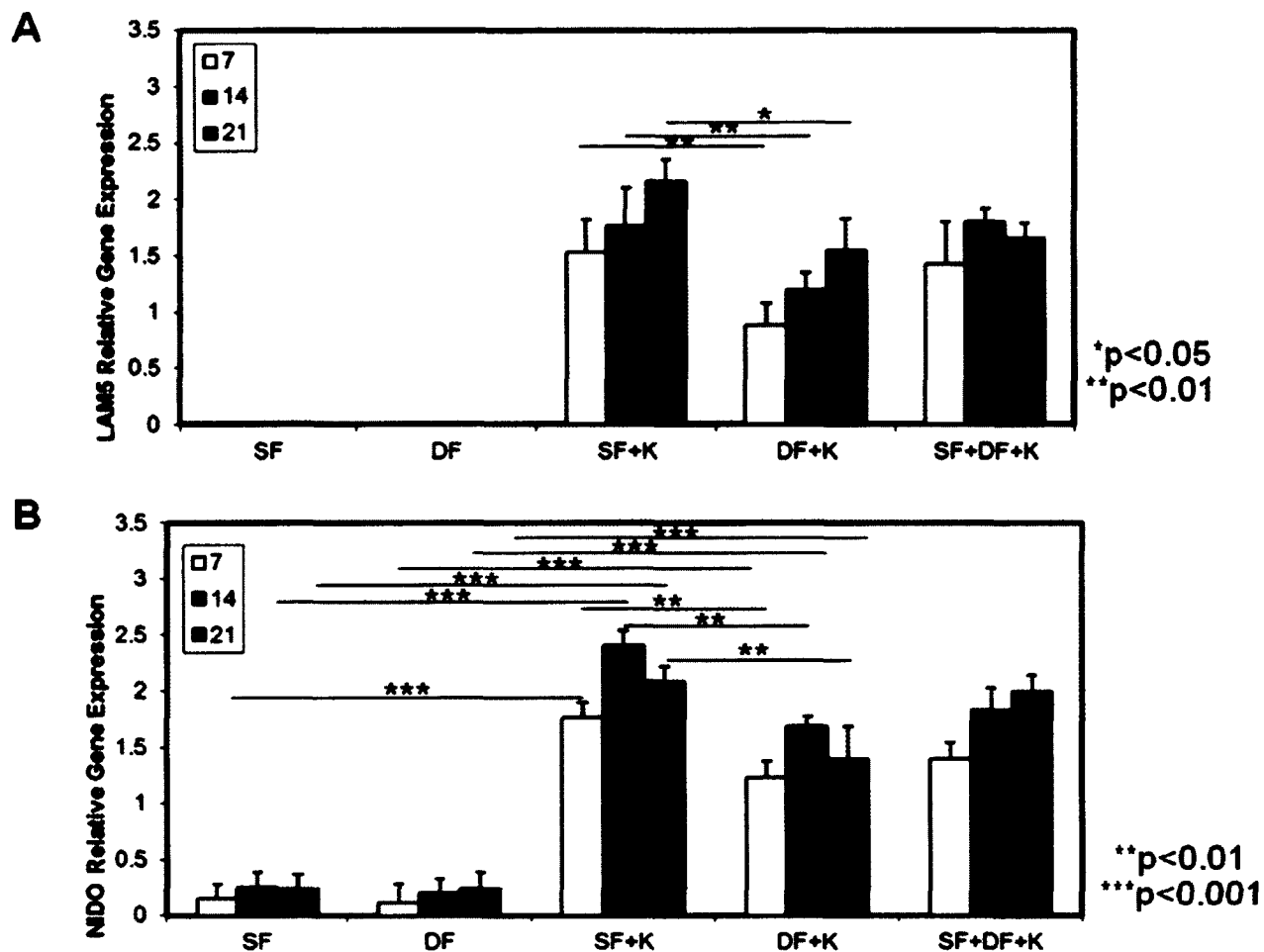


Figure 3.5A-B: Assessment of Relative Gene Expression of Basement Membrane Proteins in Tissue Engineered Skin by qRT-PCR.

mRNA was isolated on days 7, 14 and 21, and reverse transcribed using specific primers (Table 3.1). cDNA was subsequently amplified and relative gene expression was analyzed by qRT-PCR. Each bar represents Mean \pm standard

error relative gene expression (n = 3 abdominoplasty patients). **A.** Relative gene expression for laminin-5 (LAM5). Significant differences between tissue engineered skin with SF and K, DF and K on days 7, 14 ($p < 0.01$) and 21 ($p < 0.05$). **B.** Relative gene expression for Nidogen (NIDO). Significant differences between tissue engineered skin with SF and K and DF and K on days 7, 14 and 21 ($p < 0.01$). Significant differences between tissue engineered skin with SF or DF and K and matrices with fibroblasts alone at all time points ($p < 0.001$).

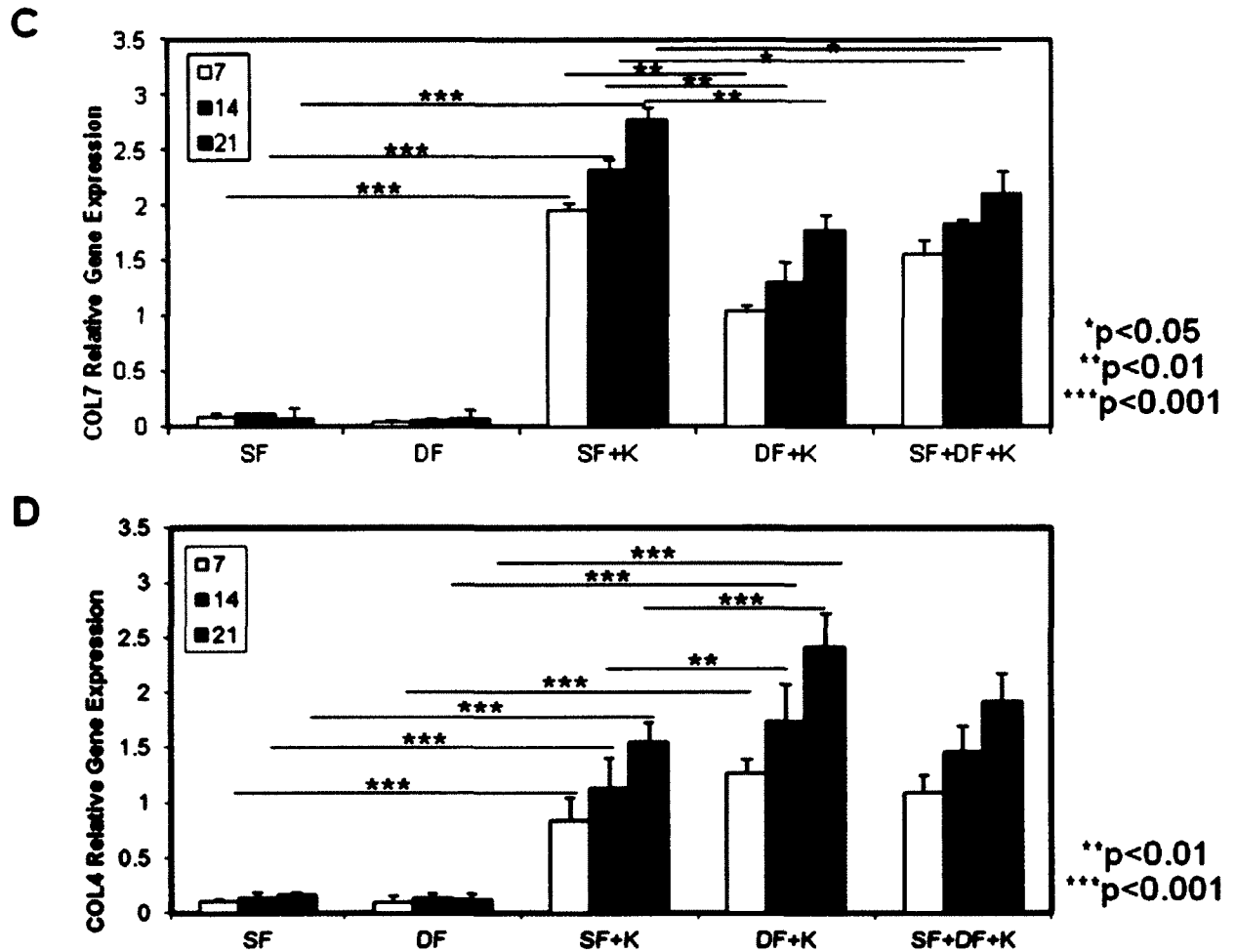


Figure 3.5C-D: Assessment of Relative Gene Expression of Basement Membrane Proteins in Tissue Engineered Skin by qRT-PCR.

mRNA was isolated on days 7, 14 and 21, and reverse transcribed using specific primers (Table 3.1). cDNA was subsequently amplified and relative gene expression was analyzed by qRT-PCR. Each bar represents Mean \pm standard

error relative gene expression (n = 3 abdominoplasty patients). **C.** Relative gene expression for Collagen type VII (COL7). Significant differences between tissue engineered skin with SF and K and DF and K on days 7, 14 and 21 ($p < 0.01$). Significant differences between tissue engineered skin with SF and K and SF, DF and K on days 14 and 21 ($p < 0.05$). Significant differences between tissue engineered skin with SF or DF and K and matrices with fibroblasts alone at all time points ($p < 0.001$). **D.** Relative gene expression for Collagen type IV (COL4). Significant differences between tissue engineered skin with SF and K and DF and K on days 14 ($p < 0.01$) and 21 ($p < 0.001$). Significant differences between tissue engineered skin with SF or DF and K and matrices with fibroblasts alone at all time points ($p < 0.001$).

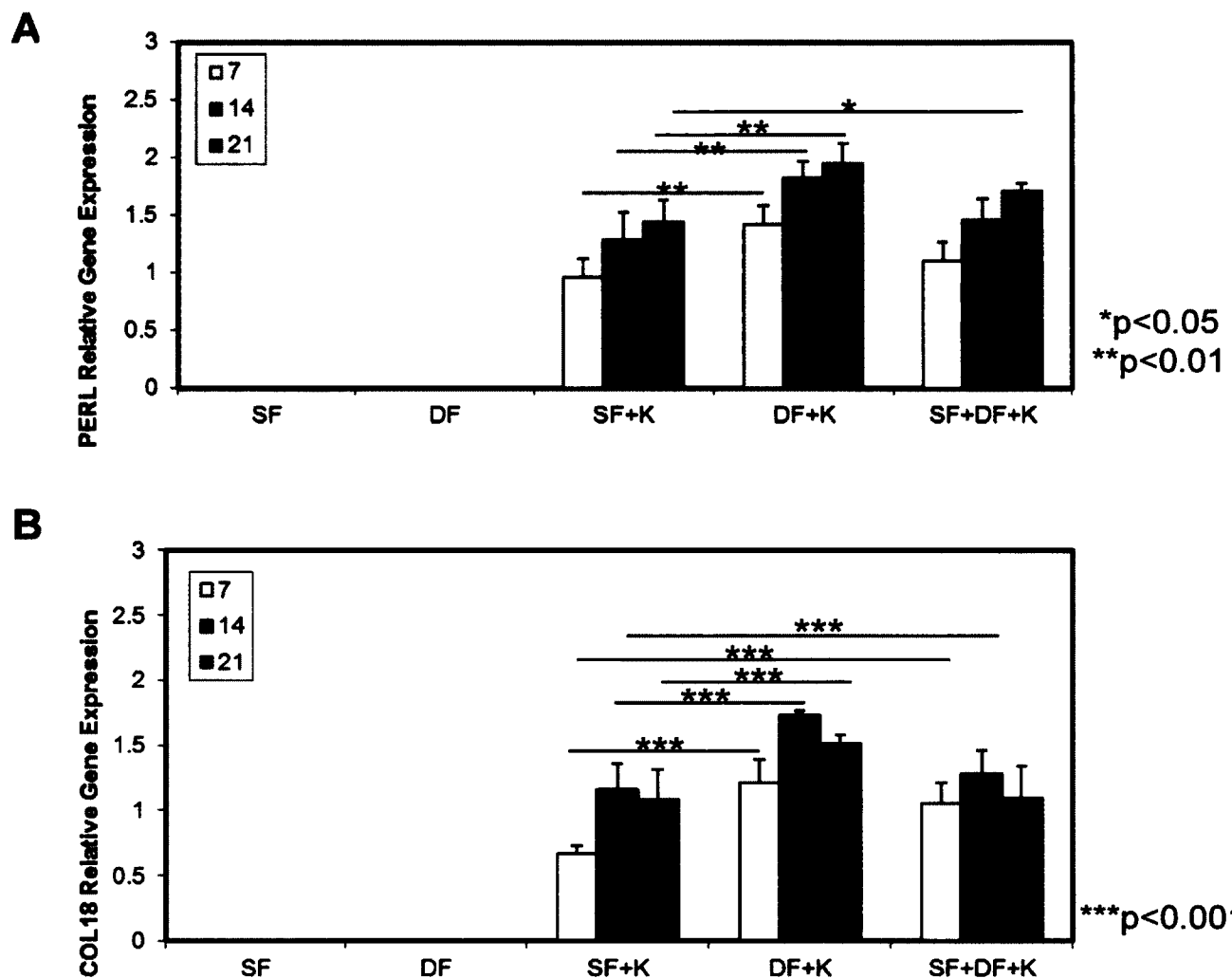


Figure 3.6: Assessment of Relative Gene Expression of Basement Membrane Proteoglycans in Tissue Engineered Skin by qRT-PCR.

mRNA was isolated on days 7, 14 and 21, and reverse transcribed using specific primers (Table 3.1). cDNA was subsequently amplified and relative gene expression was analyzed by qRT-PCR. Each bar represents Mean \pm standard error relative gene expression (n = 3 abdominoplasty patients). **A.** Relative gene expression for perlecan (PERL). Significant differences between tissue engineered skin with SF and K and DF and K at all time points ($p < 0.01$). Significant differences between tissue engineered skin with SF and K and that with SF, DF and K at day 7 ($p < 0.05$). **B.** Relative gene expression for Collagen type XVIII (COL18). Significant differences between tissue engineered skin with SF and K and DF and K at all time points ($p < 0.001$). Significant differences between tissue engineered skin with SF and K and SF, DF and K at days 7 and 14 ($p < 0.001$).

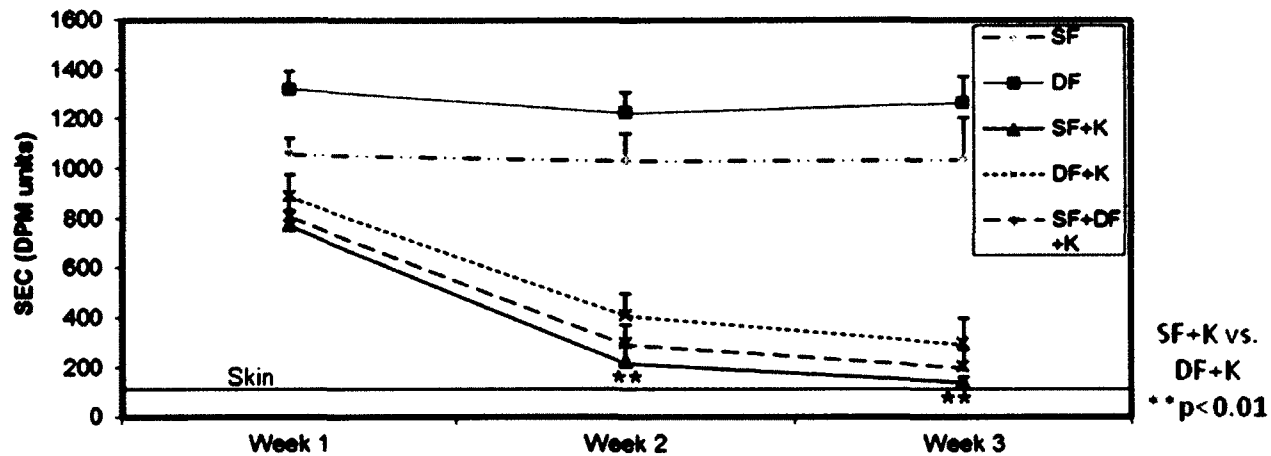


Figure 3.7: Surface Electrical Capacitance (SEC) Measurements of Tissue Engineered Skin.

Using the Nova dermal phase meter, SEC measurements of tissue engineered skin with SF and K, DF and K, or SF, DF and K were taken on week 1, 2 and 3. Each data point refers to Mean SEC \pm standard error of 5 independent measurements done in triplicate for $n = 3$ abdominoplasty patients. Continuous line indicates SEC measurements obtained for normal human skin. Significant differences between tissue engineered skin with SF and K, DF and K on week 2 and 3 ($p < 0.01$).

3.6 References

- [1] Aumailley M, Rousselle P. Laminins of the dermo-epidermal junction. *Matrix Biol.* 1999;18:19-28.
- [2] Timpl R, Brown JC. Supramolecular assembly of basement membranes. *Bioessays.* 1996;18:123-32.
- [3] Fleischmajer R, Kuhn K, Sato Y, MacDonald ED, 2nd, Perlish JS, Pan TC, et al. There is temporal and spatial expression of alpha1 (IV), alpha2 (IV), alpha5 (IV), alpha6 (IV) collagen chains and beta1 integrins during the development of the basal lamina in an "in vitro" skin model. *The Journal of investigative dermatology.* 1997;109:527-33.
- [4] Smola H, Stark HJ, Thiekotter G, Mirancea N, Krieg T, Fusenig NE. Dynamics of basement membrane formation by keratinocyte-fibroblast interactions in organotypic skin culture. *Exp Cell Res.* 1998;239:399-410.
- [5] Yamane Y, Yaoita H, Couchman JR. Basement membrane proteoglycans are of epithelial origin in rodent skin. *The Journal of investigative dermatology.* 1996;106:531-7.
- [6] Fusenig NE. Epithelial-mesenchymal interactions regulate keratinocyte growth and differentiation in vitro. In: Leigh I, Lane, B., Watt, F., editor. *The Keratinocyte Handbook.* Cambridge: Cambridge University Press; 1994. p. 71–94.
- [7] Werner S, Krieg T, Smola H. Keratinocyte-fibroblast interactions in wound healing. *J Invest Dermatol.* 2007;127:998-1008.

- [8] Sorrell JM, Baber MA, Caplan AI. Site-matched papillary and reticular human dermal fibroblasts differ in their release of specific growth factors/cytokines and in their interaction with keratinocytes. *J Cell Physiol.* 2004;200:134-45.
- [9] Wang J, Dodd C, Shankowsky HA, Scott PG, Tredget EE. Deep dermal fibroblasts contribute to hypertrophic scarring. *Lab Invest.* 2008;88:1278-90.
- [10] Varkey M, Ding J, Tredget EE. Differential collagen-glycosaminoglycan matrix remodeling by superficial and deep dermal fibroblasts: potential therapeutic targets for hypertrophic scar. *Biomaterials.* 2011;32:7581-91.
- [11] Honardoust D, Varkey M, Marcoux Y, Shankowsky HA, Tredget EE. Reduced decorin, fibromodulin, and transforming growth factor-beta3 in deep dermis leads to hypertrophic scarring. *J Burn Care Res.* 2012;33:218-27.
- [12] Christiano AM, Uitto J. Molecular complexity of the cutaneous basement membrane zone. Revelations from the paradigms of epidermolysis bullosa. *Exp Dermatol.* 1996;5:1-11.
- [13] Spirito F, Chavanas S, Prost-Squarcioni C, Pulkkinen L, Freitag S, Bodemer C, et al. Reduced expression of the epithelial adhesion ligand laminin 5 in the skin causes intradermal tissue separation. *J Biol Chem.* 2001;276:18828-35.
- [14] Aberdam D, Galliano MF, Vailly J, Pulkkinen L, Bonifas J, Christiano AM, et al. Herlitz's junctional epidermolysis bullosa is linked to mutations in the gene (LAMC2) for the gamma 2 subunit of nicein/kalinin (LAMININ-5). *Nat Genet.* 1994;6:299-304.

- [15] Chan LS, Lapiere JC, Chen M, Traczyk T, Mancini AJ, Paller AS, et al. Bullous systemic lupus erythematosus with autoantibodies recognizing multiple skin basement membrane components, bullous pemphigoid antigen 1, laminin-5, laminin-6, and type VII collagen. *Arch Dermatol.* 1999;135:569-73.
- [16] Uitto J, Christiano AM. Molecular basis for the dystrophic forms of epidermolysis bullosa: mutations in the type VII collagen gene. *Arch Dermatol Res.* 1994;287:16-22.
- [17] De Luca M, Pellegrini G, Mavilio F. Gene therapy of inherited skin adhesion disorders: a critical overview. *The British journal of dermatology.* 2009;161:19-24.
- [18] Uitto J, McGrath JA, Rodeck U, Bruckner-Tuderman L, Robinson EC. Progress in epidermolysis bullosa research: toward treatment and cure. *The Journal of investigative dermatology.* 2010;130:1778-84.
- [19] Fine JD. Inherited epidermolysis bullosa: past, present, and future. *Ann N Y Acad Sci.* 2010;1194:213-22.
- [20] Chino T, Tamai K, Yamazaki T, Otsuru S, Kikuchi Y, Nimura K, et al. Bone marrow cell transfer into fetal circulation can ameliorate genetic skin diseases by providing fibroblasts to the skin and inducing immune tolerance. *Am J Pathol.* 2008;173:803-14.
- [21] Tolar J, Ishida-Yamamoto A, Riddle M, McElmurry RT, Osborn M, Xia L, et al. Amelioration of epidermolysis bullosa by transfer of wild-type bone marrow cells. *Blood.* 2009;113:1167-74.

- [22] Prockop DJ, Olson SD. Clinical trials with adult stem/progenitor cells for tissue repair: let's not overlook some essential precautions. *Blood*. 2007;109:3147-51.
- [23] Fritsch A, Loeckermann S, Kern JS, Braun A, Bosl MR, Bley TA, et al. A hypomorphic mouse model of dystrophic epidermolysis bullosa reveals mechanisms of disease and response to fibroblast therapy. *J Clin Invest*. 2008;118:1669-79.
- [24] Boyce ST, Kagan RJ, Yakuboff KP, Meyer NA, Rieman MT, Greenhalgh DG, et al. Cultured skin substitutes reduce donor skin harvesting for closure of excised, full-thickness burns. *Ann Surg*. 2002;235:269-79.
- [25] Wang J, Ding J, Jiao H, Honardoust D, Momtazi M, Shankowsky HA, et al. Human hypertrophic scar-like nude mouse model: characterization of the molecular and cellular biology of the scar process. *Wound repair and regeneration : official publication of the Wound Healing Society [and] the European Tissue Repair Society*. 2011;19:274-85.
- [26] Takagi R, Yamato M, Murakami D, Kondo M, Yang J, Ohki T, et al. Preparation of keratinocyte culture medium for the clinical applications of regenerative medicine. *J Tissue Eng Regen Med*. 2011;5:e63-73.
- [27] Powell HM, Boyce ST. EDC cross-linking improves skin substitute strength and stability. *Biomaterials*. 2006;27:5821-7.
- [28] Honardoust D, Varkey M, Hori K, Ding J, Shankowsky HA, Tredget EE. Small leucine-rich proteoglycans, decorin and fibromodulin, are reduced in postburn

hypertrophic scar. *Wound repair and regeneration* : official publication of the Wound Healing Society [and] the European Tissue Repair Society. 2011;19:368-78.

[29] Andriessen MP, Niessen FB, Van de Kerkhof PC, Schalkwijk J. Hypertrophic scarring is associated with epidermal abnormalities: an immunohistochemical study. *The Journal of pathology*. 1998;186:192-200.

[30] Machesney M, Tidman N, Waseem A, Kirby L, Leigh I. Activated keratinocytes in the epidermis of hypertrophic scars. *Am J Pathol*. 1998;152:1133-41.

[31] Borradori L, Sonnenberg A. Structure and function of hemidesmosomes: more than simple adhesion complexes. *The Journal of investigative dermatology*. 1999;112:411-8.

[32] Fuchs E, Dowling J, Segre J, Lo SH, Yu QC. Integrators of epidermal growth and differentiation: distinct functions for beta 1 and beta 4 integrins. *Curr Opin Genet Dev*. 1997;7:672-82.

[33] Burgeson RE, Christiano AM. The dermal-epidermal junction. *Curr Opin Cell Biol*. 1997;9:651-8.

[34] Clark RA, Ghosh K, Tonnesen MG. Tissue engineering for cutaneous wounds. *The Journal of investigative dermatology*. 2007;127:1018-29.

[35] Nguyen BP, Gil SG, Carter WG. Deposition of laminin 5 by keratinocytes regulates integrin adhesion and signaling. *J Biol Chem*. 2000;275:31896-907.

- [36] Ryan MC, Lee K, Miyashita Y, Carter WG. Targeted disruption of the LAMA3 gene in mice reveals abnormalities in survival and late stage differentiation of epithelial cells. *J Cell Biol.* 1999;145:1309-23.
- [37] Marionnet C, Pierrard C, Vioux-Chagnoleau C, Sok J, Asselineau D, Bernerd F. Interactions between fibroblasts and keratinocytes in morphogenesis of dermal epidermal junction in a model of reconstructed skin. *The Journal of investigative dermatology.* 2006;126:971-9.
- [38] Nischt R, Schmidt C, Mirancea N, Baranowsky A, Mokkapati S, Smyth N, et al. Lack of nidogen-1 and -2 prevents basement membrane assembly in skin-organotypic coculture. *The Journal of investigative dermatology.* 2007;127:545-54.
- [39] Kohfeldt E, Sasaki T, Gohring W, Timpl R. Nidogen-2: a new basement membrane protein with diverse binding properties. *J Mol Biol.* 1998;282:99-109.
- [40] Engel J, Hunter I, Schulthess T, Beck K, Dixon TW, Parry DA. Assembly of laminin isoforms by triple- and double-stranded coiled-coil structures. *Biochem Soc Trans.* 1991;19:839-43.
- [41] Aumailley M, Battaglia C, Mayer U, Reinhardt D, Nischt R, Timpl R, et al. Nidogen mediates the formation of ternary complexes of basement membrane components. *Kidney Int.* 1993;43:7-12.
- [42] Fleischmajer R, Schechter A, Bruns M, Perlish JS, Macdonald ED, Pan TC, et al. Skin fibroblasts are the only source of nidogen during early basal lamina formation in vitro. *The Journal of investigative dermatology.* 1995;105:597-601.

[43] Bachinger HP, Morris NP, Lunstrum GP, Keene DR, Rosenbaum LM, Compton LA, et al. The relationship of the biophysical and biochemical characteristics of type VII collagen to the function of anchoring fibrils. *J Biol Chem.* 1990;265:10095-101.

[44] Ortiz-Urda S, Garcia J, Green CL, Chen L, Lin Q, Veitch DP, et al. Type VII collagen is required for Ras-driven human epidermal tumorigenesis. *Science.* 2005;307:1773-6.

[45] Poschl E, Schlotzer-Schrehardt U, Brachvogel B, Saito K, Ninomiya Y, Mayer U. Collagen IV is essential for basement membrane stability but dispensable for initiation of its assembly during early development. *Development.* 2004;131:1619-28.

[46] Whitelock JM, Melrose J, Iozzo RV. Diverse cell signaling events modulated by perlecan. *Biochemistry.* 2008;47:11174-83.

[47] Farach-Carson MC, Brown AJ, Lynam M, Safran JB, Carson DD. A novel peptide sequence in perlecan domain IV supports cell adhesion, spreading and FAK activation. *Matrix Biol.* 2008;27:150-60.

[48] Sher I, Zisman-Rozen S, Eliahu L, Whitelock JM, Maas-Szabowski N, Yamada Y, et al. Targeting perlecan in human keratinocytes reveals novel roles for perlecan in epidermal formation. *J Biol Chem.* 2006;281:5178-87.

[49] Utriainen A, Sormunen R, Kettunen M, Carvalhaes LS, Sajanti E, Eklund L, et al. Structurally altered basement membranes and hydrocephalus in a type XVIII collagen deficient mouse line. *Hum Mol Genet.* 2004;13:2089-99.

- [50] Seppinen L, Sormunen R, Soini Y, Elamaa H, Heljasvaara R, Pihlajaniemi T. Lack of collagen XVIII accelerates cutaneous wound healing, while overexpression of its endostatin domain leads to delayed healing. *Matrix Biol.* 2008;27:535-46.
- [51] Schluter H, Wepf R, Moll I, Franke WW. Sealing the live part of the skin: the integrated meshwork of desmosomes, tight junctions and curvilinear ridge structures in the cells of the uppermost granular layer of the human epidermis. *Eur J Cell Biol.* 2004;83:655-65.
- [52] Brandner JM, Kief S, Grund C, Rendl M, Houdek P, Kuhn C, et al. Organization and formation of the tight junction system in human epidermis and cultured keratinocytes. *Eur J Cell Biol.* 2002;81:253-63.
- [53] Tunggal JA, Helfrich I, Schmitz A, Schwarz H, Gunzel D, Fromm M, et al. E-cadherin is essential for in vivo epidermal barrier function by regulating tight junctions. *Embo J.* 2005;24:1146-56.
- [54] Fuchs E. Scratching the surface of skin development. *Nature.* 2007;445:834-42.

Chapter 4

Keratinocytes Alter Biomechanical Characteristics and Reduce Fibrotic Remodeling of Tissue Engineered Skin made with Deep Dermal Fibroblasts*

*Parts of this chapter are being published as: Varkey M, Ding J and Tredget EE. (2013) Keratinocytes alter biomechanical characteristics and reduce fibrotic remodeling of 3-D scaffolds by deep dermal fibroblasts. Manuscript to be submitted.

4 Keratinocytes Alter Biomechanical Characteristics and Reduce Fibrotic Remodeling of Tissue Engineered Skin made with Deep Dermal Fibroblasts

4.1 Introduction

Wound healing following burns and other injuries occurs rarely by regeneration but more commonly by fibrosis [1], depending on the depth of injury in the skin [2]. Regeneration restores the native organization and architecture of skin, whereas fibrosis results in replacement of native tissue with dysfunctional and disorganized tissue called scar [1]. Scar tissue formation occurs due to the growth of connective tissue in place of the normal parenchymal tissue. Fibrosis affects most organs, and can ultimately lead to organ failure as seen in the case of idiopathic pulmonary fibrosis, liver cirrhosis, cardiovascular fibrosis, systemic sclerosis, and renal fibrosis [3]. Skin fibrosis could typically lead to aesthetic and functional problems as seen for the dermal fibroproliferative disorders, hypertrophic scarring (HTS) and keloids [4, 5]. Recovery from HTS depends on a variety of factors including extent of injury and treatment regimen followed. Two-thirds of burn patients with deep dermal injury are affected by hypertrophic scarring, for which there are few clinically effective therapies. Excessive scarring and contracture that occurs during post-burn HTS

can be reduced by early autologous skin transplantation or use of tissue engineered skin in the case of more extensive injuries.

Currently available tissue engineered skin consists of heterogeneous dermal fibroblasts co-cultured with keratinocytes on collagen-glycosaminoglycan (C-GAG) matrices [6]. Dermal fibroblasts are heterogeneous in biophysical and biochemical characteristics, and have been shown to differentially remodel C-GAG matrices [7-10]. Also, the remodeled matrices have different biomechanical characteristics [8]. Deep dermal fibroblasts are pro-fibrotic, they produce more TGF- β 1 and type I collagen compared to superficial dermal fibroblasts which are anti-fibrotic and express more MMP-1 and the small leucine-rich proteoglycans, decorin and fibromodulin [7, 8]. This may have significant implications on wound healing and tissue repair following injury. Further, fibroblast heterogeneity has an effect on epithelial-mesenchymal interactions; we recently found that superficial dermal fibroblasts enhanced basement membrane and epidermal barrier formation in tissue engineered skin compared to deep dermal fibroblasts. Crosstalk between keratinocytes and fibroblasts has been shown to affect cell proliferation and matrix production in the dermis; keratinocytes regulate collagen deposition and collagenase production by fibroblasts [11, 12]. However, it is not clear yet whether keratinocytes affect fibrotic characteristics of only a subset of dermal fibroblasts and whether there is a differential effect on biomechanical ECM remodelling by superficial and deep dermal fibroblasts.

The aim of this study was to determine the effect epidermal keratinocytes have on fibrotic matrix remodelling by superficial and deep dermal fibroblasts in tissue engineered skin. Tissue engineered skin made of superficial or deep dermal fibroblasts was examined for matrix contraction, expression of fibrotic and anti-fibrotic factors and proteoglycans, collagen and TGF- β 1 production, and myofibroblast differentiation.

4.2 Materials and Methods

4.2.1 Preparation of C-GAG Matrices

Acellular C-GAG matrices were prepared by freeze-drying a co-precipitate of type I collagen and chondroitin-6-sulfate as reported previously [8]. Briefly, collagen powder (0.5 wt %; Devro Pty. Ltd., Bathurst, NSW, Australia) was co-precipitated with chondroitin-6-sulfate (0.05 wt %; Sigma, St. Louis, MO, USA) in 0.5 M acetic acid, degassed under vacuum (2 h, room temperature), cast into sheets, frozen to -40°C and freeze-dried (FreeZone⁶Plus, Labconco, Kansas City, MI, USA) to produce highly porous matrices. The matrices were cut into 30 mm discs and cross-linked by dehydrothermal treatment in a drying oven (vacuum, 140°C , 48 h; APT.Line VD, Binder GmbH, Germany). Subsequently, the matrix discs were rinsed with phosphate buffered saline (PBS; 2 \times , 15 min) and cell culture medium (DMEM, 10% FBS, 1% Antibiotic-antimycotic; 2 \times , 15 min).

4.2.2 Preparation of Tissue Engineered Skin

Tissue engineered skin was prepared by culturing superficial or deep dermal fibroblasts and keratinocytes on dehydrothermal-treated C-GAG matrices. The cells were obtained from lower abdominal tissue of three patients who underwent elective abdominoplasty surgery following informed consent. The protocols for human tissue sampling used in this study were approved by the University of Alberta Hospital's Health Research Ethics Board. Superficial and deep dermal fibroblasts and keratinocytes were isolated as reported previously [8]; briefly, tissue samples were horizontally sectioned into five layers (referred to as layers 1 to 5) using a dermatome (Padgett Instruments, Plainsboro, NJ, USA) set approximately at 0.5 mm. The superficial dermal layer (layer 1) was treated overnight with dispase (25 U/mL, 4°C; Gibco, Grand Island, NY, USA) to remove the epidermis, which was digested with trypsin to isolate keratinocytes. On the other hand, the superficial dermal layer and the deep dermal layer (layer 5) were separately treated with collagenase (455.3 U/mL, 18 h, 37°C, 60 rpm; Gibco Grand Island, NY, USA) to isolate the superficial (SF) and deep (DF) dermal fibroblasts, respectively. The keratinocyte (K) and fibroblast cell suspensions were passed through 100 µm cell strainers and centrifuged at 800 rpm for 10 minutes. The epidermal and dermal cell pellets were then re-suspended in the respective cell culture media and serially expanded in tissue culture flasks till the desired number of K, SF and DF were obtained. Passage 4 SF or DF were seeded onto cross-linked C-GAG discs at a density of 0.5×10^6

cells/cm² and cultured (at 37°C, 5% CO₂). Two days later, K were seeded on top of the fibroblast-populated matrices at a density of 1.0×10^6 cells/cm² and medium was replaced with co-culture medium containing serum (DMEM-HG and nutrient mixture F-12 Ham (3:1), 2 nM triiodothyronine, 5% FBS, 0.5% insulin–transferrin–selenium-G supplement, 1 nM cholera toxin, 10 ng/ml EGF, 0.4 µg/ml hydrocortisone, 5 µg/ml transferrin, 1% antibiotic-antimycotic;[13]). Tissue engineered skin made of SF, DF and K were used as a control for tissue engineered skin made of heterogeneous fibroblasts while matrices with SF or DF alone were used as K-free controls, wherein the number of cells was adjusted so as to make the number of cells on the matrices comparable to those that had K. The submerged culture was continued for 5 additional days and then lifted to the air-liquid interface on a steel platform to enable epidermal stratification. The tissue engineered skin and controls were used in assays at different time points as described below.

4.2.3 Analysis of Contraction of Tissue Engineered Skin

To determine the extent of contraction, the different tissue engineered skin and controls were photographed on days 7, 14 and 21, and the images were analyzed using NIH image J. The values are reported as mean percentage contraction ± standard error.

4.2.4 Assessment of Collagen Content in Conditioned Medium of Tissue Engineered Skin

The total collagen content in the conditioned medium (DMEM, 2% FBS, 50 $\mu\text{g}/\text{mL}$ ascorbic acid, 50 $\mu\text{g}/\text{mL}$ β -amino propionitrile, 0.1 mM proline) of the different tissue engineered skin was determined by measuring hydroxyproline. The amount of hydroxyproline, which is a protein marker for collagen, was quantified on days 7, 14 and 21 of culture. Conditioned media of C-GAG matrices without cells were used as controls. Briefly, acetonitrile was added to conditioned media to precipitate collagen. The samples were centrifuged (15 min, 4°C) and precipitates were hydrolyzed overnight (6 N HCl, 110°C). A known amount of N-methyl-proline was added to the hydrolysate after drying, to obtain the N-butyl ester derivative of hydroxyproline. The samples were then subjected to liquid chromatography/ mass spectrometry using a HP 1100 Liquid Chromatograph hooked up to a HP 1100 Mass Selective detector and the ions 186 (N-butyl ester of N-methyl-proline) and 188 (N-butyl ester of 4-hydroxyproline) were monitored. Each sample was analyzed with respect to a standard curve of 4-hydroxyproline (generated under identical conditions) and the results are presented as mean \pm standard error.

4.2.5 Immunohistochemical Analysis

5 mm punch biopsies were collected from the different tissue engineered skin and controls at days 7, 14 and 21 of culture for immunohistochemical staining of alpha-smooth muscle actin (α -SMA). α -SMA is a marker for myofibroblasts. C-GAG matrices with fibroblasts but no keratinocytes were used as controls. Briefly, the samples were fixed with 4% paraformaldehyde (12 h) and 70% ethanol (12 h), paraffin embedded and sectioned at 5 μ m and mounted on microscope slides. The sections were then deparaffinized with xylene and rehydrated in descending series of ethanol, and subsequently blocked with 10% BSA in PBS for 60 min to avoid non-specific protein binding. The sections were incubated overnight with primary mouse anti- α -SMA antibody (4°C, 1:50 dilution; Dako, Denmark), and later on washed with PBS (3 \times , 5 min). Non-immune human IgG at 1:50 dilution was used as the negative control. Endogenous peroxide activity was quenched with 0.3% H₂O₂ (15 min) and subsequently the sections were incubated with fluorescent secondary antibody Alexa Fluor 488-conjugated goat anti-mouse IgG (60 min, room temp., 1:500 dilution; Invitrogen, Oakville, ON, Canada). The stained sections were then mounted with DAPI containing ProLong Gold reagent, and viewed by fluorescent microscopy at 100 \times magnification and photographed.

4.2.6 Gene Expression Studies

5 mm punch biopsies were collected from the different tissue engineered skin and the controls at days 7, 14 and 21 of culture and snap frozen in liquid nitrogen for subsequent gene expression analysis. The frozen matrices were homogenized (2000 rpm, 2 min; Mikro-Dismembrator S, B. Braun Biotech International), and treated with Trizol reagent (Invitrogen, Carlsbad, CA, USA); the resultant supernatant was stored at -80°C for subsequent analyses. Later, total RNA was extracted from all the supernatants using RNeasy Mini Kit (Qiagen, Mississauga, ON, Canada) following manufacturer's instructions, and quantified using Nano Drop 1000 spectrophotometer (Thermo Fisher Scientific, Wilmington, DE). RNA extract of each sample (0.5 µg) was used for first-strand cDNA synthesis using M-MLV Reverse Transcriptase (Invitrogen, Carlsbad, CA, USA) by incubation at three different conditions, 25°C for 10 min followed by 37°C for 50 min and 70°C for 15 min. The resulting cDNA was used as a template for quantitative Real Time Polymerase Chain Reaction (qRT-PCR) amplification of genes of interest. The gene specific primers used in qRT-PCR were designed using Primer Express 3.0 (Table 4.1). qRT-PCR was done using Power Sybr Green™ PCR master mix (ABI, Foster, CA, USA) in a total reaction volume of 25 µl containing 5 µl of a 1:10 dilution of cDNA product from the first-strand reaction and 1 µM gene-specific forward and reverse primers on a StepOne Plus qRT-PCR system (ABI, Foster, CA, USA). The amplification conditions included initial denaturation at 95°C for 3 min followed by 40 cycles of denaturation at

95°C for 15 sec and annealing and primer extension at 60°C for 30 sec. The amplification of genes was measured in terms of cycle threshold (C_T) values, and the obtained C_T values were normalized with the C_T value of a house-keeping gene. Gene expression levels are shown as mean fold change \pm standard error.

4.2.7 Protein Expression Analysis

Conditioned medium from the different tissue engineered skin and controls were collected on days 7, 14 and 21 and stored at -80°C to analyze TGF- β 1 protein expression using Enzyme-linked immunosorbent assay (ELISA). The analysis of TGF- β 1 was done as reported previously [8]; briefly, 48 h before collecting conditioned medium at the respective time points the culture medium was changed from 10% FBS-DMEM to 0.2% FBS-DMEM and cells were allowed to grow. To quantify latent TGF- β 1 200 μ l of conditioned medium was directly used, while for active TGF- β 1 conditioned medium was first acidified (1 N HCl, 10 min) and neutralized (1.2 N NaOH, 0.5 M HEPES, 1 min) before analysis. In both cases, samples along with TGF- β 1 standards were diluted in assay buffer (0.1% BSA, 0.1% Tween 20, 150 mM NaCl, 100 mM Tris) and added to 96-well microtitre plates that were coated overnight with 2 μ g/mL of TGF- β 1 mouse monoclonal antibody (R&D Systems, Minneapolis, MN, USA) and incubated for 2 h at 37°C. Subsequently chicken anti-TGF- β 1 antibody (R&D Systems, Minneapolis, MN, USA) was added and the plates were incubated for 1 h at 37°C. Alkaline phosphatase conjugated rabbit anti-chicken IgG (Jackson

ImmunoResearch, West Grove, PA, USA) was then added at a dilution of 1:5000 and incubated for 1 h at 37°C followed by addition of *p*-nitrophenyl phosphate substrate solution (1 mg/ml in diethanolamine buffer). The colored product obtained was quantified at 405 nm on a microplate reader (THERMOmax, Molecular Devices, Sunnyvale, CA, USA).

4.2.8 Statistical Analysis

Experiments were conducted in triplicates and data are expressed as mean \pm standard error. Statistical analyses were done using ANOVA with significance set at $P < 0.05$, $P < 0.01$ and $P < 0.001$ using Microsoft Excel 8.0.

4.3 Results

4.3.1 Contraction of the Different Tissue Engineered Skin

SF, DF and K were isolated from lower abdominal tissue from three abdominoplasty patients and serially expanded. Passage 4 SF and DF were then independently cultured with or without K on cross-linked C-GAG matrices and analyzed at different time points to determine the extent of matrix contraction. The percentage of matrix contraction was calculated by determining the change in area of the matrices at each time point with respect to the original area; the original area of the matrix before seeding the fibroblasts was considered as 100%. C-GAG matrices with SF and DF alone were used as controls for

fibroblast-mediated contraction while matrices without cells were used as controls for matrix contraction that may be due to longer extent of exposure to culture medium. Matrices with DF alone were more contracted than tissue engineered skin made of DF and K, which was significant on days 14 ($p < 0.01$) and 21 ($p < 0.001$). Tissue engineered skin made of SF, DF and K was significantly more contracted than that made of SF and K ($p < 0.001$); however, there were no differences in contraction of matrices with SF and tissue engineered skin made of SF and K. Also, matrices with DF were more contracted than matrices with SF, which was significant on days 14 and 21 ($p < 0.001$; Fig. 4.1).

4.3.2 Collagen Production

The amount of collagen produced by the cells was determined at different time points by quantifying hydroxyproline present in conditioned medium by mass spectrometry. The conditioned medium taken from tissue engineered skin made of DF and K had significantly greater amounts of hydroxyproline than that made of SF and K at all time points ($p < 0.001$; Fig. 4.2). However, tissue engineered skin made of DF and K had significantly lower hydroxyproline level than matrices with DF alone, which was significant at all time points ($p < 0.001$, 0.05). Also, conditioned media of matrices with DF alone had significantly higher hydroxyproline levels than that with SF alone ($p < 0.001$). Hydroxyproline levels

for tissue engineered skin made of SF, DF and K was significantly lower than that with DF and K at all time points ($p < 0.001$, $p < 0.05$).

4.3.3 Expression of Pro- and Anti-Fibrotic Factors and Proteoglycans

To understand the effect of keratinocytes on the anti- and pro-fibrotic characteristics of SF and DF, expression of 6 different genes was analyzed by qRT-PCR. Genes coding for FIN, CTGF, MMP-1, DCN, VEGF and FMOD were examined. The obtained gene expression data was normalized with respect to the house-keeping gene hypoxanthineguanine phosphoribosyl transferase (HPRT). Tissue engineered skin made of DF and K had significantly higher expression of FIN compared to those with SF and K at days 7, 14 ($p < 0.001$) and 21 ($p < 0.0001$) (Fig. 4.3A), but significantly lower than matrices with DF alone on days 14 and 21 ($p < 0.0001$). Also, FIN expression for matrices with DF alone was significantly higher than those for SF alone on days 7 and 14 ($p < 0.001$) and 21 ($p < 0.0001$). FIN expression for tissue engineered skin made of SF, DF and K was lower than that for matrices with DF alone and was significant on day 21 ($p < 0.0001$), but comparable to tissue engineered skin made of DF and K. Tissue engineered skin with DF and K had significantly lower CTGF expression than matrices with DF alone at all time points ($p < 0.001$). CTGF expression for tissue engineered skin made of SF, DF and K was significantly lower than that with DF and K at all time points ($*p < 0.05$, $**p < 0.001$). Further, CTGF expression for

matrices with DF alone was significantly greater than those with SF alone at days 7, 14 ($p < 0.001$) and 21 ($p < 0.0001$). Tissue engineered skin made of DF and K had lower expression of MMP-1 compared to that with SF and K, which was significant on days 7 and 14 ($p < 0.001$) (Fig. 4.3C), but comparable to that with SF, DF, and K, or matrices with DF alone. Matrices with DF alone had lower expression of MMP-1 than those with SF alone, which was significant at all time points ($p < 0.001$, $p < 0.0001$). Tissue engineered skin with DF and K had lower expression of decorin than those with SF and K, which was significant on days 7 ($p < 0.05$), 14 ($p < 0.001$) and 21 ($p < 0.0001$), but comparable to those with SF, DF and K (Fig. 4.4A). Matrices with SF alone had significantly higher decorin expression than those with DF alone at all time points ($p < 0.001$). Expression profile for FMOD was similar to that of decorin, tissue engineered skin with DF and K had lower expression of FMOD than those with SF and K, which was significant on days 7 ($p < 0.05$), 14 ($p < 0.001$) and 21 ($p < 0.0001$), but comparable to those with SF, DF and K (Fig. 4.4B). Matrices with SF alone had significantly higher FMOD expression than those with DF alone at all time points ($p < 0.001$). In the case of VER, tissue engineered skin with DF and K had higher expression than those with SF and K, which was significant on days 7, 14 ($p < 0.001$) and 21 ($p < 0.0001$) (Fig. 4.4C). Tissue engineered skin with DF and K also had significantly higher VER expression than those with SF, DF and K at all time points ($p < 0.001$). Matrices with DF alone had significantly higher VER expression than those with SF alone at all time points ($p < 0.0001$).

4.3.4 Myofibroblast Differentiation

Myofibroblasts that mediate wound contraction that occurs during wound healing are rich in α -SMA. α -SMA staining of the different tissue engineered skin and controls was done to determine the extent of myofibroblast differentiation. α -SMA staining was maximum in the different tissue engineered skin at day 14 (Fig. 4.5A, data not shown for days 7 and 21). Matrices with DF had more α -SMA staining than tissue engineered skin made with DF and K or SF, DF and K. Interestingly, matrices with SF or tissue engineered skin made with SF and K had negligible α -SMA staining (data not shown). The gene expression data for α -SMA was consistent with the observed α -SMA staining (Fig. 4.5B); matrices with DF alone had significantly higher expression compared to tissue engineered skin with DF and K ($p < 0.0001$). Tissue engineered skin with DF and K had significantly higher expression of α -SMA compared to that with SF and K ($p < 0.0001$) or SF, DF and K ($p < 0.001$).

4.3.5 TGF- β 1 Production

TGF- β 1, which is believed to be one of the primary mediators of fibrosis, is overexpressed in deep dermal fibroblasts [14] and HTS [15]. In order to determine the amount of TGF- β 1 protein produced for the different types of tissue engineered skin, the respective conditioned media of the tissue engineered

skin with SF and K, DF and K, SF, DF and K, and matrices with SF or DF alone were analyzed by ELISA. The amount of TGF- β 1 was found to increase progressively with time for the different types of tissue engineered skin. Tissue engineered skin with DF and K produced significantly more latent TGF- β 1 as well as total TGF- β 1 compared to those with SF and K ($p < 0.01$) or SF, DF and K ($p < 0.05$, $p < 0.001$, $p < 0.0001$) (Fig. 4.6). Interestingly, tissue engineered skin with DF and K produced significantly lower amounts of TGF- β 1 compared to matrices with DF alone at all time points ($p < 0.001$). Tissue engineered skin with SF and K had similar levels of TGF- β 1 compared to matrices with SF alone.

4.4 Discussion

Wound healing is a finely orchestrated spatiotemporal process that involves hemostasis, proliferation, migration, differentiation of cells, and deposition of type I collagen and other ECM molecules that results in the formation of scar tissue that gets remodelled over time. Hypertrophic scar (HTS) formation is a major clinical problem especially in the case of burns that result in deep dermal injury. Dermal fibroblasts, the cells that mediate wound healing and hypertrophic scarring, have been shown to be heterogeneous by us and others. We had previously reported that deep dermal fibroblasts may play a significant role in the formation of HTS [7, 8]. Currently, there are no clinically effective therapies for treatment of HTS. Matrix molecules associated with HTS such as

type I collagen and glycosaminoglycans are produced by fibroblasts, however there is evidence that their production is regulated by fibroblast-keratinocyte interactions [7], suggesting that epidermal-mesenchymal interaction may have a significant influence on wound healing and HTS formation. Recently, we showed that superficial and deep dermal fibroblasts differentially remodel C-GAG matrices and differentially contribute to the formation of HTS. The current study aimed to determine how K affect the fibrotic characteristics of SF and DF and the biomechanical properties and remodelling of tissue engineered skin made with these specific dermal sub-populations.

In order to reduce variability due to different cell sources, fibroblasts and keratinocytes were obtained from the same patients; the cells were chosen such that ages of the patients were similar as much as possible (29, 32 and 47 years). As we have seen in previous studies there were no differences in viability of SF and DF cultured alone on the matrices [8], but this was significantly lower than the viability observed for tissue engineered skin made of SF or DF cultured with K (data not shown). Contraction of the matrices was monitored as an index for contraction observed during the course of wound healing. Co-culture of SF or DF with K reduced the degree of fibroblast-mediated matrix contraction, but the reduction was significant only in the case of DF. The fact that there was no significant reduction in contraction of tissue engineered skin made of SF and K compared to matrices with SF alone indicates that K do not have a contraction-inhibiting anti-fibrotic effect on SF but only on DF. Clinically, delayed re-

epithelialization has been observed to increase the severity of fibrosis and scar tissue formation. Also, use of autologous split-thickness skin grafts or autologous and allogeneic cultured keratinocytes sheets has been observed to promote wound healing and suppress scar formation in large wounds [8, 9]. The scar-inhibitory effect keratinocytes have on fibroblasts is possibly mediated through soluble keratinocyte-releasable factors that ultimately act on dermal fibroblasts in a paracrine manner [10]. The differential contraction-inhibition observed in the case of DF as opposed to SF may possibly be due to higher levels of these keratinocyte-releasable factors in the DF micro-environment.

Collagen homeostasis in the skin, which is normally maintained due to the fine balance in collagen synthesis and degradation, is compromised in the case of HTS and other fibroproliferative diseases leading to excess deposition of collagen and characteristic features observed for such diseases. In order to determine the effect keratinocytes have on collagen deposition by SF and DF, the respective conditioned medium was analyzed for hydroxyproline content. Previously we showed that DF produce more collagen type I compared to SF [7, 8]; in this study we found that co-culture with K reduced collagen production in the case of DF but not SF compared to the respective fibroblasts cultured alone. This clearly suggests that keratinocytes have an inhibitory effect on collagen production of DF but not SF. Previous studies involving co-culture of heterogeneous dermal fibroblasts with keratinocytes or treatment with keratinocyte-conditioned medium have shown that the presence of keratinocytes results in lower collagen mRNA

and protein expression levels, suggesting that collagen production by fibroblasts is regulated by certain keratinocyte-releasable factors [16].

In order to understand the molecular basis of differences in fibrotic remodelling of the different tissue engineered skin gene expression of the pro-fibrotic FIN and CTGF, anti-fibrotic MMP-1, DCN and FMOD and large proteoglycan VER were analyzed on days 7, 14 and 21. DF had significantly higher FIN and CTGF expression compared to SF, which was significantly reduced on culture with K in the case of DF but not SF. In the case of MMP-1, both SF alone and SF and K had significantly higher expression than DF and DF and K, respectively. Previously, keratinocytes have been shown to down regulate CTGF activity during end-stage wound healing through secretion of interleukin-1 α [17]. One of the factors found in keratinocyte-conditioned medium, stratifin, stimulates matrix MMP-1 production [13]. For the small proteoglycans DCN and FMOD, SF had significantly higher expression than DF, which is consistent with previous studies. DCN and FMOD play an important role in TGF- β 1 inhibition and collagen fibrillogenesis [18]. Interestingly, co-culture with K did not affect their expression in the case of SF but significantly increased their expression in the case of DF. For VER, which is important for cell adhesion, migration and proliferation [19], the trend was similar for co-culture, resulting in higher expression for DF but no effect for SF. The increase in small proteoglycan expression observed in the case of DF co-cultured with K, may be partly responsible for the observed reduction in fibrotic characteristics.

The key cellular mediator of fibrosis, myofibroblasts, have characteristically higher contractile ability and expression of α -SMA and collagen [20]. They mediate wound contraction that enables to bring the wound edges closer and facilitate the wound healing process. Previous studies have shown that the extent of differentiation to myofibroblasts is significantly more for DF compared to SF [7, 8]. Interestingly, in this study we found that K had an inhibitory effect on differentiation of DF to myofibroblasts but not that of SF, which may possibly be due to differences in characteristics of the SF and DF as well as their cellular microenvironment. Of the known factors implicated in wound healing and fibrosis, TGF- β 1, the central pro-fibrotic factor, is understood to be vital since it is essential for differentiation to myofibroblasts and their maintenance [21], and as well direct mediation of collagen production [22]. DF were significantly more differentiated into myofibroblasts compared to SF; which was reduced on co-culture with K. Reduction in TGF- β 1 production on co-culture with K for DF but not SF indicates a K-mediated anti-fibrotic effect on the former. Keratinocytes have been shown to release factors into their conditioned media that inhibit fibroblast mediated-production of TGF- β 1 and its downstream mediator CTGF [11]. Overall the results from this study show that keratinocytes have a role in suppressing ECM production and deposition specifically in the case of DF.

4.5 Conclusions

Currently, there are few fully effective *in vitro* models to study HTS. Some research groups including that of Moulin V from LOEX institute (Quebec, Canada) are working on using keloid and HTS fibroblasts with tissue engineered skin to develop *in vitro* models. This is the first study to assess fibrotic characteristics of tissue engineered skin made of pure sub-populations of dermal fibroblasts as opposed to the conventional heterogeneous dermal fibroblasts. The use of a keratinocytes-fibroblast co-culture system on C-GAG matrices enabled us to assess the anti-fibrotic role of keratinocytes on superficial and deep dermal fibroblasts in a 3-D microenvironment and their effect on keratinocyte-induced differential biomechanical and biochemical remodelling of the matrices. Taken together our results demonstrate that keratinocytes particularly influence biomechanical properties and fibrotic remodelling of tissue engineered skin made specifically of DF and not SF. This could lead to the development of novel non-scarring tissue engineered skin which could be used to treat burn patients who are prone to fibroproliferative diseases such as HTS and keloids.

4.6 Table and Figures

Table 4.1: Primers Used in qRT-PCR for Amplification of Genes of Interest

| Gene | Forward Primer | Reverse Primer |
|---|------------------------------|-------------------------------|
| Versican | GCAGCTGAACGGGAA TGC | CGTGAGACAGGATGC TTGTGA |
| Decorin | TGTCATAGAACTGGG CACCAAT | GGAAAGCCCCATTTT CAATTC |
| Fibromodulin | TTTTATCATCGTTCTG CCTTCATG | TGTTTGCGGGACCTT AGGAA |
| TGF- β 1 | GGGAAATTGAGGGCT TTCG | AGTGTGTTATCCCTG CTGTCACA |
| CTGF | TCCACCCGGGTTACC AATG | CAGGCGGCTCTGCTT CTCTA |
| Fibronectin | CCAATTCCTTGCTGG TATCATG | TCATACTTGATGATG TAGCCGGTAA |
| MMP-1 | CCTCGCTGGGAGCAA ACA | TTGGCAAATCTGGCG TGTA |
| α -SMA | GCTCACGGAGGCACC CCTGAA | TCCAGAGTCCAGCAG ATG |
| Hypoxanthine guanine phospho- ribosyl transferase (house-keeping gene) | GACCAGTCAACAGGG GACA | ACACTTCGTGGGGTC CTTTT |

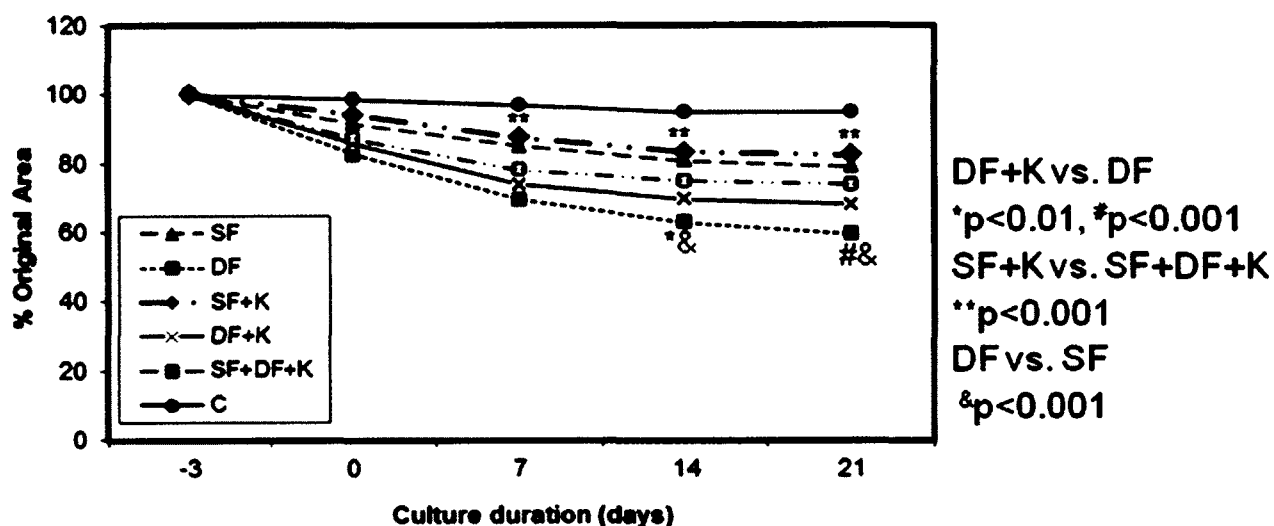


Figure 4.1: Contraction of Tissue Engineered Skin made of SF or DF and K.

SF and DF were independently co-cultured with K on C-GAG matrices for 21 days. Digital photographs of the matrices were taken just before the fibroblasts were seeded (-3), on the day keratinocytes were seeded (0) and further on days 7, 14 and 21 of culture and the extent of contraction was measured using NIH Image J. Each data point represents Mean \pm SE contraction ($n = 3$ abdominoplasty patients). Significant differences in contraction were observed between tissue engineered skin made of DF and K and matrices with DF alone on days 14 ($p < 0.01$) and 21 ($p < 0.001$). Significant differences in contraction were

also observed between tissue engineered skin made of SF and K and those with SF, DF and K on days 7, 14 and 21($p < 0.001$). Also, matrices with DF were more significantly contracted than those with SF on days 14 and 21($p < 0.001$).

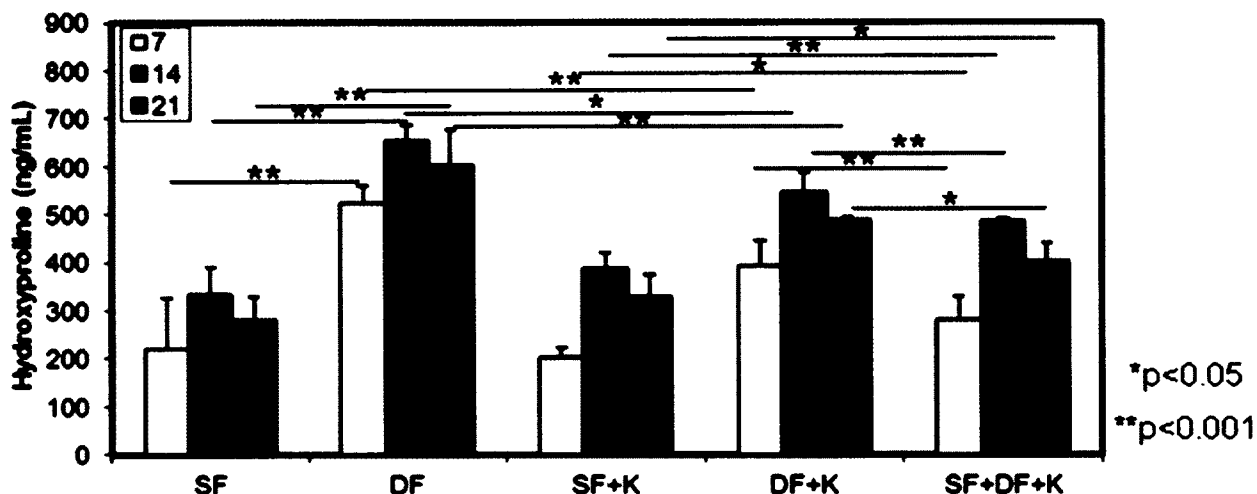


Figure 4.2: Measurement of Collagen Production for Tissue Engineered Skin made of SF or DF and K.

SF and DF were independently co-cultured with K on C-GAG matrices for 21 days. Collagen production was measured by LC/MS assessment of hydroxyproline on days 7, 14 and 21 of culture. Each bar represents Mean \pm SE Hyp (n = 3 abdominoplasty patients). SF and DF cultured with or without K on C-GAG matrices in co-culture medium and 48 h before each time point the medium was changed to 2% FBS/DMEM. The supernatants were collected and assessed by LC/MS. Significant differences were observed in level of hydroxyproline in conditioned media of tissue engineered skin made of DF and K and matrices with

DF alone on days 7, 14 and 21 ($p < 0.0001$). Significant differences were also observed between tissue engineered skin made of SF and K and DF and K on days 7 and 14 ($p < 0.001$) and 21 ($p < 0.0001$), tissue engineered skin made of DF and K had significantly different hydroxyproline levels compared with those that had SF, DF and K on days 7 ($p < 0.001$) and 14 and 21 ($p < 0.0001$). Further matrices with DF alone and SF alone had significant differences in hydroxyproline on days 7 and 14 ($p < 0.001$) and 21 ($p < 0.0001$).

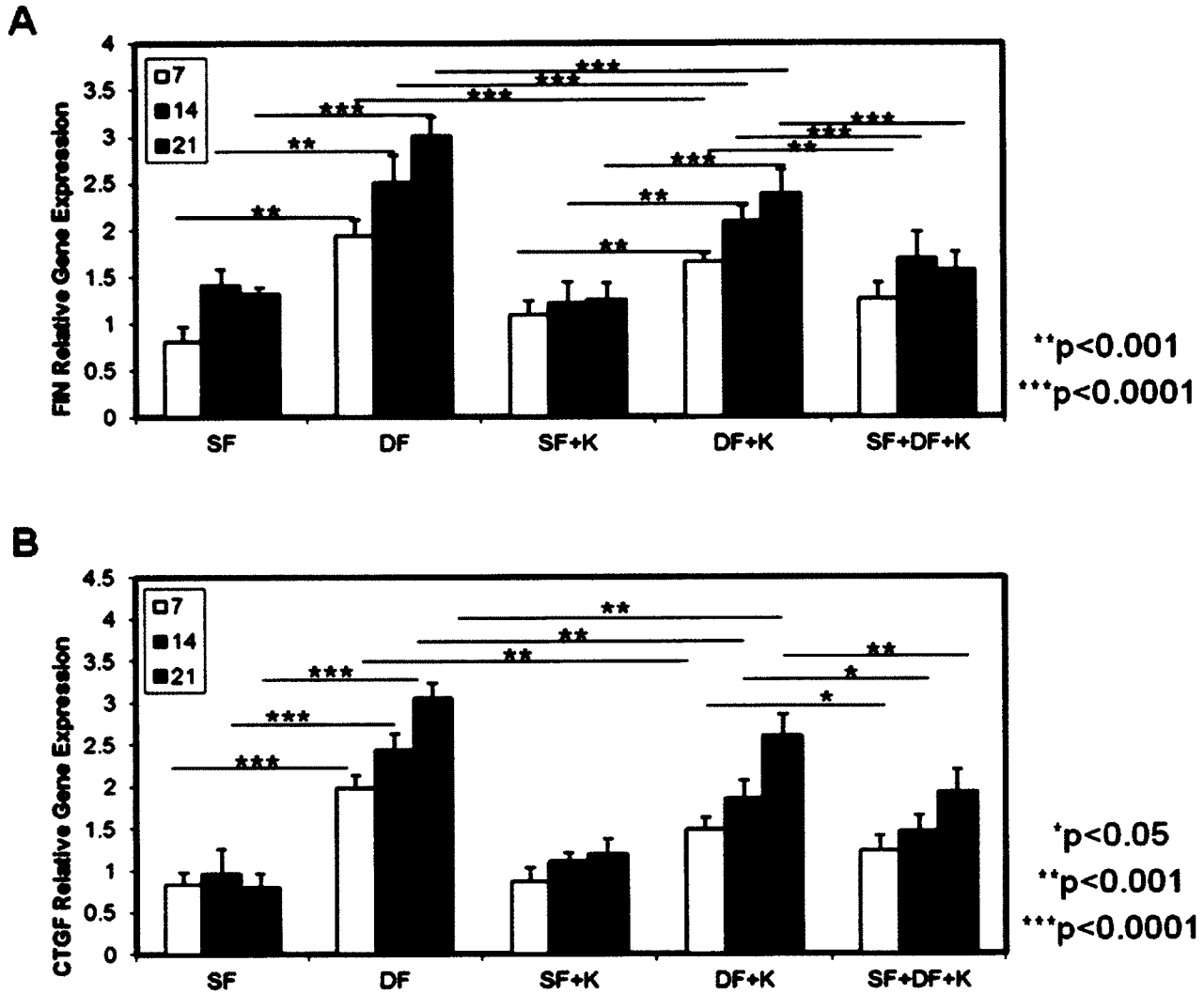


Figure 4.3A-B: Assessment of Relative Gene Expression of Fibrotic Marker Proteins for Tissue Engineered Skin made of SF or DF and K.

SF and DF were independently co-cultured with K on C-GAG matrices for 21 days. mRNA was isolated on days 7, 14 and 21, and reverse transcribed using specific primers (Table 4.1). cDNA was subsequently amplified and relative gene expression was analyzed by qRT-PCR. Each bar represents Mean \pm standard error relative gene expression (n = 3 abdominoplasty patients). **A.** Relative gene expression for FIN. Significant differences between tissue engineered skin made of DF and K and matrices with DF alone on days 7, 14 and 21 ($p < 0.0001$). Also, significant differences between tissue engineered skin made of SF and K and DF and K on days 7 and 14 ($p < 0.001$) and 21 ($p < 0.0001$) and between tissue engineered skin made of DF and K and SF, DF and K on days 7 ($p < 0.001$) and 14 and 21 ($p < 0.0001$). Further, significant differences between matrices with DF alone and SF alone on days 7 and 14 ($p < 0.001$) and 21 ($p < 0.0001$). **B.** Relative gene expression for CTGF. Significant differences between tissue engineered skin made of DF and K and matrices with DF alone on days 7, 14 and 21 ($p < 0.001$). Also, significant differences between tissue engineered skin made of DF and K and SF, DF and K on days 7 and 14 ($p < 0.05$) and 21 ($p < 0.001$). Further, significant differences between matrices with DF alone and SF alone on days 7, 14 and 21 ($p < 0.0001$).

C

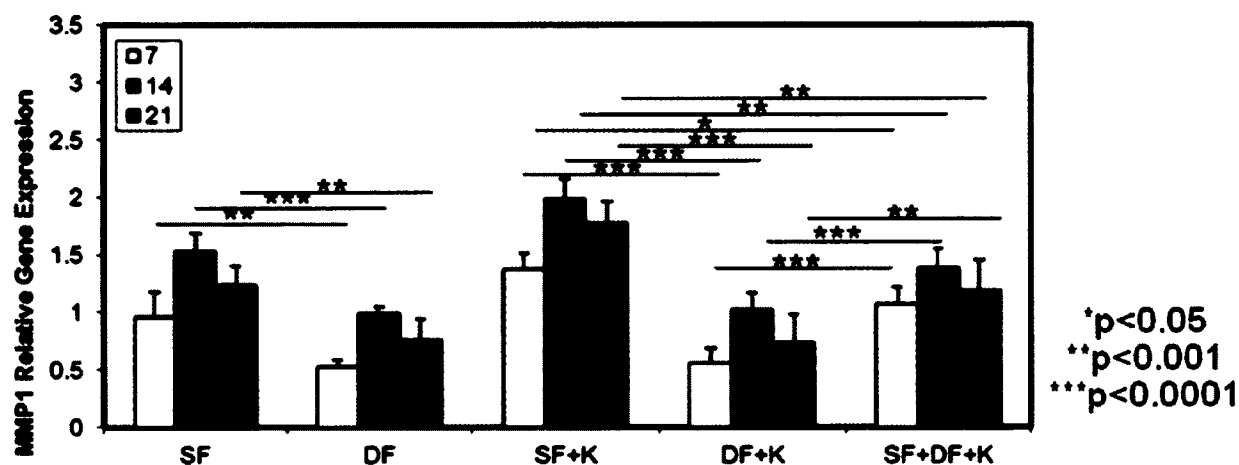


Figure 4.3C: Assessment of Relative Gene Expression of Fibrotic Marker Proteins for Tissue Engineered Skin made of SF or DF and K.

SF and DF were independently co-cultured with K on C-GAG matrices for 21 days. mRNA was isolated on days 7, 14 and 21, and reverse transcribed using specific primers (Table 4.1). cDNA was subsequently amplified and relative gene expression was analyzed by qRT-PCR. Each bar represents Mean \pm standard error relative gene expression (n = 3 abdominoplasty patients). **C.** Relative gene expression for MMP1. Significant differences between tissue engineered skin made of SF and K and DF and K on days 7, 14 and 21 (p<0.0001). Also, significant differences between tissue engineered skin made of DF and K and SF,

DF and K on days 7 and 14 ($p < 0.0001$) and 21 ($p < 0.001$). Further, significant differences between tissue engineered skin made of SF and K and SF, DF and K on days 7 ($p < 0.05$) and 14 and 21 ($p < 0.001$), and between matrices with SF alone and DF alone on days 7, 14 and 21 ($p < 0.001$, $p < 0.0001$, $p < 0.001$).

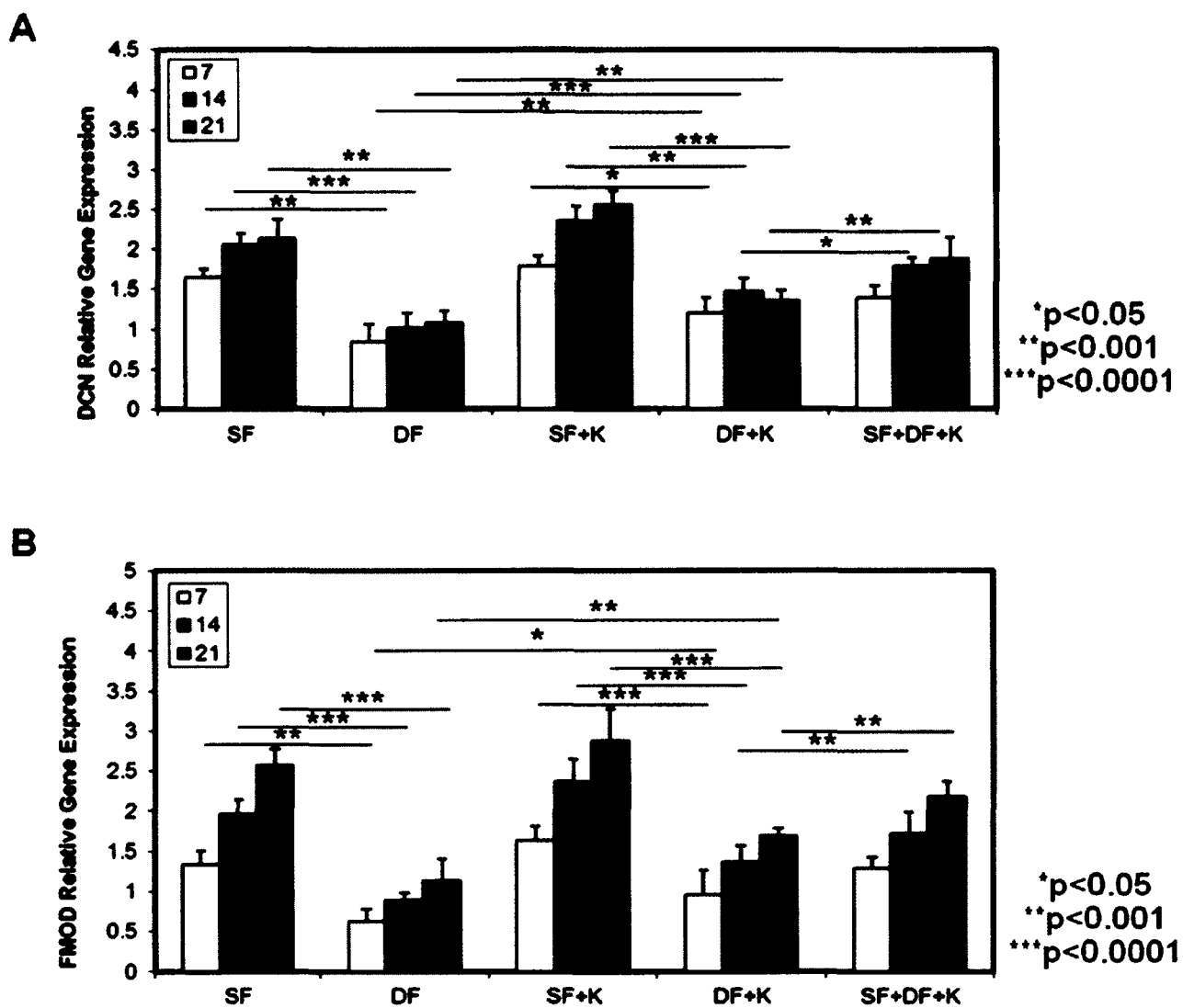


Figure 4.4A-B: Assessment of Relative Gene Expression of Proteoglycans for Tissue Engineered Skin made of SF or DF and K.

SF and DF were independently co-cultured with K on C-GAG matrices for 21 days. mRNA was isolated on days 7, 14 and 21, and reverse transcribed using specific primers (Table 4.1). cDNA was subsequently amplified and relative gene expression was analyzed by qRT-PCR. Each bar represents Mean \pm standard error relative gene expression (n = 3 abdominoplasty patients). **A.** Relative gene expression for DCN. Significant differences between tissue engineered skin made of DF and K and matrices with DF alone on days 7 ($p < 0.001$), 14 ($p < 0.0001$) and 21 ($p < 0.001$). Also, significant differences between tissue engineered skin made of SF and K and DF and K on days 7 ($p < 0.05$), 14 ($p < 0.001$) and 21 ($p < 0.0001$) and between tissue engineered skin made of DF and K and SF, DF and K on days 14 ($p < 0.05$) and 21 ($p < 0.001$). Further, significant differences between matrices with DF alone and SF alone on days 7 ($p < 0.001$), 14 ($p < 0.0001$) and 21 ($p < 0.001$). **B.** Relative gene expression for FMOD. Significant differences between tissue engineered skin made of DF and K and matrices with DF alone on days 7 ($p < 0.05$) and 14 ($p < 0.001$). Also, there were significant differences between tissue engineered skin made of SF and K and DF and K on days 7, 14 and 21 ($p < 0.0001$), and between tissue engineered skin made of DF and K and SF, DF and K on days 14 and 21 ($p < 0.001$). Further, there were significant differences between matrices with DF alone and SF alone on days 7 ($p < 0.001$), and 14 and 21 ($p < 0.0001$).

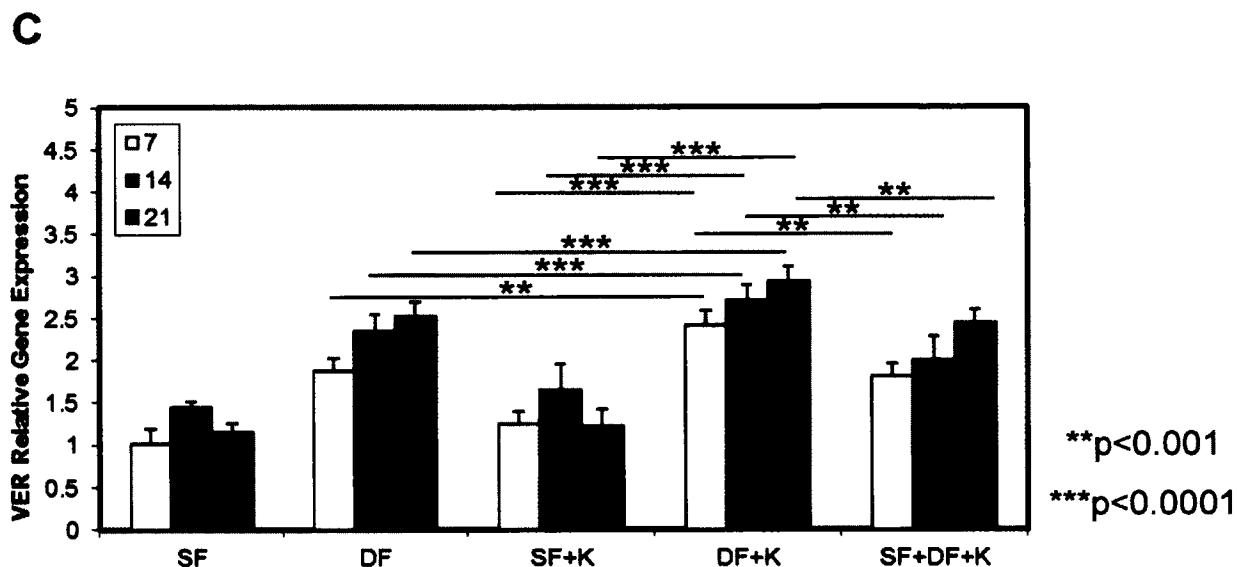


Figure 4.4C: Assessment of Relative Gene Expression of Proteoglycans for Tissue Engineered Skin made of SF or DF and K.

SF and DF were independently co-cultured with K on C-GAG matrices for 21 days. mRNA was isolated on days 7, 14 and 21, and reverse transcribed using specific primers (Table 4.1). cDNA was subsequently amplified and relative gene expression was analyzed by qRT-PCR. Each bar represents Mean \pm standard error relative gene expression ($n = 3$ abdominoplasty patients). **C.** Relative gene expression for VER. Significant differences between tissue engineered skin made of DF and K and DF alone on days 7 ($p < 0.001$), 14 and 21 ($p < 0.0001$). Also, there were significant differences between tissue engineered skin made of SF and K and DF and K on days 7, 14 and 21 ($p < 0.0001$), and between tissue engineered skin made of DF and K and SF, DF and K on days 7, 14 and 21 ($p < 0.001$).

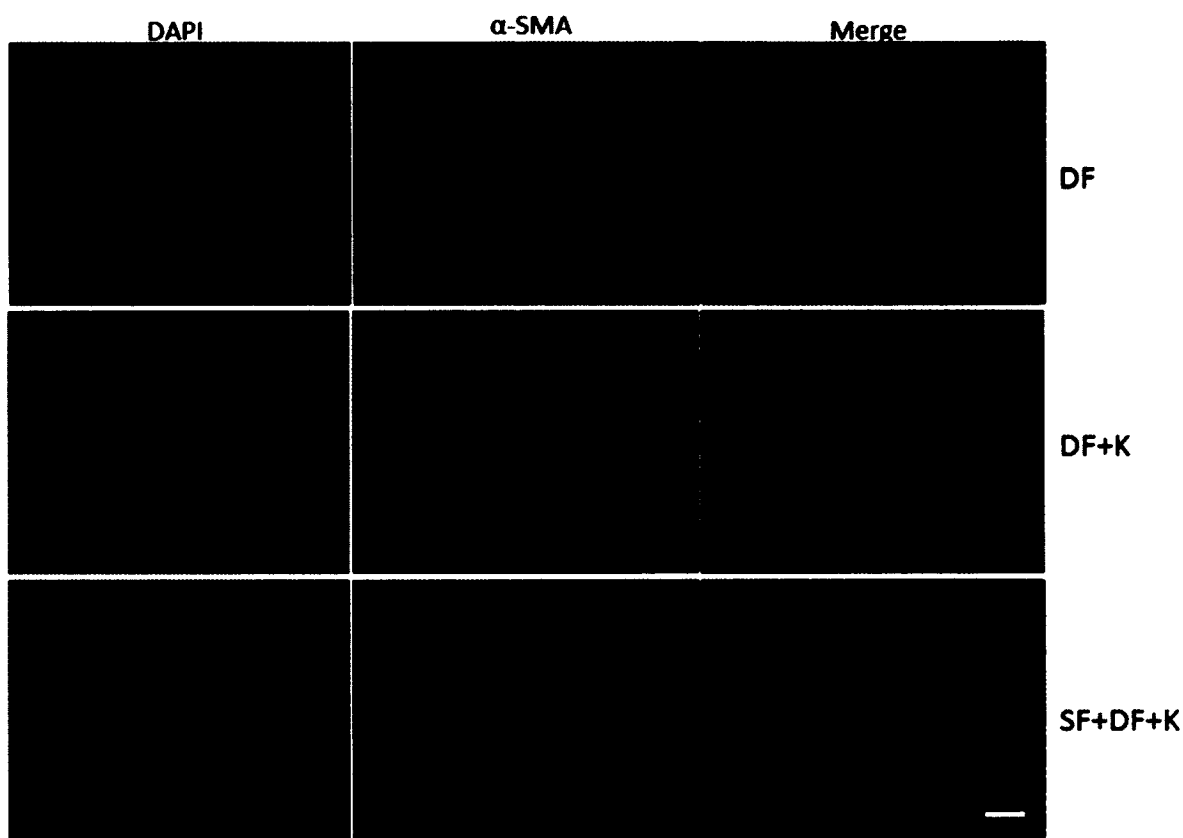


Figure 4.5A: Assessment of Myofibroblast Differentiation for Tissue Engineered Skin made of SF or DF and K.

SF and DF were independently co-cultured with K on C-GAG matrices for 21 days. **A.** Week 2 α -SMA staining for tissue engineered skin made of SF and K, DF and K, or SF, DF and K at 100 \times magnification. Scale bar = 100 μ m. Blue indicates DAPI staining of nuclei on matrices while green indicates presence of α -SMA.

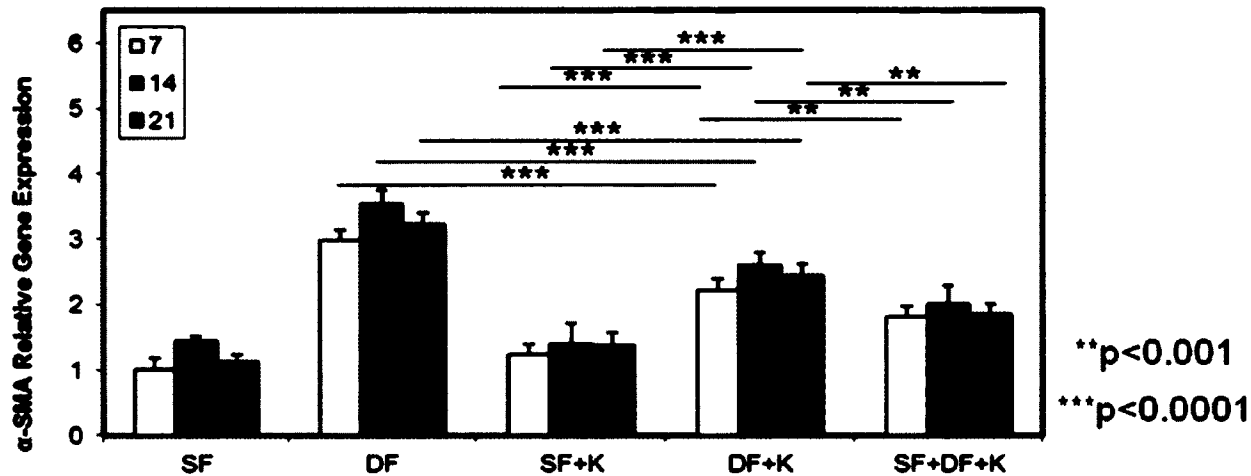
B

Figure 4.5B: Assessment of Myofibroblast Differentiation for Tissue Engineered Skin made of SF or DF and K.

SF and DF were independently co-cultured with K on C-GAG matrices for 21 days. **B.** Relative gene expression for α -SMA. Significant differences between tissue engineered skin made of DF and K and matrices with DF alone on days 7, 14 and 21 ($p < 0.0001$). Also, there were significant differences between tissue engineered skin made of SF and K and DF and K on days 7, 14 and 21 ($p < 0.0001$), and between tissue engineered skin made of DF and K and SF, DF and K on days 7, 14 and 21 ($p < 0.001$).

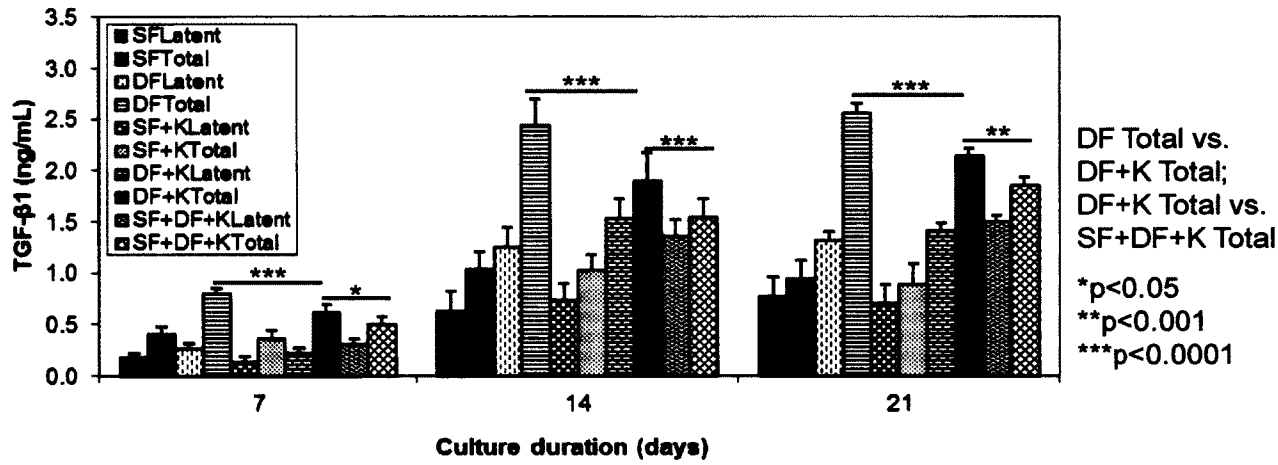


Figure 4.6: Analysis of Latent and Total TGF-β1 Expression for Tissue Engineered Skin made of SF or DF and K.

SF and DF were independently co-cultured with K on C-GAG matrices for 21 days. Latent and total TGF-β1 expression for tissue engineered skin made of SF or DF and K was analyzed using ELISA on days 7, 14 and 21 of culture. 48 h before each time point, media was changed from co-culture medium to 0.2% FBS/DMEM. Conditioned media was directly used in the assay to quantify latent TGF-β1, while to quantify active TGF-β1 the conditioned media was acidified and then neutralized before use in assay. Total TGF-β1 includes latent and active TGF-β1. Each bar represents Mean ± SE TGF-β1 (n = 3 abdominoplasty

patients). Significant differences between tissue engineered skin made of DF and K and matrices with DF alone on days 7, 14 and 21 ($p < 0.0001$). Also, there were significant differences between tissue engineered skin made of DF and K and SF, DF and K on days 7 ($p < 0.05$), 14 ($p < 0.0001$) and 21 ($p < 0.001$).

4.7 References

- [1] Gurtner GC, Werner S, Barrandon Y, Longaker MT. Wound repair and regeneration. *Nature*. 2008;453:314-21.
- [2] Dunkin CS, Pleat JM, Gillespie PH, Tyler MP, Roberts AH, McGrouther DA. Scarring occurs at a critical depth of skin injury: precise measurement in a graduated dermal scratch in human volunteers. *Plastic and reconstructive surgery*. 2007;119:1722-32; discussion 33-4.
- [3] Wynn TA. Cellular and molecular mechanisms of fibrosis. *The Journal of pathology*. 2008;214:199-210.
- [4] Armour A, Scott PG, Tredget EE. Cellular and molecular pathology of HTS: basis for treatment. *Wound repair and regeneration : official publication of the Wound Healing Society [and] the European Tissue Repair Society*. 2007;15 Suppl 1:S6-17.
- [5] Bock O, Schmid-Ott G, Malewski P, Mrowietz U. Quality of life of patients with keloid and hypertrophic scarring. *Arch Dermatol Res*. 2006;297:433-8.
- [6] Boyce ST, Kagan RJ, Yakuboff KP, Meyer NA, Rieman MT, Greenhalgh DG, et al. Cultured skin substitutes reduce donor skin harvesting for closure of excised, full-thickness burns. *Ann Surg*. 2002;235:269-79.
- [7] Wang J, Dodd C, Shankowsky HA, Scott PG, Tredget EE. Deep dermal fibroblasts contribute to hypertrophic scarring. *Lab Invest*. 2008;88:1278-90.

- [8] Varkey M, Ding J, Tredget EE. Differential collagen-glycosaminoglycan matrix remodeling by superficial and deep dermal fibroblasts: potential therapeutic targets for hypertrophic scar. *Biomaterials*. 2011;32:7581-91.
- [9] Azzarone B, Macieira-Coelho A. Heterogeneity of the kinetics of proliferation within human skin fibroblastic cell populations. *J Cell Sci*. 1982;57:177-87.
- [10] Sorrell JM, Baber MA, Caplan AI. Site-matched papillary and reticular human dermal fibroblasts differ in their release of specific growth factors/cytokines and in their interaction with keratinocytes. *J Cell Physiol*. 2004;200:134-45.
- [11] Garner WL. Epidermal regulation of dermal fibroblast activity. *Plast Reconstr Surg*. 1998;102:135-9.
- [12] Harrison CA, Gossiel F, Bullock AJ, Sun T, Blumsohn A, Mac Neil S. Investigation of keratinocyte regulation of collagen I synthesis by dermal fibroblasts in a simple in vitro model. *Br J Dermatol*. 2006;154:401-10.
- [13] Takagi R, Yamato M, Murakami D, Kondo M, Yang J, Ohki T, et al. Preparation of keratinocyte culture medium for the clinical applications of regenerative medicine. *J Tissue Eng Regen Med*. 2011;5:e63-73.
- [14] Wang J, Dodd C, Shankowsky HA, Scott PG, Tredget EE. Deep dermal fibroblasts contribute to hypertrophic scarring. *Lab Invest*. 2008;88:1278-90.
- [15] Wang R, Ghahary A, Shen Q, Scott PG, Roy K, Tredget EE. Hypertrophic scar tissues and fibroblasts produce more transforming growth factor-beta1 mRNA and protein than normal skin and cells. *Wound Repair Regen*. 2000;8:128-37.

- [16] Ghaffari A, Kilani RT, Ghahary A. Keratinocyte-conditioned media regulate collagen expression in dermal fibroblasts. *J Invest Dermatol.* 2009;129:340-7.
- [17] Nowinski D, Hoijer P, Engstrand T, Rubin K, Gerdin B, Ivarsson M. Keratinocytes inhibit expression of connective tissue growth factor in fibroblasts in vitro by an interleukin-1alpha-dependent mechanism. *The Journal of investigative dermatology.* 2002;119:449-55.
- [18] Hildebrand A, Romaris M, Rasmussen LM, Heinegard D, Twardzik DR, Border WA, et al. Interaction of the small interstitial proteoglycans biglycan, decorin and fibromodulin with transforming growth factor beta. *Biochem J.* 1994;302 (Pt 2):527-34.
- [19] Wight TN. Versican: a versatile extracellular matrix proteoglycan in cell biology. *Curr Opin Cell Biol.* 2002;14:617-23.
- [20] Hinz B, Phan SH, Thannickal VJ, Galli A, Bochaton-Piallat ML, Gabbiani G. The myofibroblast: one function, multiple origins. *Am J Pathol.* 2007;170:1807-16.
- [21] Wipff PJ, Rifkin DB, Meister JJ, Hinz B. Myofibroblast contraction activates latent TGF-beta1 from the extracellular matrix. *J Cell Biol.* 2007;179:1311-23.
- [22] Tredget EE. Pathophysiology and treatment of fibroproliferative disorders following thermal injury. *Ann N Y Acad Sci.* 1999;888:165-82.

Chapter 5

Conclusions and Future Avenues

5 Conclusions and Future Avenues

5.1 Conclusions

Fibroblasts from different depths of the dermis were independently cultured on C-GAG matrices to investigate C-GAG matrix remodelling by superficial and deep dermal fibroblasts, assess potential differences in biochemical and biomechanical properties of the remodelled matrices, and analyze the role of these fibroblasts in formation of HTS [1]. Interestingly, superficial and deep dermal fibroblasts were found to differentially remodel the ECM; deep fibroblasts contracted and stiffened the matrices significantly more and decreased their ultimate tensile strength compared to superficial fibroblasts. Deep fibroblasts were also found to express significantly more OPN, ANG-II and PPAR- α , and significantly less TNF- α , PPAR- β/δ , PPAR- γ and FMOD compared to superficial fibroblasts. The newly identified molecular targets described above interact with the critical regulator, TGF- β 1, and therefore are ideal candidates to develop novel strategies to control HTS and promote regenerative healing of the skin.

Superficial and deep dermal fibroblasts were independently co-cultured with keratinocytes on C-GAG matrices to investigate the specific effects and interactions of the two fibroblast sub-populations with keratinocytes, and assess potential differences in epidermis, basement membrane formation and epidermal barrier function. Interestingly, of the developed tissue engineered skin, the

construct made of superficial fibroblasts and keratinocytes formed superior epidermis with enhanced barrier function and a better basement membrane with increased expression of dermo-epidermal adhesive and anchoring proteins such as laminin-5 and collagen type VII compared to the others made of deep fibroblasts or the conventional heterogeneous fibroblasts and keratinocytes. The novel tissue engineered skin made specifically with superficial fibroblasts and keratinocytes may therefore be beneficial for treatment of patients with basement membrane disorders such as EB and other skin blistering diseases. Further work including studies in animal models is necessary for effective translation of this treatment modality to the clinic.

In order to assess the effect keratinocytes have on fibrotic characteristics of superficial and deep dermal fibroblasts, they were independently co-cultured with keratinocytes on C-GAG matrices and subsequently the biomechanical characteristics of the remodelled matrices and production of fibrotic markers was analyzed. Co-culture with keratinocytes significantly reduced matrix contraction and collagen production in the case of deep fibroblasts but not superficial fibroblasts or heterogeneous fibroblasts. Also, co-culture with keratinocytes significantly reduced gene expression of the pro-fibrotic CTGF and fibronectin, and increased expression of the anti-fibrotic MMP-1 for deep fibroblasts but not significantly for superficial or heterogeneous fibroblasts. Furthermore, co-culture with keratinocytes significantly increased expression of the small proteoglycans, decorin and fibromodulin in the case of superficial fibroblasts and not deep

fibroblasts, while co-culture increased expression of the large proteoglycan, versican, in the case of deep fibroblasts and not superficial fibroblasts. In addition, co-culture with keratinocytes significantly reduced TGF- β 1 mRNA and protein production and differentiation to myofibroblasts for deep fibroblasts but not significantly for superficial or heterogeneous fibroblasts. Co-culture with keratinocytes significantly altered fibrotic effects and biomechanical properties of the remodelled matrices in the case of deep fibroblasts but not for superficial or heterogeneous fibroblasts.

Overall, this work has demonstrated that superficial and deep dermal fibroblasts differ in fibrotic characteristics, differentially remodel ECM, and the resulting tissue engineered skin shows differences in the formed epidermis, basement membrane and epidermal barrier function. Use of a pure population of superficial fibroblasts to make tissue engineered skin may therefore be more beneficial for wound healing and minimizing post-burn HTS compared to heterogeneous dermal fibroblasts that are conventionally used in tissue engineered skin. The use of superficial fibroblasts with keratinocytes in tissue engineered skin may also help promote regenerative wound healing due to their anti-fibrotic characteristics, as opposed to fibrosis often observed when heterogeneous dermal fibroblasts are used.

5.2 Future Avenues

This project has provided valuable information about differences in matrix remodelling by superficial and deep dermal fibroblasts. *In vitro* assessment of tissue engineered skin with superficial and deep dermal fibroblasts revealed that tissue engineered skin with superficial fibroblasts forms continuous epidermis and basement membrane and a better epidermal barrier. *In vitro* analyses of also revealed that tissue engineered skin made with superficial fibroblasts has anti-fibrotic characteristics as opposed to tissue engineered skin made with deep fibroblasts, which is pro-fibrotic. These characteristics of both types of tissue engineered skin need to be further confirmed *in vivo*. In this direction, immunodeficient nude mouse can be used as a promising model to test functional differences in tissue engineered skin made with superficial or deep dermal fibroblasts [2]. Nude mice lack thymus and cannot generate mature T lymphocytes, therefore they are unable to mount most immune responses including antibody formation, cell-mediated immune responses, killing of malignant cells and graft-rejection [3]. Nude mice have previously been used for assessment of tissue engineered skin made of heterogeneous fibroblasts [4]. For *in vivo* assessment, tissue engineered skin made with superficial or deep fibroblasts could be applied to wounds on the back of nude mice, and the mice could be monitored for rates of engraftment and formation of scars, if any. Further, the applied tissue engineered skin can be tested for barrier function by SEC measurements using a dermal phase meter and assessed by qRT-PCR for

different pro-fibrotic and anti-fibrotic markers of wound healing. These experiments will enable assessment of the role of superficial dermal fibroblasts in mediating anti-fibrotic wound healing and fibrosis post-deep dermal injury.

Future work should be focussed on improving this novel tissue engineered skin and making it more 'native-skin like'. Some studies show that the rapid freezing process used in fabrication of the C-GAG scaffolds could lead to variable heat transfer from C-GAG suspension, resulting in scaffolds with a heterogeneous pore structure and large variation in pore diameter at different locations in the scaffold [5]. Further the C-GAG scaffolds are structurally different from the native ECM; the native ECM is fibrillar with micron to sub-micron fibres while C-GAG scaffolds contain pore walls that are several microns thick. To generate C-GAG scaffolds that are more homogeneous and homologous to the native ECM, with fibre structures in the range of sub-micron to nanometer range, electrospinning can be utilized [6]. It is an inexpensive process, wherein, the C-GAG suspension will be pumped through a syringe needle that is electrically charged [7]. A charge will be induced on the liquid droplet at the tip of the needle by the electric potential between the needle and a grounded collection plate. When the electric field reaches a threshold, the repulsive electric force within the liquid overcomes the surface tension of the C-GAG solution, causing a charged jet of solution to be ejected from the droplet of C-GAG solution. The C-GAG jet is then accelerated towards the oppositely charged or grounded collection plate. This process generates non-woven nanometre to micron-sized fibers. By altering factors such

as concentration of the C-GAG suspension, flow rate, surface tension, etc. the fibre diameter and morphology of the electrospun scaffold can be controlled.

An essential requirement for the fast and efficient preparation of tissue engineered skin is availability of large number of cells to culture on C-GAG scaffolds. Expansion of cells in tissue culture flasks, the method employed for cell procurement in this project, has a slower turn over period. The use of bio-reactors for expansion of fibroblasts and keratinocytes could enable quicker and efficient supply of cells for use in preparation of tissue engineered skin.

Further, to make tissue engineered skin similar to 'native skin' other appendages such as sweat glands, hair follicles and pigment cells need to be included in the engineered skin. In this direction, co-culture protocols and reagents for inclusion of other cells such as Langerhans cells, melanocytes, endothelial cells, Merkel cells and adipocytes need to be developed and optimized; directed differentiation of stem cells [8, 9] seeded on C-GAG scaffolds into a variety of cells could be a promising approach for this.

Finally, for successful and widespread translation of this novel tissue engineered skin from bench-side to clinic for use in burn patients with extensive skin loss, cell culture media free of animal components (serum-free) and alternative dermal substitute materials in place of bovine collagen that present lower risks need to be explored.

5.3 References

- [1] Varkey M, Ding J, Tredget EE. Differential collagen-glycosaminoglycan matrix remodeling by superficial and deep dermal fibroblasts: potential therapeutic targets for hypertrophic scar. *Biomaterials*. 2011;32:7581-91.
- [2] Wang J, Ding J, Jiao H, Honardoust D, Momtazi M, Shankowsky HA, et al. Human hypertrophic scar-like nude mouse model: characterization of the molecular and cellular biology of the scar process. *Wound repair and regeneration* : official publication of the Wound Healing Society [and] the European Tissue Repair Society. 2011;19:274-85.
- [3] Mecklenburg L, Tychsen B, Paus R. Learning from nudity: lessons from the nude phenotype. *Exp Dermatol*. 2005;14:797-810.
- [4] Powell HM, Boyce ST. Wound closure with EDC cross-linked cultured skin substitutes grafted to athymic mice. *Biomaterials*. 2007;28:1084-92.
- [5] O'Brien FJ, Harley BA, Yannas IV, Gibson L. Influence of freezing rate on pore structure in freeze-dried collagen-GAG scaffolds. *Biomaterials*. 2004;25:1077-86.
- [6] Telemeco TA, Ayres C, Bowlin GL, Wnek GE, Boland ED, Cohen N, et al. Regulation of cellular infiltration into tissue engineering scaffolds composed of submicron diameter fibrils produced by electrospinning. *Acta Biomater*. 2005;1:377-85.
- [7] Chew SY, Wen Y, Dzenis Y, Leong KW. The role of electrospinning in the emerging field of nanomedicine. *Curr Pharm Des*. 2006;12:4751-70.

- [8] Sasaki M, Abe R, Fujita Y, Ando S, Inokuma D, Shimizu H. Mesenchymal stem cells are recruited into wounded skin and contribute to wound repair by transdifferentiation into multiple skin cell type. *J Immunol.* 2008;180:2581-7.
- [9] Pittenger MF, Mackay AM, Beck SC, Jaiswal RK, Douglas R, Mosca JD, et al. Multilineage potential of adult human mesenchymal stem cells. *Science.* 1999;284:143-7.